



Norwegian University of  
Science and Technology

# Current Distribution in Bipolar Cell Systems for the Chlor-alkali Industry

**Per Sverre Iversen**

Chemical Engineering and Biotechnology

Submission date: June 2018

Supervisor: Svein Sunde, IMA

Co-supervisor: Egil Rasten, Inovyn

Norwegian University of Science and Technology  
Department of Materials Science and Engineering





Norwegian University of  
Science and Technology

# Current Distribution in Bipolar Cell Systems for the Chlor-alkali Industry

**Per Sverre Iversen**

21st June 2018

MASTER THESIS

Norwegian University of Science and Technology  
Department of Materials Science and Engineering

Supervisor: Svein Sunde, NTNU,  
Co-supervisor: Egil Rasten, Inovyn

This page is intentionally left blank

## Preface

This master thesis was written in the spring semester of 2018 at NTNU. The project was done for the company INOVYN, which is a subsidiary of INEOS. The reason for the project was to one day being able to predict the lifetime of the electrodes in-situ in a bipolar cell system for the chlor-alkali process. The anodic and cathodic sample preparations were done in Porsgrunn at INOVYN and the experimental work was done in Trondheim at NTNU. Samples of the commercial anodes and cathodes, which were used in the experiments, was provided by INOVYN.

I would like to thank Svein Sunde (NTNU) for his tremendous efforts in helping and guiding me throughout the project. I would also like to thank Eqil Rasten (INOVYN) for help and guidance throughout the project and Ingmarie Libberger (INOVYN) for all help in the laboratory at Porsgrunn. I would also like to thank INOVYN which provided the electrode samples and gave me the opportunity to work on this project.

Trondheim, 21st June 2018

(signature)

Per Sverre Iversen

## Abstract

The chlor-alkali industry is one of Europe's largest chemical industries and produces chlorine gas, hydrogen gas and sodium hydroxide. One of the main production methods is to use membrane cells that are assembled into a bipolar cell system. Operating such a cell system uses a lot of energy, in addition to consuming rare metals such as ruthenium and iridium by degradation of the electrode coatings. During the replacements of the electrodes, most of them are sent back to recoating, without being fully worn out. By increasing the current efficiency and to predict the lifetime of the coatings in-situ, the operating cost of the chlor-alkali process could be reduced.

The aim of this master thesis was to be able to dynamically simulate the current distributions throughout the bipolar cell system, including shunt currents. The simulations would be used to look at what degree of impact the different inlet tube lengths had on the current distribution during steady state operation and during the discharge stage. Also, to look at what impact the different capacitance values have for the electrodes had on the discharge rate, in order to see if it was possible to predict in-situ the state of the electrode coatings, based on discharge data.

A theoretical model for the potentials in the electrolytes throughout the bipolar cell system was constructed. The model was then used as the basis for programming a code that would be able to dynamically simulate the potentials during steady state operation and during the discharge stage. From the potentials and the resistances in the electrolyte, the current distribution could be found. Electrochemical impedance spectroscopy was done to the anode and cathode samples in order to determine the capacitance of the electrodes.

It was found that the longer the anodic and cathodic inlet tubes were, the more current went through the cell system itself, during steady state operation. The increased current through the cell system led to a decrease of the current going through the headers, and therefore gave a greater power efficiency. During the discharge stage, it was found that the impact of the inlet tube lengths were significantly smaller, than during steady state operation. It was also found that the capacitance values of the electrodes significantly affected the discharge rate.

## Sammendrag

Kloralkaliindustrien er en av Europas største kjemiske industrier og produserer klorgass, hydrogengass og natriumhydroksid. En av de mest brukte produksjonsmetodene er å bruke membran-celler satt sammen til et bipolar cellsystem. Driften av et slikt cellsystem bruker mye energi, i tillegg til forbruk av sjeldne metaller som ruthenium og iridium ved nedbryting av elektrodbeleggene. Under utskifting av elektrodene blir de fleste sendt tilbake til rebelegging uten å være helt utslitt. Ved å øke strømeffektiviteten og ved å kunne forutse levetiden til beleggene in-situ, kan driftskostnaden for kloralkali-prosessen reduseres.

Målet med denne masteroppgaven var å kunne dynamisk simulere strømfordelingene i et bipolar cellsystem, inkludert for kryptstrøm. Simuleringene vil bli brukt til å se på hvordan forskjellige innløpsrørlengder påvirket strømfordelingene under drift og under utladningsfasen. I tillegg se på hvilken effekt ulike kapasitansverdier for elektrodene hadde på utladningshastigheten. Dette for å kunne vurdere om det var mulig å forutse elektrodernes levetid in-situ, basert på utladningsdata.

En teoretisk model for potensialene i elektrolytten gjennom det bipolare cellsystemet ble konstruert. Modellen ble så brukt som grunnlaget til å programmere en kode som skulle kunne dynamisk simulere potensialene under drift og under utladningsfasen. Gjennom å simulere potensialene og finne resistansen til elektrolyttene, kunne strømfordelingene bli funnet. Elektrokjemisk impedansspektroskopi ble utført på anode- og katodeprøvene for å finne kapasitansverdiene til elektrodene.

Det ble funnet at større lengde på anodisk og katodisk innløpsrør førte til at en større mengde strøm gikk gjennom det bipolare cellsystemet under drift. Den økte strømmen gjennom cellsystemet førte til at en mindre mengde strøm gikk gjennom innløpsfordeleren, noe som øker strømeffektiviteten. Under utladningstadiet ble det funnet at påvirkningen til innløpsrørlengden var betydelig mindre enn under drift. Det ble også funnet at kapasitansverdiene til elektrodene påvirket utladningshastigheten i stor grad.





# Contents

Preface . . . . .	iii
Abstract . . . . .	iv
Sammendrag . . . . .	v
<b>List of Tables</b>	<b>ix</b>
<b>List of Figures</b>	<b>xiv</b>
<b>List of Symbols</b>	<b>xv</b>
0.1 Symbol list . . . . .	xvi
<b>1 Introduction</b>	<b>1</b>
<b>2 Theory</b>	<b>3</b>
2.1 Bipolar cell systems . . . . .	3
2.2 Cyclic voltammetry . . . . .	6
2.3 RuO <sub>2</sub> kinetics . . . . .	8
2.4 Electrochemical impedance spectroscopy . . . . .	8
2.4.1 General theory . . . . .	8
2.4.2 Impedance of a capacitor . . . . .	10
2.4.3 Constant phase element . . . . .	11
2.4.4 Warburg impedance . . . . .	12
2.4.5 Measurement models . . . . .	13
<b>3 Model</b>	<b>15</b>

3.1	Transient model for bipolar electrolyser . . . . .	15
<b>4</b>	<b>Simulation</b>	<b>17</b>
4.1	GeneratingMatrixCreepCurrentDynamicSimulation . . . . .	17
<b>5</b>	<b>Experimental</b>	<b>25</b>
5.1	Electrodes . . . . .	26
5.2	Cyclic voltammetry . . . . .	26
5.3	Electrochemical impedance spectroscopy . . . . .	27
<b>6</b>	<b>Results</b>	<b>29</b>
6.1	Experimental work . . . . .	29
6.1.1	Cyclic voltammetry . . . . .	29
6.2	Electrochemical impedance spectroscopy . . . . .	30
6.2.1	Anode sample . . . . .	30
6.2.2	Cathode sample . . . . .	33
6.3	Simulations . . . . .	35
6.3.1	During operation . . . . .	35
6.3.2	Discharge by variations of shunt currents . . . . .	38
6.3.3	Discharge by variations of capacitance . . . . .	47
<b>7</b>	<b>Discussion</b>	<b>53</b>
7.1	Further work . . . . .	56
<b>8</b>	<b>Conclusion</b>	<b>57</b>
	<b>References</b>	<b>58</b>
<b>A</b>	<b>Appendix</b>	<b>61</b>
A.1	Matlab code . . . . .	61

# List of Tables

5.1	The PMI value of the anode and the cathode from a pre-set value of Ru content in the coating. . . . .	26
-----	---	----



# List of Figures

2.1	Illustrates the chlor-alkali process in a membrane cell [6] . . . . .	4
2.2	Shows the equivalent circuit of membrane cells in a bipolar cell system[17]. . .	4
2.3	Illustrates the natural discharge for the cells in a bipolar cell system, where the cell voltage is plotted against the time and cell position. The figure is obtained from a presentation given by Egil Rasten at INOVYN in connection to the training in regards of the project work. . . . .	5
2.4	Shows the shunt currents in the form of $\text{Na}^+$ and $\text{OH}^-$ ions that are moving through the inlet tubes. The figure is obtained from a presentation given by Egil Rasten at INOVYN in connection to the training in regards of the project work. . . . .	5
2.5	By plotting the potential against the time, during cyclic voltammetry, creates a waveform potential curve. Where $E_{pa}$ is the anodic turning potential and $E_{pc}$ is the cathodic turning potential. The slope of the potential curve is the scan rate, $\nu$ . . . . .	6
2.6	In a voltammogram, the current or current density is plotted against the potential. $i_{pa}$ is the anodic peak current and the $i_{pc}$ is the cathodic peak current. . . . .	7
2.7	The voltammogram of (a) is for a titanium plate and (b) is for $\text{TiO}_2$ nanofibres coated with $\text{RuO}_2$ [19]. . . . .	8
2.8	The phasor diagram shows the change and the relationship between the alternating current and potential. The phase angle between the alternating current and the potential is shown as $\phi$ [2]. . . . .	9
2.9	Vector diagram of the impedance, where $R$ is the real component and $X_C$ is the imaginary component. $\phi$ is the phase angle between the impedance vector and the real vector [2]. . . . .	10
2.10	Illustrates an equivalent R-C circuit for a capacitor [10]. . . . .	10
2.11	(a) Shows the sinusoidal curves for the potential and the current with a phase angle of $90^\circ$ [2]. (b) Shows the Nyquist plot for a capacitor [3]. . . . .	11
2.12	Illustrates the equivalent R-Q circuit of a CPE [12]. . . . .	12

---

2.13	Nyquist plot of a R-Q circuit for a CPE. . . . .	12
2.14	Shows an equivalent $R_{ct}$ -W circuit for Warburg impedance [4]. . . . .	12
2.15	Shows a vector diagram of Warburg impedance. The phase angle between the real component vector and the impedance vector is $45^0$ [2]. . . . .	13
2.16	Illustrates the Voight electrical circuit analogue with n number of elements [16].	14
4.1	Nodes are placed in the 2- dimensional model of the bipolar cell system. Each node is connected to its neighboring node. . . . .	18
4.2	Coefficient matrix A. Each blue dot corresponds to a value in the matrix. The x-axis represents position and the the y-axis represents the number of equations.	21
4.3	Column vector b. Each blue dot corresponds to a value in the column. The y-axis represents the number of equations. . . . .	22
4.4	The x-values are given as potentials values. The x-axis represents the position of the x-value and the y-axis represents its value. . . . .	22
4.5	The figure shows the potential throughout the bipolar cell system with shunt currents. The x-axis, as with this case seen as the axis with values from zero to 100, represents the i-position. The y-axis, as with this case seen as the axis with values from zero to 35, represents the j-position. The vertical z-axis, represents the potential values to the given positions. . . . .	23
4.6	The figure shows the flowchart of the GeneratingMatrixCreepCurrentDynamic-Simulation code. . . . .	24
5.1	Three-electrode-setup for a half-cell that was used in the experiments. . . . .	25
6.1	Cyclic voltammogram of the anode sample in 250 g/L NaCl and with a pH of 11. The x-axis shows the potential in V vs. Ag/AgCl and the y-axis shows the current (A). . . . .	29
6.2	Cyclic voltammogram of the cathode sample in 30 % NaOH. The x-axis shows the potential in V vs. Ag/AgCl and the y-axis shows the current (A). . . . .	30
6.3	Complex impedance plane plot of the anode sample done with a potential of 0.2 V vs. Ag/AgCl. The electrolyte consisted of 250 g/L NaCl, with a pH of 11. . . . .	31
6.4	Enlarged area of the complex impedance plane plot of the anode sample, shown by Figure 6.3. . . . .	31
6.5	Bode plot of the anode sample done with a potential of 0.2 V vs. Ag/AgCl. The electrolyte consisted of 250 g/L NaCl, with a pH of 11. . . . .	32
6.6	The upper plot shows the imaginary component error and the lower plot shows the real component error, with respect to the frequency. The plots corresponds to the EIS data, shown by Figure 6.3 for the complex impedance plane plot and Figure 6.5 for the Bode plot. . . . .	32

---

6.7	Complex impedance plane plot of the cathode sample done with a potential of -0.4 V vs. Ag/AgCl. The electrolyte consisted of 30 % NaOH. . . . .	33
6.8	Bode plot of the cathode sample done with a potential of -0.4 V vs. Ag/AgCl. The electrolyte consisted of 30 % NaOH. . . . .	34
6.9	The upper plot shows the imaginary component error and the lower plot shows the real component error, with respect to the frequency. The plots corresponds to the EIS data, shown by Figure 6.7 for the complex impedance plane plot and Figure 6.8 for the Bode plot. . . . .	34
6.10	The figure shows the potential throughout the bipolar cell system with shunt currents, for a compilation of seven membrane cells. The x-axis represents the i-position. The y-axis represents the j-position. The vertical z-axis, represents the potential values to the given position. . . . .	36
6.11	The figure shows the potential throughout the bipolar cell system with shunt currents, for a compilation of seven membrane cells. The x-axis represents the i-position. The y-axis represents the j-position. The vertical z-axis, represents the potential values to the given position. . . . .	37
6.12	The figure shows the potentials throughout the bipolar cell system with shunt currents, for a compilation of seven membrane cells. The discharge simulation was done with the time iteration step of 0.001. The x-axis represents the i-position. The y-axis represents the j-position. The vertical z-axis, represents the potential values to the given position. . . . .	39
6.13	The figure shows the potentials throughout the bipolar cell system with shunt currents, for a compilation of seven membrane cells. The discharge simulation was done with the time iteration step of 0.01. The x-axis represents the i-position. The y-axis represents the j-position. The vertical z-axis, represents the potential values to the given position. . . . .	40
6.14	The figure shows the potentials throughout the bipolar cell system with shunt currents, for a compilation of seven membrane cells. The discharge simulation was done with the time iteration step of 0.1. The x-axis represents the i-position. The y-axis represents the j-position. The vertical z-axis, represents the potential values to the given position. . . . .	41
6.15	The figure shows the potentials throughout the bipolar cell system with shunt currents, for a compilation of seven membrane cells. The discharge simulation was done with the time iteration step of 1. The x-axis represents the i-position. The y-axis represents the j-position. The vertical z-axis, represents the potential values to the given position. . . . .	42
6.16	The figure shows the potentials throughout the bipolar cell system with shunt currents, for a compilation of seven membrane cells. The discharge simulation was done with the time iteration step of 0.001. The x-axis represents the i-position. The y-axis represents the j-position. The vertical z-axis, represents the potential values to the given position. . . . .	43

6.17 The figure shows the potentials throughout the bipolar cell system with shunt currents, for a compilation of seven membrane cells. The discharge simulation was done with the time iteration step of 0.01. The x-axis represents the i-position. The y-axis represents the j-position. The vertical z-axis, represents the potential values to the given position. . . . . 44

6.18 The figure shows the potentials throughout the bipolar cell system with shunt currents, for a compilation of seven membrane cells. The discharge simulation was done with the time iteration step of 0.1. The x-axis represents the i-position. The y-axis represents the j-position. The vertical z-axis, represents the potential values to the given position. . . . . 45

6.19 The figure shows the potentials throughout the bipolar cell system with shunt currents, for a compilation of seven membrane cells. The discharge simulation was done with the time iteration step of 1. The x-axis represents the i-position. The y-axis represents the j-position. The vertical z-axis, represents the potential values to the given position. . . . . 46

6.20 The figure shows the potentials throughout the bipolar cell system with shunt currents, for a compilation of seven membrane cells. The discharge simulation was done with the time iteration step of 0.001 and with half the capacitance value of the anode and cathode. The x-axis represents the i-position. The y-axis represents the j-position. The vertical z-axis, represents the potential values to the given position. . . . . 48

6.21 The figure shows the potentials throughout the bipolar cell system with shunt currents, for a compilation of seven membrane cells. The discharge simulation was done with the time iteration step of 0.01 and with half the capacitance value of the anode and cathode. The x-axis represents the i-position. The y-axis represents the j-position. The vertical z-axis, represents the potential values to the given position. . . . . 49

6.22 The figure shows the potentials throughout the bipolar cell system with shunt currents, for a compilation of seven membrane cells. The discharge simulation was done with the time iteration step of 0.1 and with half the capacitance value of the anode and cathode. The x-axis represents the i-position. The y-axis represents the j-position. The vertical z-axis, represents the potential values to the given position. . . . . 50

6.23 The figure shows the potentials throughout the bipolar cell system with shunt currents, for a compilation of seven membrane cells. The discharge simulation was done with the time iteration step of 1 and with half the capacitance value of the anode and cathode. The x-axis represents the i-position. The y-axis represents the j-position. The vertical z-axis, represents the potential values to the given position. . . . . 51

7.1 The figure shows the discharge plot of a anode sample, performed in the previous project thesis work [11]. The black box indicates the first time interval, where the electrodes undergoes only a capacitive discharge. . . . . 54



# List of Symbols

## 0.1 Symbol list

### Symbols

$A$	: Area	[m <sup>2</sup> ]
$a_j$	: Activity of species j	[]
$C$	: Capacitance	[F]
$C^0$	: Bulk concentration	[mol/cm <sup>2</sup> ]
$C_O^*$	: Initial concentration of the oxidant	[mol/cm <sup>3</sup> ]
$c$	: Concentration of RuOOH	[mol/cm <sup>2</sup> ]
$c_0$	: Initial concentration	[mol/cm <sup>3</sup> ]
$c_{uc}$	: Maximal possible concentration of RuO <sub>2</sub>	[mol/cm <sup>2</sup> ]
$D$	: Diffusion coefficient	[cm <sup>2</sup> /s]
$E_0$	: Initial potential	[V]
$E_{pa}$	: Anodic limiting potential	[V]
$E_{pc}$	: Cathodic limiting potential	[V]
$E_t$	: Potential	[V]
$F$	: Faraday constant	[96485 C/mol]
$I_0$	: Initial current	[A]
$I_t$	: Current	[A]
$i$	: Current density	[A]
$i_0$	: Exchange current density	[A/cm <sup>2</sup> ]
$i_{pa}$	: Anodic peak current	[A/cm <sup>2</sup> ]
$i_{pc}$	: Cathodic peak current	[A/cm <sup>2</sup> ]
$j$	: $\sqrt{-1}$	[]
$n$	: Stoichiometric number of electrons	[]
$Q$	: Electric charge	[C]
$R$	: Gas constant	[8.314 J/(Kmol)]
$R$	: Resistance	[ $\Omega$ ]
$R_e$	: Electrolyte resistance	[ $\Omega$ ]
$R_m$	: External resistance	[ $\Omega$ ]
$T$	: Temperature	[K]
$t$	: Time	[s]
$U_t$	: Cell potential	[V]
$V_i$	: Initial voltage	[V]

---

$V_t$	: Electrical voltage	[V]
$x$	: Ratio	[]
$x$	: Planar distance	[cm]
$Z$	: Impedance	[ $\Omega$ ]
$Z_0$	: Initial impedance	[ $\Omega$ ]
$Z_i$	: Imaginary component of impedance	[ $\Omega$ ]
$Z_r$	: Real component of impedance	[ $\Omega$ ]
$z$	: Charge number	[]
$z_j$	: Charge number of species j	[]
$\alpha$	: Transfer coefficient	[]
$\epsilon$	: dielectric constant	[]
$\kappa$	: electrolyte conductivity	[S/m]
$\Gamma$	: Number of redox-active sites	[mol]
$\Delta_k$	: Sum of Voight element k	[]
$\theta$	: Concentration fraction	[]
$\rho$	: Charge density	[C/m <sup>3</sup> ]
$\mu_j$	: Chemical potential of species j	[kJ/mol]
$\mu_j^0$	: Standard chemical potential of species j	[kJ/mol]
$\tilde{\mu}_j$	: Electrochemical potential of species j	[kJ/mol]
$\nu$	: Scan rate	[mV/s]
$\tau$	: integration constant	[]
$\tau_k$	: Time constant for element k	[s]
$\phi$	: Phase angle, electrolyte potential	[radians, degrees], [V]
$\phi_j$	: Electrostatic potential of species j	[V]
$\omega$	: Radial frequency	[rad/s]



# 1 Introduction

In 2016, the European chlor-alkali industry accounted for 55 % of the total turnover within the European chemical industry [7]. The chlor-alkali production uses mostly membrane cells that are assembled into bipolar cell systems. During operation of these cell systems, electrode coatings and membranes experience degradation. The electrodes and the membranes have different lifetimes, which means that they have to be replaced at different intervals. The replacement intervals for the electrodes are periodic and are set in the future based on the predicted lifetime. Due to the complexity of the replacement procedure and the re-coating of electrodes, the event has to be planned preferably over a year in advance. To prevent the electrodes from going beyond their service life, a significant margin of the rest thickness in the electrode coating has to be implemented. By being able to predict the electrode lifetime in-situ, one is able to transition from periodic maintenance to a condition based maintenance. If the electrode lifetime can be predicted, the margin of the residual lifetime can be decreased, which allows for a longer utilization of the electrodes. By constantly having an overview over the remaining life time the risk associated with maintenance and operation, which can lead to unpredicted downtime or damage, is reduced. In addition, one avoids sending electrodes with sufficient residue coating to be re-coated. The consequences of being able to predict the electrode lifetime in-situ will lead to a significant reduction in operation expenses, as well as a greater control over the process.

The purpose of this work is to develop a model that can dynamically simulate the potentials throughout the cell system, during operation and during the discharge stage. By being able to simulate the potentials during the operation, the electrical distribution in the system is given by Ohm's law. Since the model will include shunt currents, the impact of these currents on the overall electrical distributions can be seen. This allows for the possibility to limit the negative consequences of the shunt currents by adjusting the dimensions of the inlet tubes. For example, by decreasing the shunt currents, the current efficiency will increase. By being able to dynamically simulate the potentials in the cell system during the discharge stage, the effect of the residual life time of the electrodes and the shunt currents, can be seen. The residual life time is dependent on the coating thickness, which in turn defines the capacitance of the electrodes. By simulating with different capacitance values, one could predict the life time in-situ by comparing the discharge graphs of the simulation with the natural discharge of the bipolar cell system.

In this project, cyclic voltammetry and electrochemical impedance spectroscopy will be performed in order to find the capacitance of the anode and the cathode used in the chlor-alkali industry for bipolar cell systems. A model of the potentials in the electrolyte will be constructed. The model will then be used as the basis for writing a code in Matlab that would be able to simulate the potentials throughout the bipolar cell system during operation, and to dynamically simulate the potentials during the discharge of the cell system.



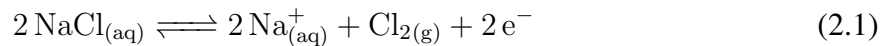
## 2 Theory

Parts of the theory are taken from the previously written project thesis from last autumn [11]. The reason for this is because much of the same theory is still relevant for the master thesis work.

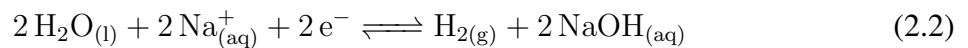
### 2.1 Bipolar cell systems

The chlor-alkali production uses primarily membrane cells that are assembled into a bipolar cell structure. Each structure or system consists of several cell elements that are connected in series, where the equivalent circuit is shown in Figure 2.2. The electrochemical process for chlor-alkali production is shown in Figure 2.1, for a single membrane cell.

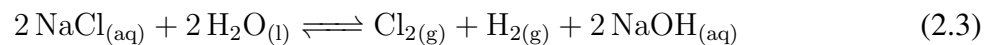
The anode is made of titanium with a coating of titanium oxide, ruthenium oxide and iridium oxide. The cathode is made of nickel with a coating of nickel oxide and ruthenium oxide. Both the electrodes have a mesh structure and are dimensionally stable. A membrane separates the anode chamber from the cathode chamber. The electrolyte in the anode chamber consists of concentrated brine and the electrolyte in the cathode chamber consists of 30-33 % NaOH. The concentrated brine solution is pumped into the anode chamber, where the chlorine ions are reduced to chlorine gas. The sodium ions diffuse through the membrane and reacts with water, to produce hydrogen gas and sodium hydroxide. The cell reaction is given by the anode reaction



and the cathode reaction



which gives the total reaction



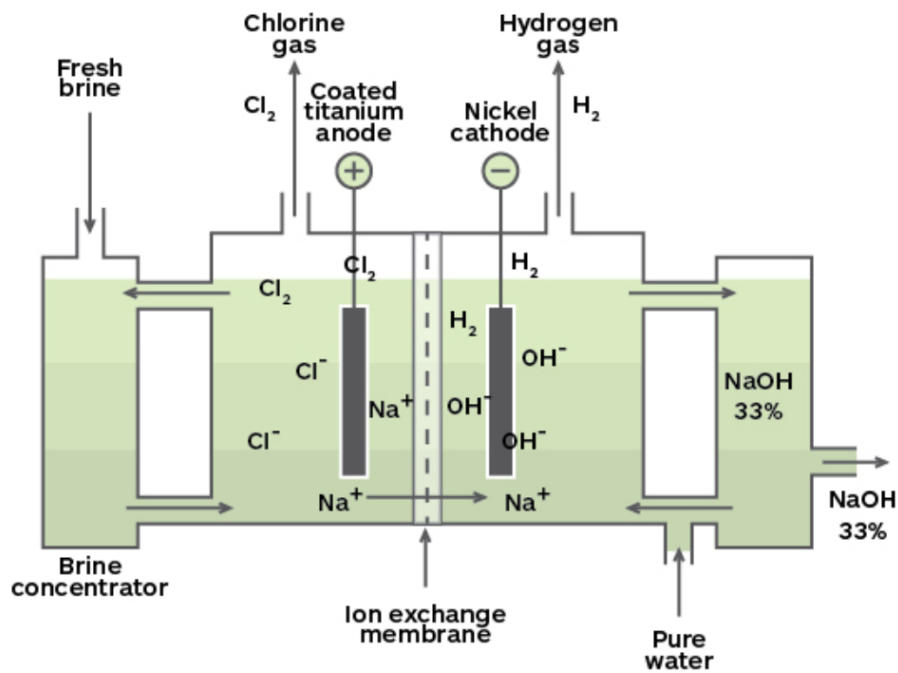


Figure 2.1: Illustrates the chlor-alkali process in a membrane cell [6]

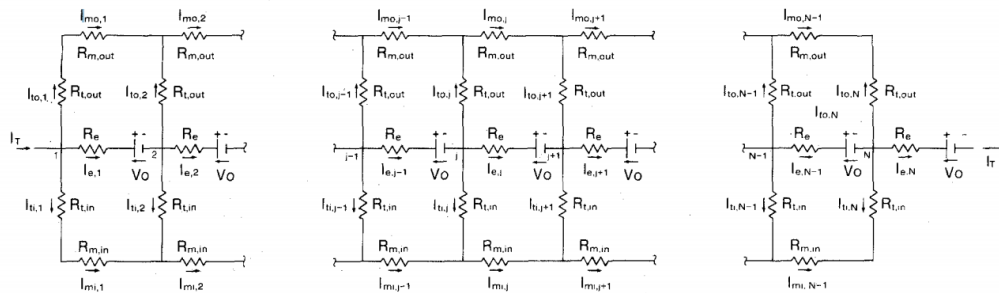
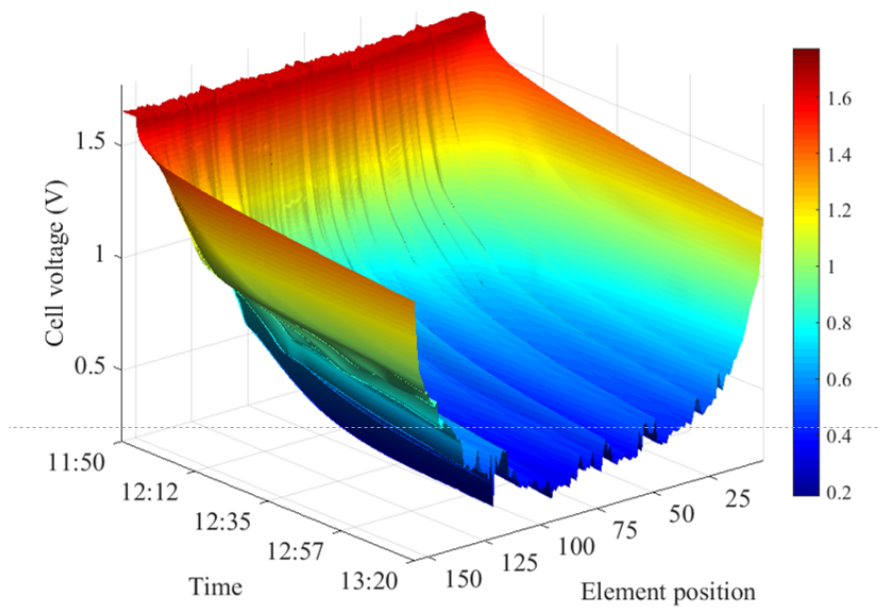


Figure 2.2: Shows the equivalent circuit of membrane cells in a bipolar cell system[17].

During the shutdown of the bipolar cell system, there is a discharge stage. The natural discharge is shown in Figure 2.3, where the potential is plotted against the time and cell position. As can be seen, the cell position affects the cell discharge. This is due to shunt currents, in the form of ion migrations, in the bipolar cell system at the inlet and outlet tubes. The shunt currents are driven by polarization gradients throughout the system. Figure 2.4 shows the current flow and the ion migration through the system during steady state operation. The figure displays how the basis for the two-dimensional model that are simulated, is constructed. From the figure, the different parts of the bipolar cell system can be seen. The parts indicated by an A, shows the anode and the parts indicated by a C, shows the cathode. The membranes are indicated by a B. The cathodic inlet tubes are indicated by a D and the cathodic header is indicated by an E. The anodic inlet tubes are indicated by a F and the anodic header is indicated by a G.





**Figure 2.3:** Illustrates the natural discharge for the cells in a bipolar cell system, where the cell voltage is plotted against the time and cell position. The figure is obtained from a presentation given by Egil Rasten at INOVYN in connection to the training in regards of the project work.

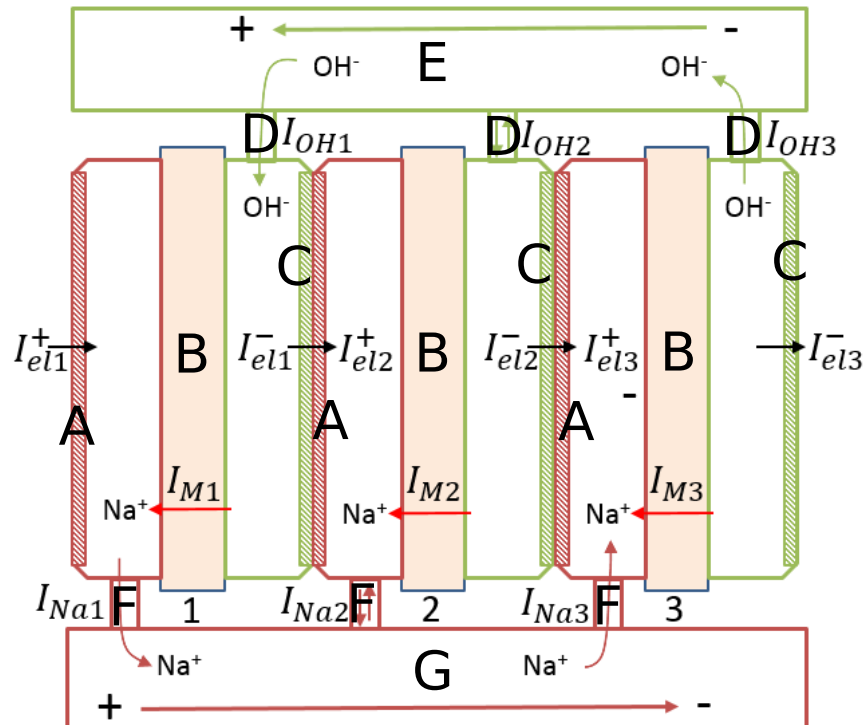


**Figure 2.4:** Shows the shunt currents in the form of  $\text{Na}^+$  and  $\text{OH}^-$  ions that are moving through the inlet tubes. The figure is obtained from a presentation given by Egil Rasten at INOVYN in connection to the training in regards of the project work.

## 2.2 Cyclic voltammetry

Cyclic voltammetry is widely used in electrochemistry to study the characteristics of electroactive species. For a three-electrode-setup, the working electrode is exposed to a potential that changes with time. The potential at the working electrode is measured against a reference electrode. As can be seen from Figure 2.5, the cyclic voltammetry applies a potential with a triangular waveform. Each cycle starts at a given potential and runs between the anodic limiting potential ( $E_{pa}$ ) and the cathodic limiting potential ( $E_{pc}$ ) [5]. The speed of which the applied potential is changing, is called the scan rate. The changes in the potential for the working electrode, creates a corresponding current between it and the counter electrode. The generated current is due to deviations from equilibrium at the interface and the equilibrium potential [1]. The potential range is set at an interval containing the redox processes of interest [18]. In an aqueous electrolyte, the anodic and cathodic turning potential,  $E_{pa}$  and  $E_{pc}$ , i.e. the limiting interval potentials, is set at the oxygen and hydrogen evolution potentials [5].

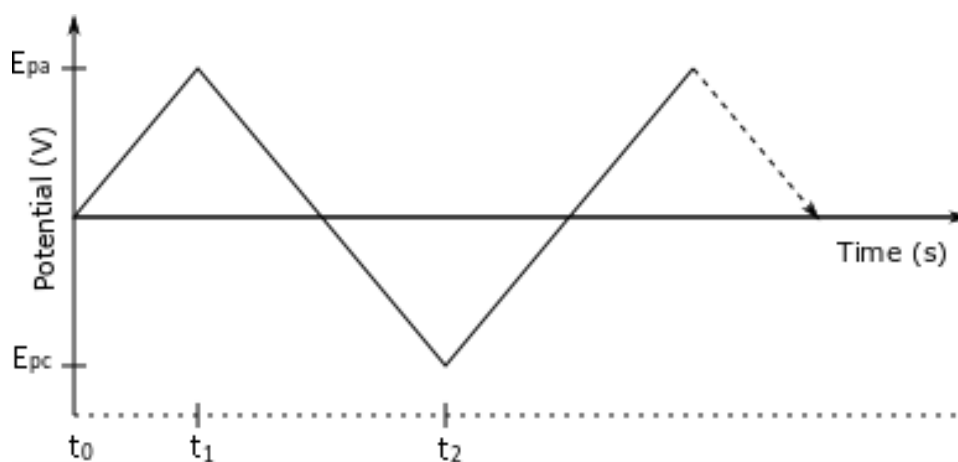


**Figure 2.5:** By plotting the potential against the time, during cyclic voltammetry, creates a waveform potential curve. Where  $E_{pa}$  is the anodic turning potential and  $E_{pc}$  is the cathodic turning potential. The slope of the potential curve is the scan rate,  $\nu$ .

Plotting the current between the working electrode and the counter electrode against the potential between the working electrode and the reference electrode, creates a voltammogram. An example of a voltammogram is shown by Figure 2.6. For a system with an aqueous electrolyte, with no active redox couples in the solution, the current is generated by formation and dissolution of chemisorbed hydrides and oxide layers on the electrode surface [5]. From point 1 in Figure 2.6, the applied potential increases. When the potential gets high enough to oxidize the electrode surface, the anodic current increases until it reaches the anodic peak current ( $i_{pa}$ ). From the point of the anodic peak current, the anodic current decreases. After reaching the anodic turning potential, a cathodic current will start to generate. The cathodic current is generated by reduction of the electrode species. The cathodic current increases until it reaches the cathodic peak potential ( $i_{pc}$ ). For cyclic voltammetry, the mentioned redox processes repeats as the potential changes as shown in Figure 2.5.

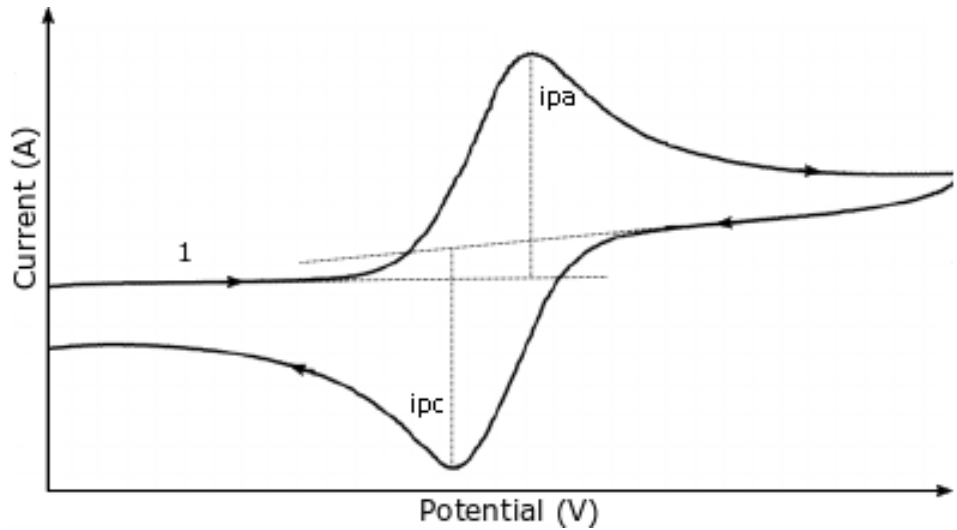


**Figure 2.6:** In a voltammogram, the current or current density is plotted against the potential.  $i_{pa}$  is the anodic peak current and the  $i_{pc}$  is the cathodic peak current.

From the voltammogram, the capacitance of the electrode can be found. L. Yanan et.al. defines the capacitance as a body's ability to store electrical charge [14]. The capacitance is given in farad which is defined by the Bureau International des Poids et Mesures as the capacitance of a capacitor between the plates of which there appears a potential difference of 1 volt when it is charged by a quantity of electricity of 1 coulomb [15]. The capacitance is given by Equation (2.4).

$$C = \frac{dQ}{dE} \quad (2.4)$$

where  $C$  is the capacitance,  $Q$  is the charge and  $E$  is the potential. The current density is given by Equation (2.5).

$$i = \frac{dQ}{dt} \quad (2.5)$$

where  $t$  is the time. By Inserting  $dQ$  from Equation (2.5) into (2.4) gives the Equation (2.6).

$$C = \frac{i}{\frac{dE}{dt}} \quad (2.6)$$

Since the scan rate is given by the change of the potential divided by the change of the time. Equation (2.6) thereby becomes Equation (2.7).

$$C = \frac{i}{\nu} \quad (2.7)$$

where  $\nu$  is the scan rate.

## 2.3 RuO<sub>2</sub> kinetics

Ruthenium is an element that can occur in many oxidation states, which in turn gives the possibility of it forming different oxides. The total capacitance of the ruthenium oxide is mainly due to the pseudocapacitance, in addition to the usual double-layer capacitance [8]. Throughout the project report, the two ruthenium species that will be taken into account are RuO<sub>2</sub> and RuOOH. The equilibrium reaction between ruthenium oxide (RuO<sub>2</sub>) and ruthenium oxyhydroxide (RuOOH) is the cause of the pseudocapacitive abilities. The equilibrium reaction is given by Reaction (2.8).



Figure 2.7 shows the voltammogram of ruthenium and titanium in 0.5 M H<sub>2</sub>SO<sub>4</sub>. As can be seen, the voltammogram of ruthenium contains an anodic and a cathodic peak current,  $i_{pa}$  and  $i_{pc}$ . The anodic current generated is due to oxidation of RuOOH to RuO<sub>2</sub>. The cathodic current is in turn generated by reduction of RuO<sub>2</sub> to RuOOH. The mechanism behind the redox reaction is proton-electron couple transfer [8].

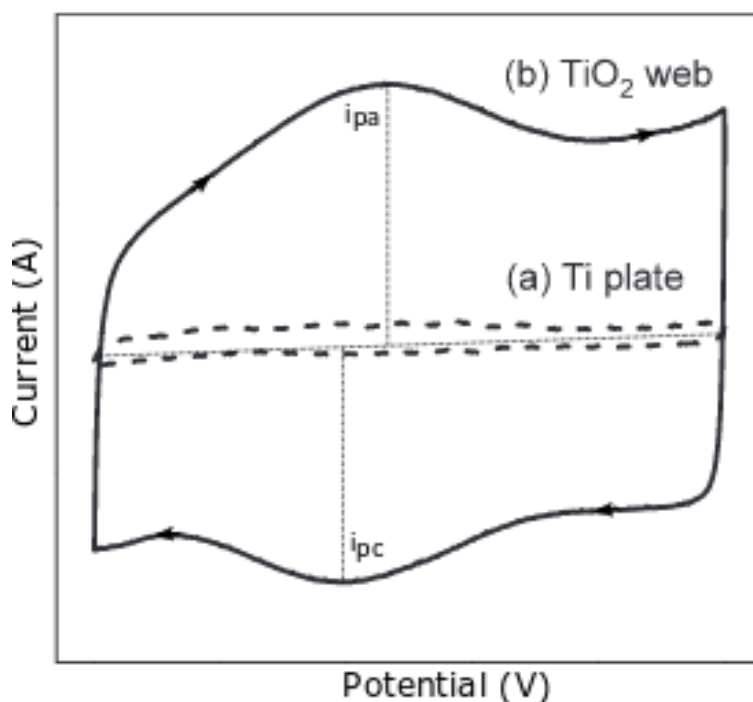


**Figure 2.7:** The voltammogram of (a) is for a titanium plate and (b) is for TiO<sub>2</sub> nanofibres coated with RuO<sub>2</sub> [19].

## 2.4 Electrochemical impedance spectroscopy

### 2.4.1 General theory

Electrochemical impedance spectroscopy is used to learn about the characteristics of electronic materials and electrochemical systems [16]. This section will address the general theory and its

application to determine the extent to which a reaction is surface limited. It will also address measurement models for analysis of impedance data.

When conducting an electrochemical impedance spectroscopy experiment, a constant potential is imposed on the cell. The potential experiences a frequency with an amplitude of, in this project, 5 mV. The frequency form a sinusoidal curve for the potential, which is given by

$$E_t = E_0 \sin(\omega t) \quad (2.9)$$

where  $E_t$  is the potential,  $E_0$  is the potential amplitude and  $\omega$  is the angular frequency. For a linear system, the frequency in the potential creates a response frequency for the current [10]. The response frequency form a sinusoidal curve as well, and can be written as

$$I_t = I_0 \sin(\omega t + \phi) \quad (2.10)$$

where  $I_t$  is the current,  $I_0$  is the current amplitude and  $\phi$  is the phase angle between the potential phasor and the current phasor. The relationship between the current phasor and the potential phasor is shown in Figure 2.8.

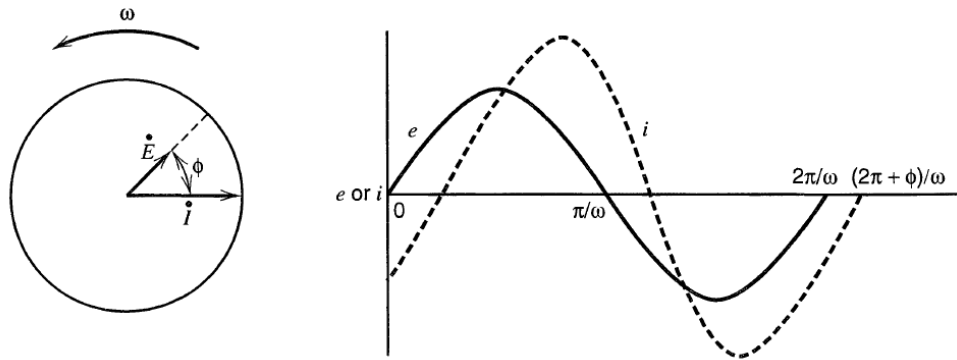


**Figure 2.8:** The phasor diagram shows the change and the relationship between the alternating current and potential. The phase angle between the alternating current and the potential is shown as  $\phi$  [2].

The impedance can be interpreted as a generalized resistance. Therefore an expression for the impedance can be written with Ohm's law

$$Z = \frac{E_t}{I_t} \quad (2.11)$$

where  $Z$  is the impedance. When inserting Equation (2.9) and (2.10) into Equation (2.11), gives the equation

$$Z = \frac{E_0 \sin(\omega t)}{I_0 \sin(\omega t + \phi)} = Z_0 \frac{\sin(\omega t)}{\sin(\omega t + \phi)} \quad (2.12)$$

With the euler's relationship of

$$\exp(j\phi) = \cos(\phi) + j \sin(\phi) \quad (2.13)$$

makes it possible to write the impedance as the complex form

$$Z = Z_0 \frac{\exp(j\omega t)}{\exp(j\omega t - \phi)} = Z_0 \exp(j\phi) = Z_0 [\cos(\phi) + j \sin(\phi)] \quad (2.14)$$

Figure 2.9 shows an example of an impedance vector diagram. Where the two vectors  $R$ , real and  $X_C$ , imaginary, creates the impedance vector,  $Z$  with the angle  $\phi$ .

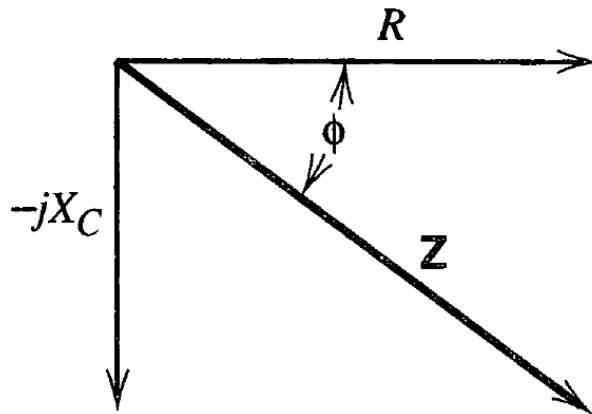


**Figure 2.9:** Vector diagram of the impedance, where  $R$  is the real component and  $X_C$  is the imaginary component.  $\phi$  is the phase angle between the impedance vector and the real vector [2].

## 2.4.2 Impedance of a capacitor

For a capacitor with its equivalent R-C circuit as shown in Figure 2.10, the impedance is written as

$$Z = R - \frac{j}{\omega C} \quad (2.15)$$

where  $R$  is the real part and  $\frac{j}{\omega C}$  is the imaginary part. Sinusoidal curves for the potential and the current for such a circuit, when performing EIS is shown in Figure 2.11(a). As can be seen from Equation (2.15), the real part is independent of the angular frequency. The real value will therefore be constant and the accompanying Nyquist plot for a capacitor is shown in Figure 2.11(b). Since the real part in the impedance for a capacitor does not change with different angular frequencies, the phase angle between the impedance vector and the real part is  $90^\circ$ . This can also be seen in the sinusoidal curves for the capacitor.

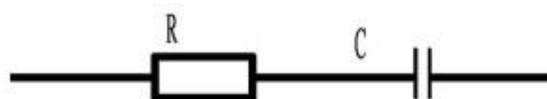


**Figure 2.10:** Illustrates an equivalent R-C circuit for a capacitor [10].

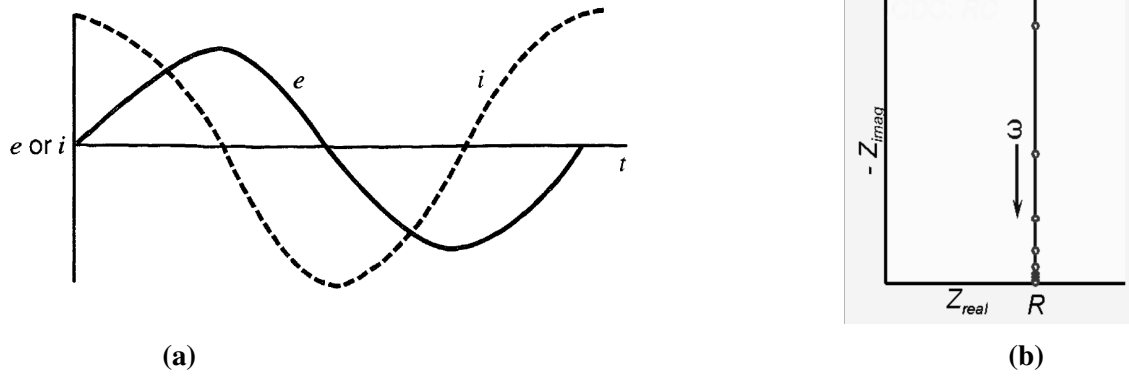


**Figure 2.11:** (a) Shows the sinusoidal curves for the potential and the current with a phase angle of  $90^\circ$  [2]. (b) Shows the Nyquist plot for a capacitor [3].

For a capacitor, the imaginary part of the impedance is given by

$$-Z_{imag} = \frac{V(\omega)}{I(\omega)} = \frac{1}{j\omega C} \quad (2.16)$$

By rewriting the equations, the capacitance is given by

$$C = \frac{1}{-Z_{imag}j\omega} \quad (2.17)$$

### 2.4.3 Constant phase element

Constant phase element, hereby denoted as CPE, corresponds to an equivalent circuit for a non-ideal capacitor [12]. The equivalent R-Q circuit for such an element is shown by Figure 2.12. The Nyquist plot for the R-Q circuit is shown by Figure 2.13, as a depressed semi-circle. The impedance for the R-Q circuit is given by

$$Z(\omega) = R + \frac{1}{Q(i\omega)^\alpha} \quad (2.18)$$

where the real part is given by

$$Z_{real} = R + \frac{\cos\left(\frac{\pi\alpha}{2}\right)}{Q\omega^\alpha} \quad (2.19)$$

and the imaginary part is given by

$$Z_{imag} = -\frac{\sin\left(\frac{\pi\alpha}{2}\right)}{Q\omega^\alpha} \quad (2.20)$$

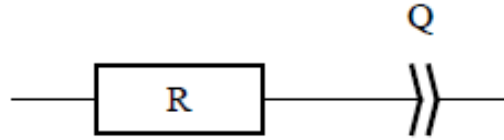


**Figure 2.12:** Illustrates the equivalent R-Q circuit of a CPE [12].

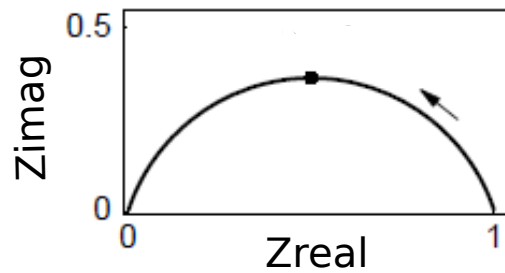


**Figure 2.13:** Nyquist plot of a R-Q circuit for a CPE.

#### 2.4.4 Warburg impedance

For a cell where the rate determine step is semi-infinte diffusion limited, has an equivalent  $R_{ct}$ -W circuit that is shown with Figure 2.14 [10].



**Figure 2.14:** Shows an equivalent  $R_{ct}$ -W circuit for Warburg impedance [4].

The Warburg impedance for such a circuit can be written as

$$Z = Z_0 [\omega^{-0.5} - j\omega^{-0.5}] \quad (2.21)$$

and  $Z_0$  is given by

$$Z_0 = \frac{RT}{(nF)^2 C^0 \sqrt{2D}} \quad (2.22)$$

where  $C^0$  is the bulk concentration [2] [3]. A Nyquist plot of the Warburg impedance is shown by Figure 2.15. The phase angle between the real part and the impedance is  $45^\circ$ .



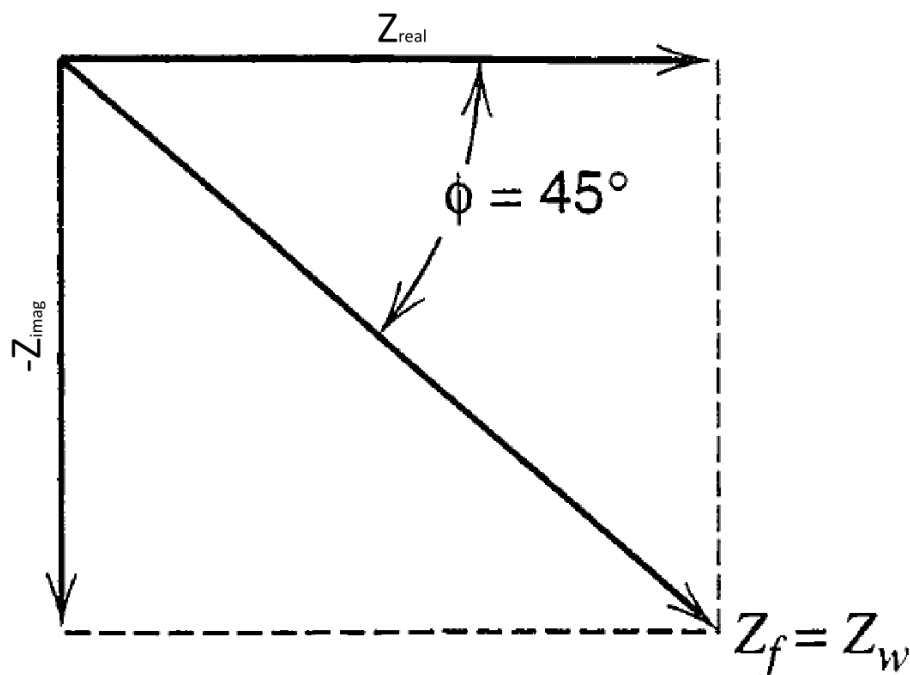


**Figure 2.15:** Shows a vector diagram of Warburg impedance. The phase angle between the real component vector and the impedance vector is  $45^\circ$  [2].

By comparing the impedance of a capacitor and for Warburg impedance, some conclusion regarding surface limited reactions can be made. An electrode with reactions that is not surface limited, but diffusion limited, will have a Nyquist plot where the phase angle is around  $45^\circ$ . However, an electrode where the reactions are completely surface limited, the electrode will have a phase angle between the impedance vector and the real component vector of  $90^\circ$ , as shown in Figure 2.11(b). Thus, by constructing a Nyquist plot from an electrochemical impedance spectroscopy measurement and checking the phase angle, an assessment of the extent to which the occurring reactions are surface limited or diffusion limited can be made.

### 2.4.5 Measurement models

Electrochemical impedance spectroscopy can also be used to determine if a system is stationary [16]. The Voight model, that uses electrical circuit analogue shown in Figure 2.16, has a corresponding impedance equation of

$$Z(\omega) = Z_0 + \sum_k \frac{\Delta_k}{1 + j\tau_k\omega} \quad (2.23)$$

which is consistent with the Kramers-Kronig relationship given by the Equations (2.24) and (2.25). By fitting the Voight model to the physical impedance data, the stationarity of the system can be evaluated. A good fit corresponds to a stationary system, which means that it is stable, causal and linear [16]. The above mentioned sub-sections about electrochemical impedance spectroscopy, addresses an assumed completely linear system. Having a good fit confirms that the system can be analyzed as linear, instead of non-linear, which is significantly harder [10].

$$Z_r(\omega) = Z_r(\infty) + \frac{2}{\pi} \int_0^\infty \frac{xZ_i(x) - \omega Z_i(\omega)}{x^2 - \omega^2} dx \quad (2.24)$$

$$Z_i(\omega) = -\frac{2\omega}{\pi} \int_0^\infty \frac{Z_r(x) - Z_r(\omega)}{x^2 - \omega^2} dx \quad (2.25)$$

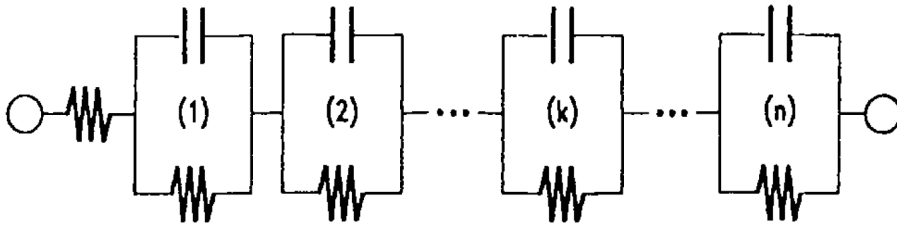


**Figure 2.16:** Illustrates the Voigt electrical circuit analogue with  $n$  number of elements [16].

# 3 Model

## 3.1 Transient model for bipolar electrolyser

The governing equation for the electrolyte is Poisson's equation

$$\nabla^2 \phi = \frac{\rho}{\epsilon} \quad (3.1)$$

where  $\rho$  is the charge density and  $\epsilon$  the dielectric constant of the solution. We assume electroneutrality ( $\rho = 0$ ), and

$$\nabla^2 \phi = 0 \quad (3.2)$$

where  $\phi$  is the potential in the electrolyte [13]. Suitable boundary conditions at electrode surfaces are

$$i = -\kappa \nabla \phi = -F\Gamma \frac{d\theta}{dt} \quad (3.3)$$

where  $i$  is the current density,  $\kappa$  the electrolyte conductivity,  $\Gamma$  to total number of redox-active sites in the catalytic layer,  $\theta$  the fraction of these that are in the reduced state, and  $t$  is the time. As initial conditions a certain value of  $\theta$  for each solid surface and  $\phi$  for each point in space may be assumed. Equation (3.2) is an elliptic partial differential equation.

We assume that the time derivative in Equation (3.4) can be related to the potential as

$$-\kappa \nabla \phi = -F\Gamma \frac{d\theta}{d\phi} \frac{d\phi}{dt} = K \frac{d\phi}{dt} \quad (3.4)$$

At membrane surfaces we assume that Ohm's law applies so that the boundary condition becomes

$$-\kappa \nabla \phi^k = j^k \quad (3.5)$$

where  $j^k$  is the current density in time-step  $k$  (not to be confused with the  $y$  coordinate index).

A numerical solution implies a discretization of the Equations (3.2) and (3.4)

$$\frac{\phi^k(i+1, j) - 2\phi^k(i, j) + \phi^k(i-1, j)}{(\Delta x)^2} + \frac{\phi^k(i, j+1) - 2\phi^k(i, j) + \phi^k(i, j-1)}{(\Delta y)^2} = 0 \quad (3.6)$$

For  $\Delta x = \Delta y$  this reduces to

$$4\phi^k(i, j) - \phi^k(i+1, j) - \phi^k(i-1, j) - \phi^k(i, j+1) - \phi^k(i, j-1) = 0 \quad (3.7)$$

For the boundary condition at the surface of an electrode for which Equation (3.4) applies (given below for the example in which the surface is placed at  $j = 1$ )

$$\frac{-3\phi^k(1, j) + 4\phi^k(2, j) - \phi^k(3, j)}{2\Delta x} = K \left[ \frac{\phi^k(1, j) - \phi^{k-1}(1, j)}{\kappa \Delta t} \right] \quad (3.8)$$

or

$$-3\phi^k(1, j) + 4\phi^k(2, j) - \phi^k(3, j) = \lambda [\phi^k(1, j) - \phi^{k-1}(1, j)] \quad (3.9)$$

where

$$\lambda = \frac{2K\Delta x}{\kappa\Delta t} \quad (3.10)$$

$k$  represents time and  $i, j$  a position in space. Equation (3.12) represents a three-point forward finite difference in space and a two-point forward difference in time. Other discretization schemes may of course also be used.

The boundary condition for inert surfaces is given by Equation (3.11)

$$-3\phi^k(1, j) + 4\phi^k(2, j) - \phi^k(3, j) = 0 \quad (3.11)$$

For the boundary condition at the surface of a membrane for which Equation (3.5) applies (given below for the example in which the surface is placed at  $j = 1$ )

$$\frac{-3\phi^k(1, j) + 4\phi^k(2, j) - \phi^k(3, j)}{2\Delta x} = -\frac{j^k}{\kappa} \quad (3.12)$$

or

$$-3\phi^k(1, j) + 4\phi^k(2, j) - \phi^k(3, j) = -\mu j^k \quad (3.13)$$

where

$$\mu = \frac{2\Delta x}{\kappa} \quad (3.14)$$

At insulating surfaces the current is zero, and so is therefore the potential. This gives another set of equations, for example

$$-3\phi^k(i, 1) + 4\phi^k(i, 2) - \phi^k(i, 3) = 0 \quad (3.15)$$

if the current is zero at the surface  $(i, 1)$ .

Equation (3.7) and the boundary conditions above give a set of linear equations to be solved for each time step  $k$ , for which the potentials for the previous time step  $\phi_{i,j}^{k-1}$  are known. The set may be represented by a sparse, partly banded, matrix for which solvers exist, e.g. in Matlab.

Note that the equations presented here only models the capacitive and ohmic processes. Potential differences caused by differences in chemical composition along the electrolyser will give significant and possibly even dominant contributions to the cell and stack potentials. However, we will argue below that such contributions can be simply included in the model, and that the model formulation above will give a good representation within the time frame relevant for diagnostics of the remaining lifetime of electrocatalytic layers at electrodes.

## 4 Simulation

The simulation was done with the `GeneratingMatrixCreepCurrentDynamicSimulation` Matlab code, attached in Appendix A. The code was written as the mayor part of this master thesis work. In short, the code builds up a 2-dimensional model of the bipolar cell system, with shunt currents going through the inlet headers. It dynamically simulates the discharge of the bipolar cell system with respect to the time. At the initial time, the code simulates the steady state of the bipolar cell system during operation. The 2d model displays the potential values, which in turn illustrates the current distribution throughout the bipolar cell system.

### 4.1 `GeneratingMatrixCreepCurrentDynamicSimulation`

The 2-dimensional model was based on the Figure 2.4. By placing theoretical nodes in the figure, where each nodes is given an  $i$  and  $j$  value, an equation setup based on Equations (3.7), (3.9), (3.11) and (3.13) can then be constructed. Figure 4.1 shows such a layout. The equation setup represents a discretized 2d model of the bipolar cell system. Due to the shunt currents of the system, Equation (3.13) has to be written as

$$-\phi^k(i-2, j) + 4\phi^k(i-1, j) - 6\phi^k(i, j) + 4\phi^k(i+1, j) - \phi^k(i+2, j) = 0 \quad (4.1)$$

This is because the current through the membrane is unknown, due to some of it going through the inlet headers.

The placement of the nodes, seen in Figure 4.1, determines which discretized equations that are applicable. The Equation (3.9) applies for nodes placed at the surface of an anode or a cathode. Equation (4.1) applies for nodes placed at the membrane surface. Equation (3.11) applies to nodes placed at inert surfaces. For nodes that are placed internally in the anodic chamber, cathodic chamber, the membrane and in the inlet tubes and headers, Equation (3.7) applies.

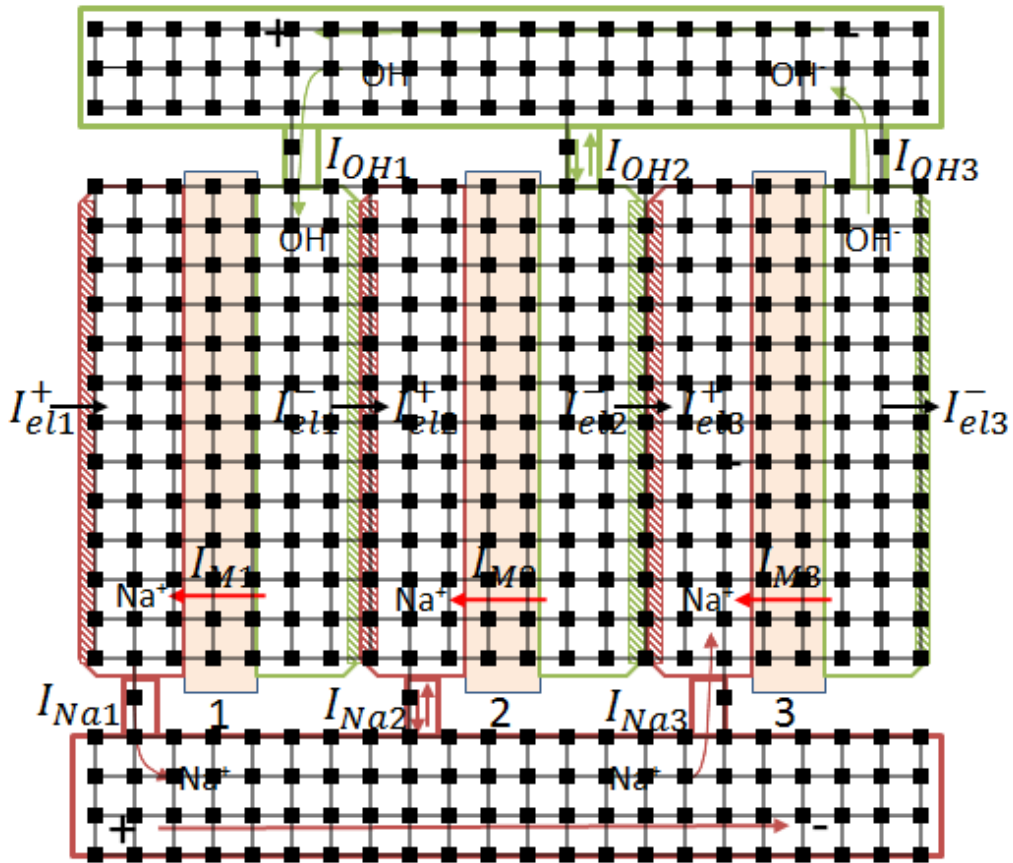


**Figure 4.1:** Nodes are placed in the 2- dimensional model of the bipolar cell system. Each node is connected to its neighboring node.

In order to build up the model, the written Matlab code goes through the node structure and recognizes what kind of placement the nodes are given, based on dimensional parameters. The code uses several for loops which goes through the  $i$  and  $j$  directions, and adds the corresponding discretized equation or equations to that node. The discretized equation sets are represented by a coefficient matrix,  $\mathbf{A}$  and the column vector  $\mathbf{b}$ . Because of the discretization of the Equations (3.1) and (3.2), the set of linear equations can be represented by

$$\mathbf{A} \cdot \mathbf{x} = \mathbf{b} \quad (4.2)$$

Where  $\mathbf{A}$  represents the coefficient matrix,  $\mathbf{b}$  represents column vectors and  $\mathbf{x}$  is the unknown. For the given model, the unknown  $\mathbf{x}$ -values represents the potential in the electrolyte at a given  $(i,j)$ -position.

Figure 4.2 shows an example of a generated coefficient matrix  $\mathbf{A}$ , done by GeneratingMatrixCreepCurrentDynamicSimulation code. Each blue dot represents a value in the given matrix. The matrix represents a small model with only three cells in a bipolar cell system. Figure 4.3 shows the corresponding column vector  $\mathbf{b}$ , where the blue dots represents a value in the given column vector. By dividing the column vector  $\mathbf{b}$ , with the coefficient matrix  $\mathbf{A}$ , the x-values are given. These x-values are shown by Figure 4.4. Where the x-axis represents the position of the value and the y-axis represents the potential value of the position.

By plotting the x-values with respect of the (i,j)-position, Figure 4.5 is given. The x-axis represents the i-position and the y-axis represents the j-position. The potential values of x are given by the z-axis. The middle "wave" in the figure, represents the bipolar cells with anodes, cathodes and membranes. The outer "waves" represents the inlet headers and its connections between the middle "wave", represents the inlet tubes to the anode and cathode compartment. The different parts of the cell system is indicated in Figure 4.5 in the same manner as that of Figure 2.4.

Figure 4.6 shows the flowchart as a diagrammatic representation of the algorithm in the GeneratingMatrixCreepCurrentDynamicSimulation code. The code uses inputs such as model dimensions, capacitance values and the size of the time iteration steps, as a way of defining the system. There are major limitations of the model dimensions, due to insufficient capacity of the processor and the RAM of a common computer. In order to do a full dimensional simulation, a supercomputer has to be used. The figure also indicates the different parts of the bipolar cell system, which could be compared Figure 2.4. Where an A indicates the placement of the anodes and a C indicates the placement of the cathodes. The membranes are indicated by a B. The cathodic inlet tubes are indicated by a D, and the cathodic header is indicated by an E. The anodic inlet tubes are indicated by a F and the anodic header is indicated by a G.

The capacitance values found by the EIS experiments are inserted into Equation (3.4). By definition, the capacitance is given by

$$C = \frac{dQ}{d\phi} \quad (4.3)$$

By multiplying with  $d\phi$  and dividing with  $dt$ , Equation (4.3) becomes

$$C \frac{d\phi}{dt} = \frac{dQ}{dt} = i \quad (4.4)$$

By combining Equation (4.4) with the equation

$$Q = \Gamma \theta F \quad (4.5)$$

gives the equation

$$C \frac{d\phi}{dt} = \Gamma F \frac{d\theta}{dt} \quad (4.6)$$

From the Equation (3.4) and (4.6), the constant,  $K$ , is thereby given as  $K = -C$ .

The conductance,  $\kappa$  of the anodic electrolyte, of 250 g/L NaCl and the cathodic electrolyte, of 30 % NaOH, are found to be approximately  $20.5344 \text{ Sm}^{-1}$  and  $32.25 \text{ Sm}^{-1}$  [9]. Thus the  $\lambda$  value from Equation (3.10), varies with the size of the time iteration step,  $\Delta t$ .



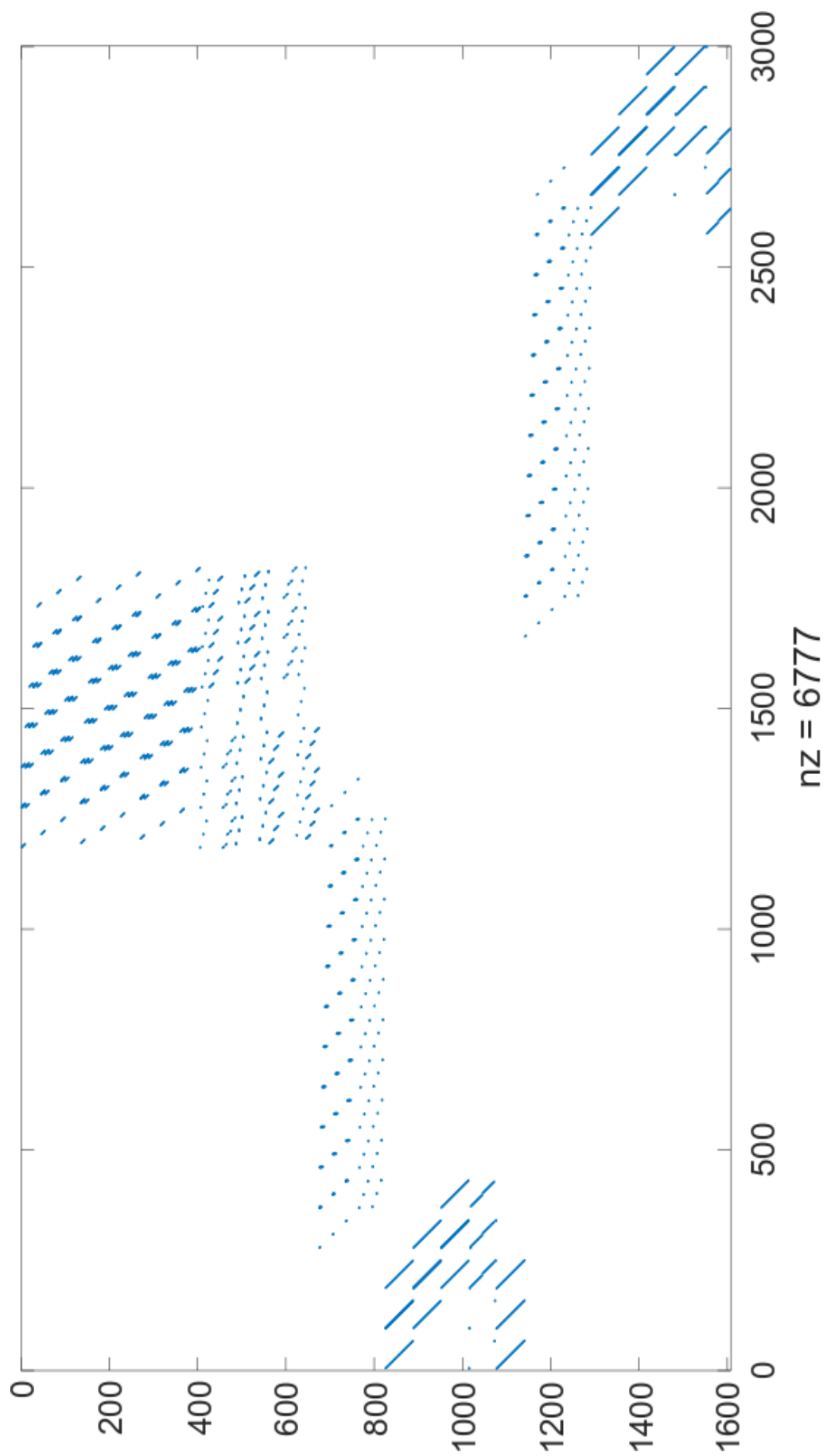


**Figure 4.2:** Coefficient matrix A. Each blue dot corresponds to a value in the matrix. The x-axis represents position and the y-axis represents the number of equations.



**Figure 4.3:** Column vector  $b$ . Each blue dot corresponds to a value in the column. The y-axis represents the number of equations.

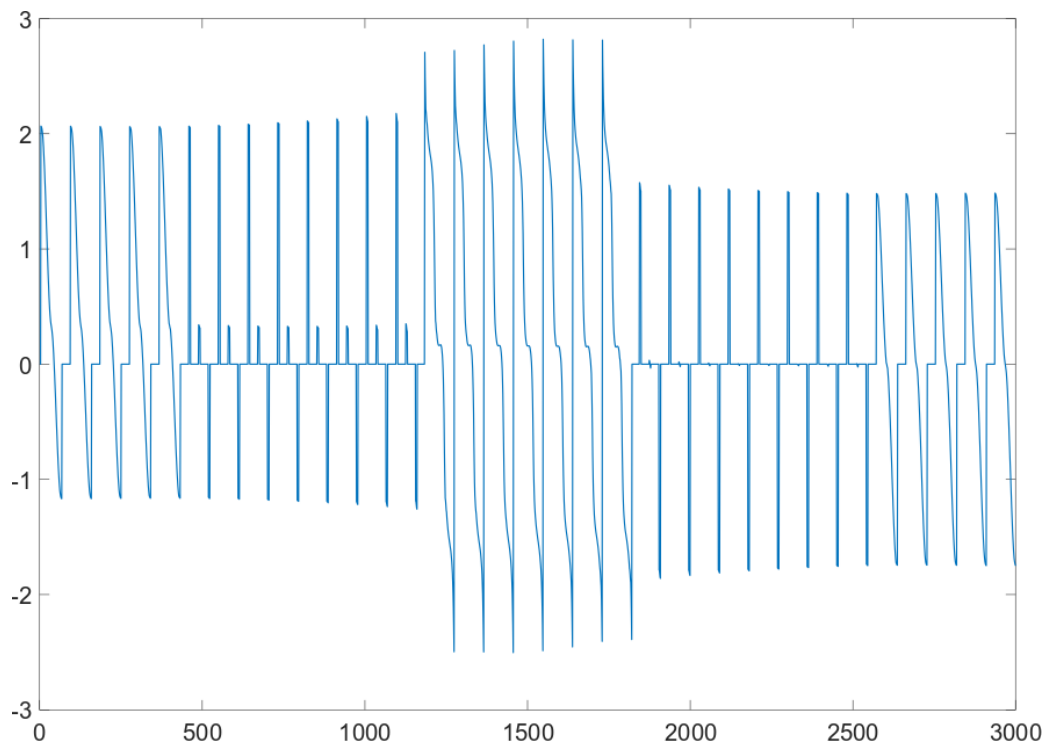


**Figure 4.4:** The x-values are given as potentials values. The x-axis represents the position of the x-value and the y-axis represents its value.

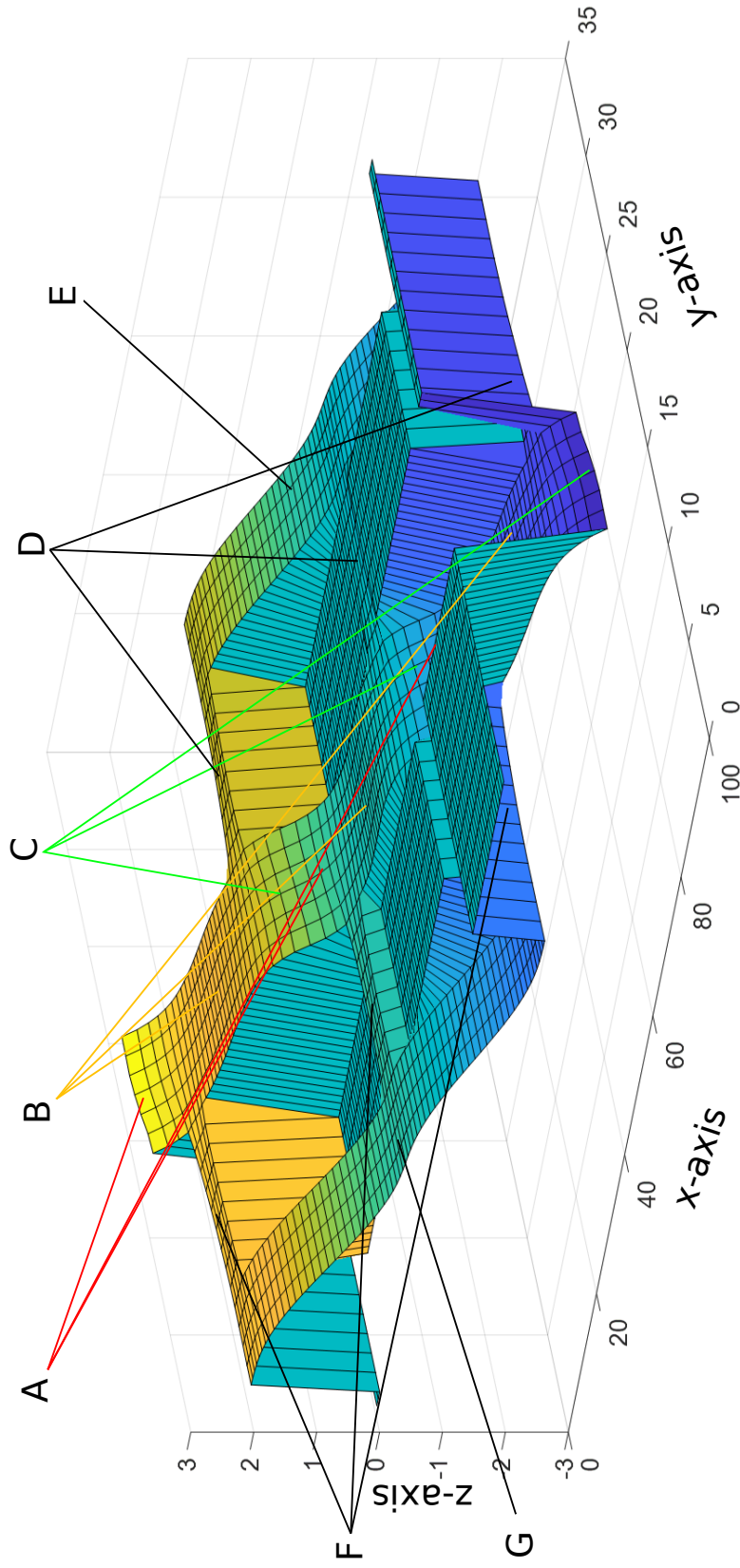


**Figure 4.5:** The figure shows the potential throughout the bipolar cell system with shunt currents. The x-axis, as with this case seen as the axis with values from zero to 100, represents the i-position. The y-axis, as with this case seen as the axis with values from zero to 35, represents the j-position. The vertical z-axis, represents the potential values to the given positions.

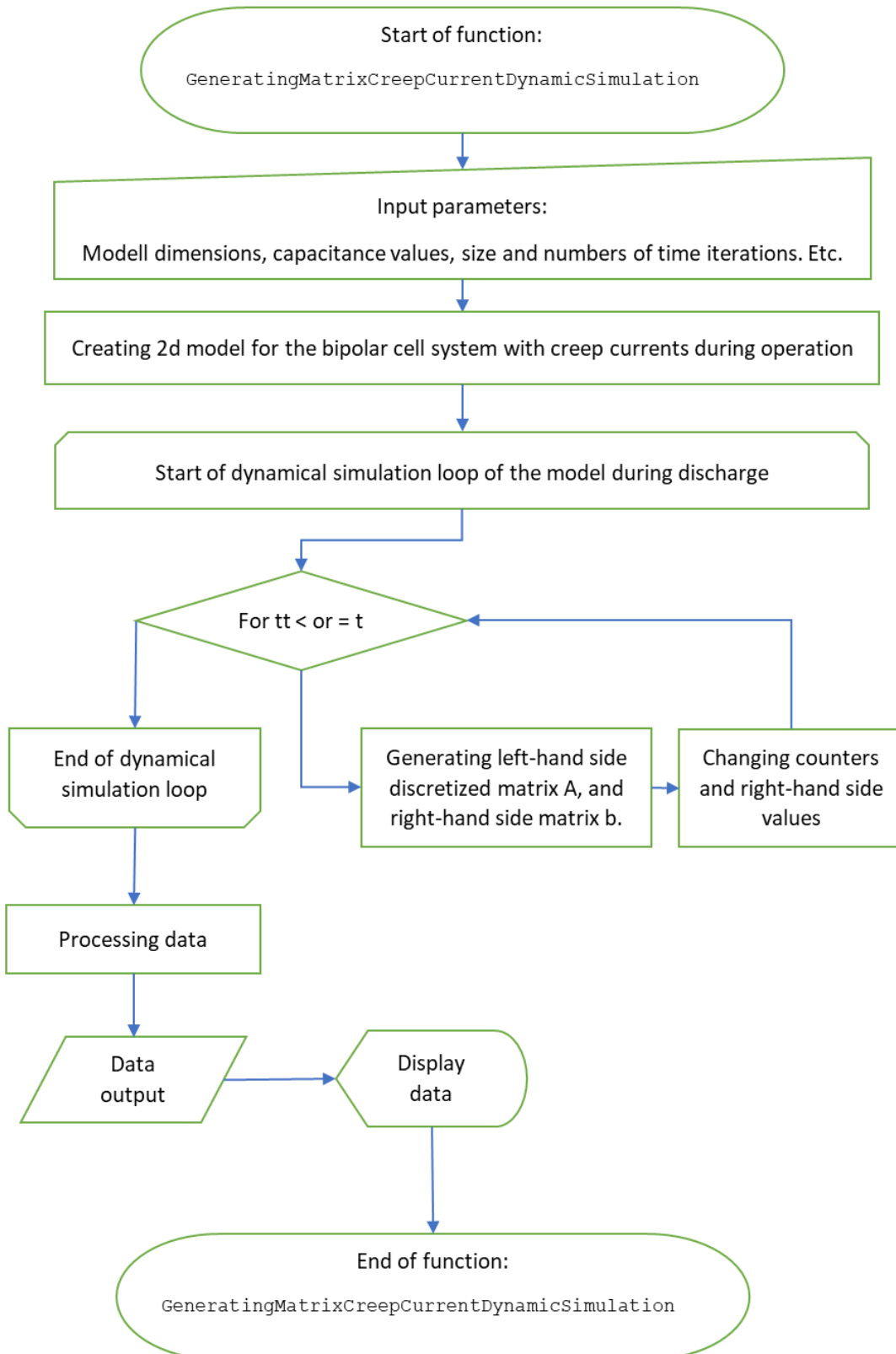


**Figure 4.6:** The figure shows the flowchart of the `GeneratingMatrixCreepCurrentDynamicSimulation` code.

## 5 Experimental

The experimental work consisted of cyclic voltammetry and electrochemical impedance spectroscopy. An air-tight three-electrode-setup configuration for a half cell was used to carry out the experiments. Such a setup is shown by Figure 5.1. In addition, the three-electrode-setup had one inlet tube and one outlet tube for nitrogen purging. The inlet tube could be lowered or raised in order to purge oxygen from the electrolyte and the space above it. The end of the outlet tube was placed in a cylinder containing water to measure the nitrogen overpressure. A platinum plate was used as the counter electrode and an Ag/AgCl reference electrode was used as the reference electrode. For the experiments with the anode as working electrode, a solution of 250 g/L NaCl with a pH of 11 was used as the electrolyte. For the experiments with the cathode as working electrode, a solution of 30% NaOH was used as the electrolyte. The Autolab PGSTAT30 with the associated NOVA 2.0 software was used as the potentiostat.

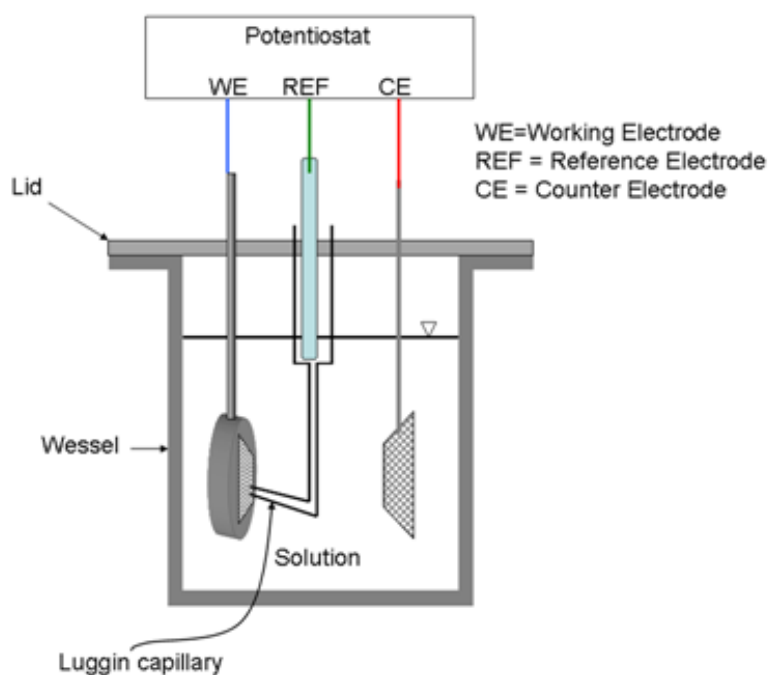


**Figure 5.1:** Three-electrode-setup for a half-cell that was used in the experiments.

## 5.1 Electrodes

The anode and the cathode that were used in the experiments are of the same commercial type that is used in the chlor-alkali industry. The commercial anode has a mesh structure and is made of titanium, with a coating of TiO, RuO<sub>2</sub> and IrO<sub>2</sub>. The commercial cathode also has a mesh structure and is made of nickel, with a coating of NiO<sub>2</sub> and RuO<sub>2</sub>. In order to measure the state of the electrodes, a positive material identification, hereby denoted as PMI, was used. The PMI uses X-ray fluorescence (XFR) to identify the composition of a metal or an alloy. The PMI measurements gave a percentage value of Ru from a pre-set standard of Ru content in the coating. A value of 100 % is the equivalent of that of a new anode. The results from the PMI measurements of the anode and the cathode, that were used in the experiments, are shown in Table 5.1.

Electrodes	PMI (%)
Anode	102.8
Cathode	114.1

**Table 5.1:** The PMI value of the anode and the cathode from a pre-set value of Ru content in the coating.

In order to make the electrode samples, small parts from the anode mesh and the cathode mesh were sawed-off. The small anode parts were spot welded to a titanium wire and the small cathode parts were spot welded to a nickel wire. The spot welding resulted in damaged areas on the electrodes. To make these areas inert, apiezon wax was soldered on to the electrodes. Before the experiments commenced, the anode was driven with chlorine development and the cathode was driven with hydrogen development, for two hours. This was done to make sure that the oxide composition in the coatings were normal.

## 5.2 Cyclic voltammetry

Cyclic voltammetry, hereby denoted as CV, was used to determine which potential range the electrochemical impedance spectroscopy experiments could be run within. The results from the CV is shown in Figure 6.1 and Figure 6.2.

The CV experiment with the anode as the working electrode used a platinum electrode as the counter electrode and an Ag/AgCl reference electrode as the reference electrode. The electrolyte consisted of 250 g/L NaCl, with a pH of 11. Before the experiment, the electrolyte was purged with nitrogen for ten minutes. The inlet tube was then raised to purge the space above it throughout the experiment. The CV was run with a series of five cycles. The scan rate was 100 mV/s and the potential range was between  $-0.6$  V vs. Ag/AgCl and  $0.8$  V vs. Ag/AgCl.

The CV experiment with the cathode as working electrode used a platinum electrode as the counter electrode and an Ag/AgCl reference electrode as the reference electrode. The electrolyte consisted of 30 % NaOH. Before the experiment, the electrolyte was purged with nitrogen for ten minutes. The inlet tube was then raised to purge the space above it throughout the experiment. The CV was run with a series of five cycles. The scan rate was 100 mV/s and the potential range was between  $-1.05$  V vs. Ag/AgCl and  $-0.1$  V vs. Ag/AgCl.

## 5.3 Electrochemical impedance spectroscopy

Electrochemical impedance spectroscopy, hereby denoted as EIS, was used in order to find the capacitance of the anode and the cathode. The results are shown in Section 6.2.

The EIS experiment with the anode as the working electrode used a platinum electrode as the counter electrode and an Ag/AgCl reference electrode as the reference electrode. The electrolyte consisted of 250 g/L NaCl, with a pH of 11. Before the experiment, the electrolyte was purged with nitrogen for ten minutes. The inlet tube was then raised to purge the space above it throughout the experiment. A magnetic stirrer was also used during the pre-experimental purging and during the execution of the experiment. The frequency range of EIS was from  $1 \cdot 10^5$  to 0.1 Hz and had an amplitude of 5 mV. The EIS was run with five different potentials of  $-0.2$ , 0, 0.2, 0.4 and 0.6 V vs. Ag/AgCl, where each potentials was held for 5 minutes before commencing and during the experiment. The results from the EIS experiment with the held potential of 0.2 V vs. Ag/AgCl, was used further on to find the capacitance.

The EIS experiment with the cathode as the working electrode used a platinum electrode as the counter electrode and an Ag/AgCl reference electrode as the reference electrode. The electrolyte consisted of 30 % NaOH. Before the experiment, the electrolyte was purged with nitrogen for ten minutes. The inlet tube was then raised to purge the space above it throughout the experiment. A magnetic stirrer was also used during the pre-experimental purging and during the execution of the experiment. The frequency range of EIS was from  $1 \cdot 10^5$  to 0.05 Hz and had an amplitude of 5 mV. The EIS was run with four different potentials of  $-0.8$ ,  $-0.6$ ,  $-0.4$  and  $-0.2$  V vs. Ag/AgCl, where each potentials was held for 5 minutes before the commencing and during the experiment. The results from the EIS experiment with the held potential of  $-0.4$  V vs. Ag/AgCl, was used further on to find the capacitance.



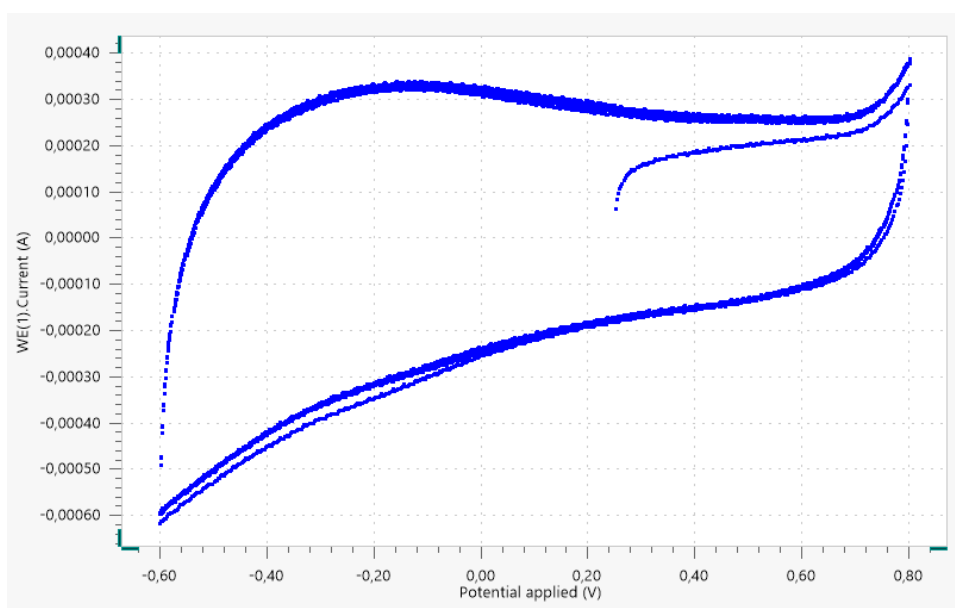


# 6 Results

## 6.1 Experimental work

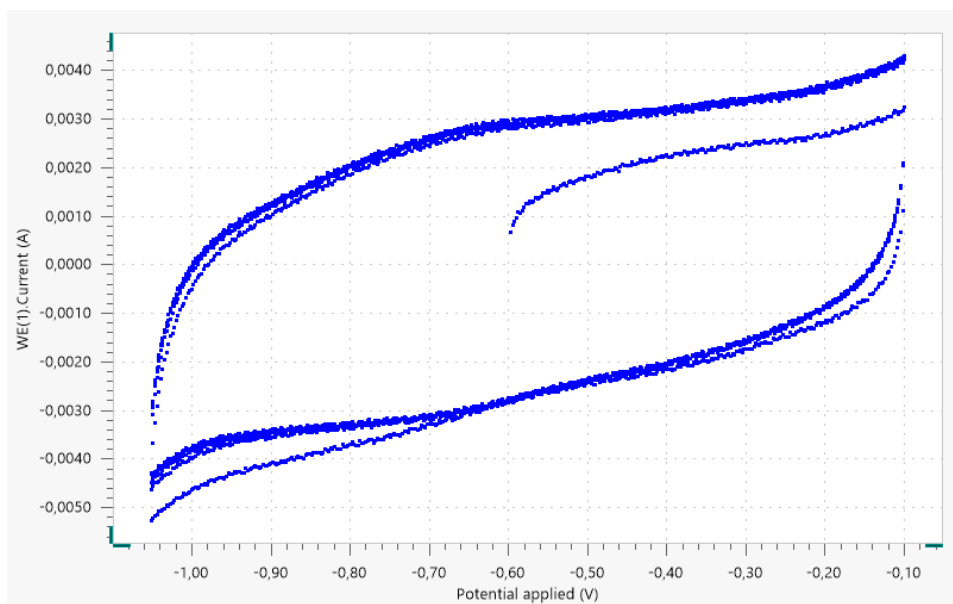
### 6.1.1 Cyclic voltammetry

Figure 6.1 shows the voltammogram of the anode sample. The experiment was done with a scan rate of 100 mV/s. The electrolyte consisted of 250 g/L NaCl, with a pH of 11. The cell was purged with nitrogen before and during the experiment. The potential range was between -0.6 and 0.8 V vs. Ag/AgCl. From the voltammogram, it was decided that the EIS experiment for the anode could be run with the potentials of -0.2, 0, 0.2 and 0.6 V vs. Ag/AgCl.



**Figure 6.1:** Cyclic voltammogram of the anode sample in 250 g/L NaCl and with a pH of 11. The x-axis shows the potential in V vs. Ag/AgCl and the y-axis shows the current (A).

Figure 6.2 shows the voltammogram of the cathode sample. The experiment was done with a scan rate of 100 mV/s. The electrolyte consisted of 30 % NaOH. The cell was purged with nitrogen before and during the experiment. The potential range was between -1.05 and -0.1 V vs. Ag/AgCl. From the voltammogram, it was decided that the EIS experiment for the cathode could be run with the potentials of -0.8, -0.6, -0.4, and -0.2 V vs. Ag/AgCl.



**Figure 6.2:** Cyclic voltammogram of the cathode sample in 30 % NaOH. The x-axis shows the potential in V vs. Ag/AgCl and the y-axis shows the current (A).

## 6.2 Electrochemical impedance spectroscopy

### 6.2.1 Anode sample

Figures 6.3 and 6.4, show the complex impedance plane plot, normally called a Nyquist plot, for the anode sample. Figure 6.5 shows its corresponding Bode plot and Figure 6.6 shows the real and imaginary error at the given frequency. The EIS experiment to which these data belongs to was conducted with a potential of 0.2 V vs. Ag/AgCl and with an amplitude of 5 mV. The frequency varied from  $1 \times 10^5$  to 0.1 Hz. The electrolyte consisted of 250 g/L NaCl, with a pH of 11.

The red data points in the Figures 6.3, 6.4 and 6.5, are the physical impedance data, while the blue data points is the simulated ones. As can be seen, there is a good fit between the simulation and the physical data. For the simulation, a Voight electrical circuit analogue for CPE, with two Voight elements as shown in Figure 2.16, were used.

As can be seen from Figure 6.3, the real component of the impedance changes little, with respect to the frequency, compared to the imaginary component. The complex impedance plane plot is therefore quite similar to that of a capacitor. Figure 6.4 shows the enlargement of the area at around 1 to 4.5 for the real component of the impedance and -0.5 to 2 for the imaginary part of the impedance. The complex impedance plane plot of this area shows similarities with Nyquist plots of a CPE, shown by Figure 2.13.

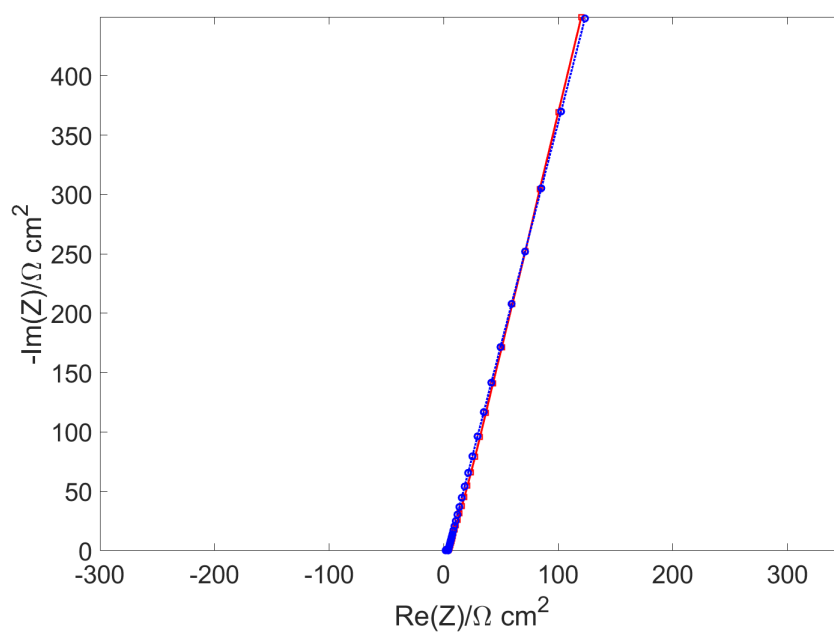


**Figure 6.3:** Complex impedance plane plot of the anode sample done with a potential of 0.2 V vs. Ag/AgCl. The electrolyte consisted of 250 g/L NaCl, with a pH of 11.

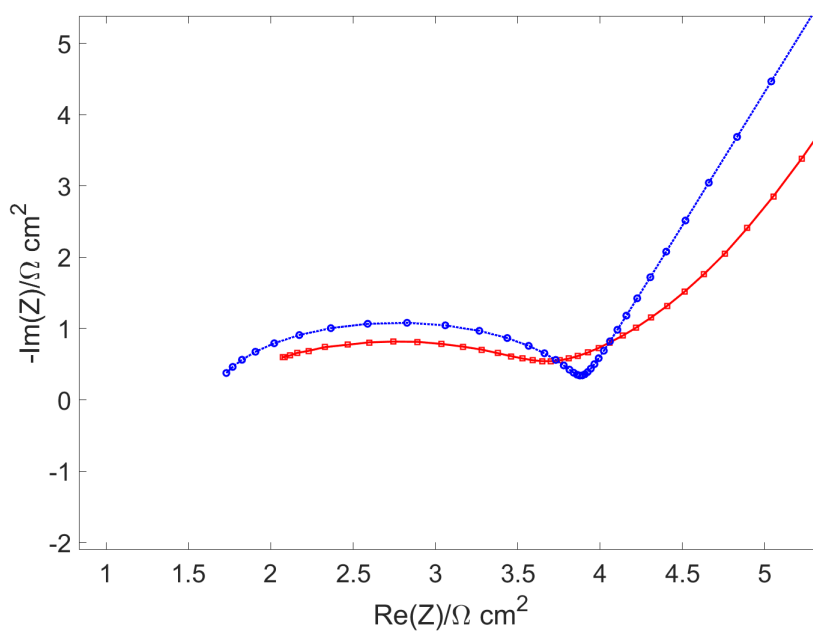


**Figure 6.4:** Enlarged area of the complex impedance plane plot of the anode sample, shown by Figure 6.3.

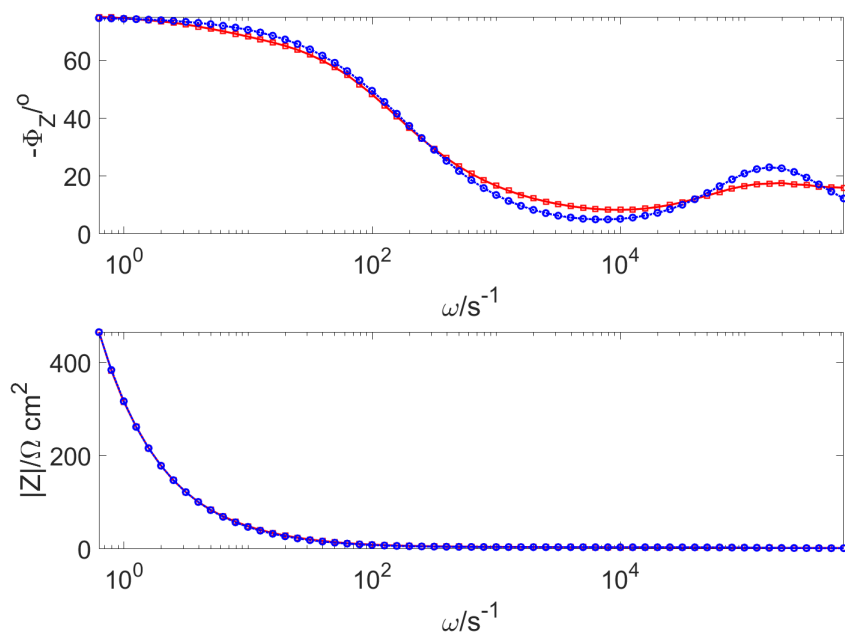


**Figure 6.5:** Bode plot of the anode sample done with a potential of 0.2 V vs. Ag/AgCl. The electrolyte consisted of 250 g/L NaCl, with a pH of 11.

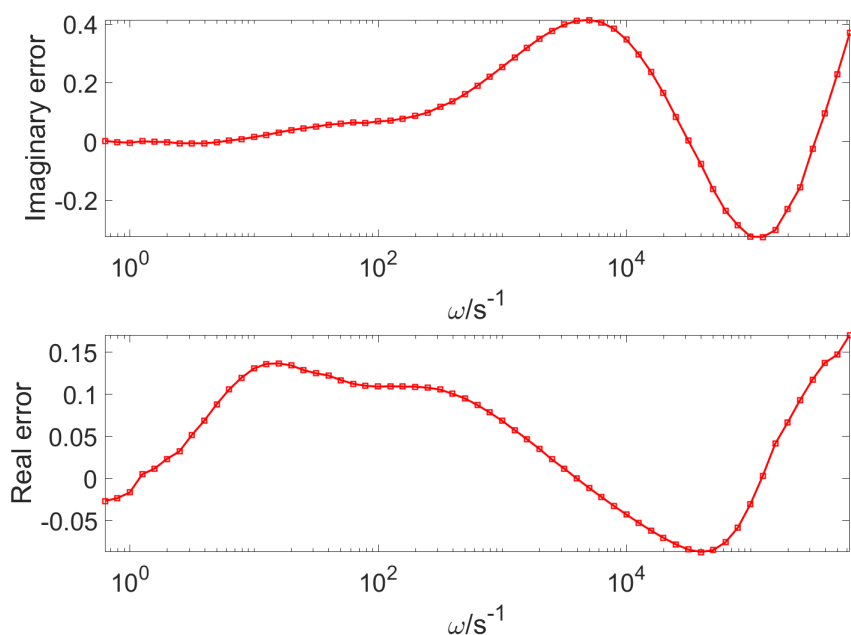


**Figure 6.6:** The upper plot shows the imaginary component error and the lower plot shows the real component error, with respect to the frequency. The plots corresponds to the EIS data, shown by Figure 6.3 for the complex impedance plane plot and Figure 6.5 for the Bode plot.

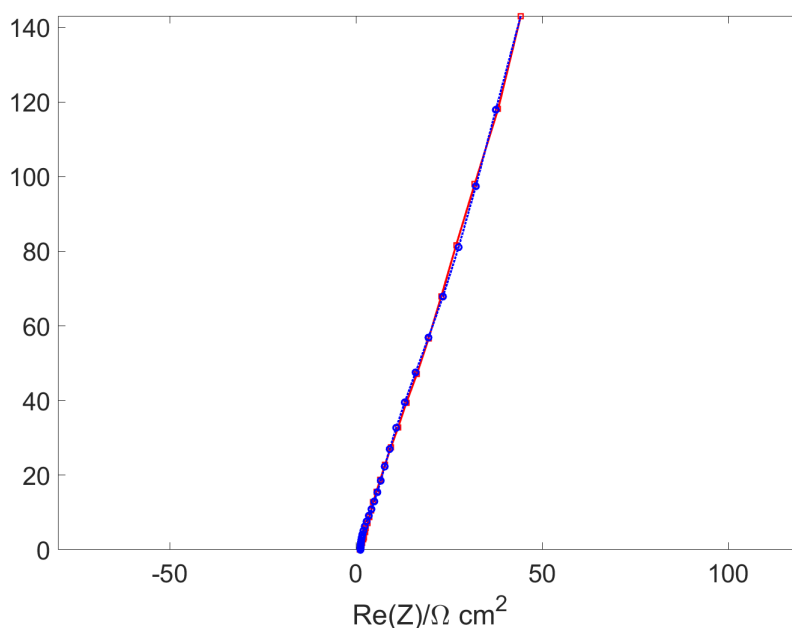
Assuming that the anode possesses the properties of a capacitor, the capacitance could be calculated by Equation 2.17. From the EIS experiment, it was found that the capacitance of the anode sample was around  $3.54 \times 10^{-3}$  F. The impedance data points from the area where the

anode sample showed the properties to that of a CPE, where ignored during the calculation.

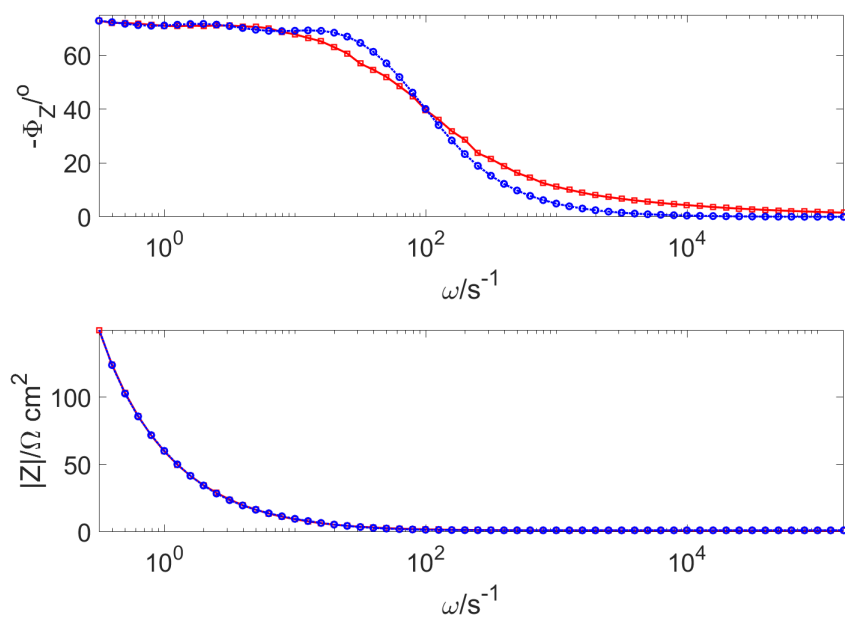
### 6.2.2 Cathode sample

Figure 6.7 shows the complex impedance plane plot, normally called Nyquist plot, for the cathode sample. Figure 6.8 shows its corresponding Bode plot and Figure 6.9 shows the real and imaginary error at the given frequency. The EIS experiment to which these data belongs to, was conducted with a potential of  $-0.4$  V vs. Ag/AgCl and with an amplitude of 5 mV. The frequency varied from  $1 * 10^5$  to 0.05 Hz. The electrolyte consisted of 30 % NaOH.

The red data points in the Figures 6.7 and 6.8, are the physical impedance data, while the blue data points is the simulated ones. As can be seen, there is a good fit between the simulation and the physical data. For the simulation, a Voight electrical circuit analogue with three Voight elements as shown in Figure 2.16, were used. As can be seen from Figure 6.7, the real component of the impedance changes little with respect to the frequency, compared to the imaginary component. The complex impedance plane plot is therefore quite similar to that of a capacitor.



**Figure 6.7:** Complex impedance plane plot of the cathode sample done with a potential of  $-0.4$  V vs. Ag/AgCl. The electrolyte consisted of 30 % NaOH.



**Figure 6.8:** Bode plot of the cathode sample done with a potential of -0.4 V vs. Ag/AgCl. The electrolyte consisted of 30 % NaOH.

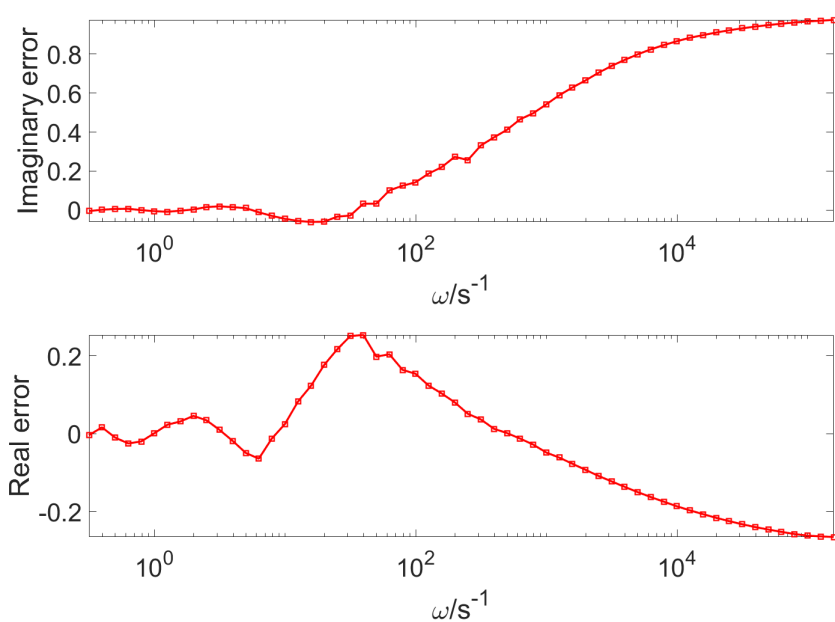


**Figure 6.9:** The upper plot shows the imaginary component error and the lower plot shows the real component error, with respect to the frequency. The plots corresponds to the EIS data, shown by Figure 6.7 for the complex impedance plane plot and Figure 6.8 for the Bode plot.

Assuming that the cathode possesses the properties of a capacitor, the capacitance could be calculated by Equation (2.17). From the EIS experiment, it was found that the capacitance of the anode sample was around 0.022 F.

## 6.3 Simulations

### 6.3.1 During operation

The initial condition of the dynamical simulation of the bipolar cell system discharge, shows the model under steady-state operation. The dynamical simulations were done by the `GeneratingMatrixCreepCurrentDynamicSimulation` code, written in Matlab as the mayor part of the master thesis work. Figures 6.10 and 6.11 show the potentials throughout the bipolar cell system, inlet tubes and headers, during operation. The cell system is compiled by seven membrane cells. The difference between these two models are that the anodic and cathodic inlet tubes are five times longer than in Figure 6.11 then for Figure 6.10.

The simulation, shown by Figure 6.10, has a potential drop of 25.21 V through the bipolar cell system. The potential drops through the anodic header and the cathodic header are respectively 21.13 V and 21.13 V. The simulation, shown by Figure 6.11, has a potential drop of 27.57 V through the bipolar cell system. The potential drops through the anodic header and the cathodic header are respectively 15.14 V and 15.14 V. By increasing the anodic and cathodic inlet tubes by five times, the potential drop through the cell system increases by 2.36 V, and the potential drops through the headers decreases by 5.99 V.

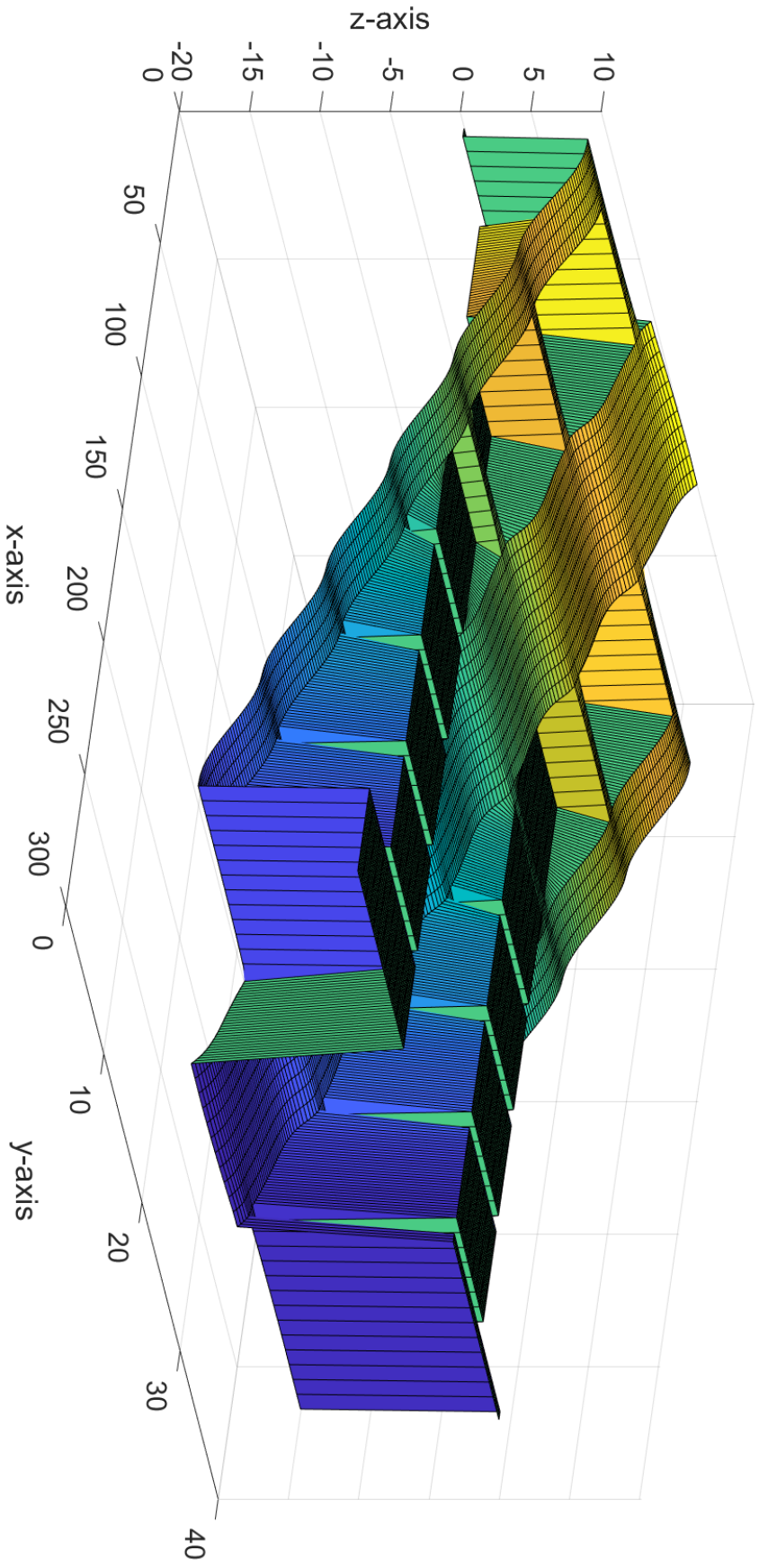


**Figure 6.10:** The figure shows the potential throughout the bipolar cell system with shunt currents, for a compilation of seven membrane cells. The x-axis represents the  $i$ -position. The y-axis represents the  $j$ -position. The vertical z-axis, represents the potential values to the given position.



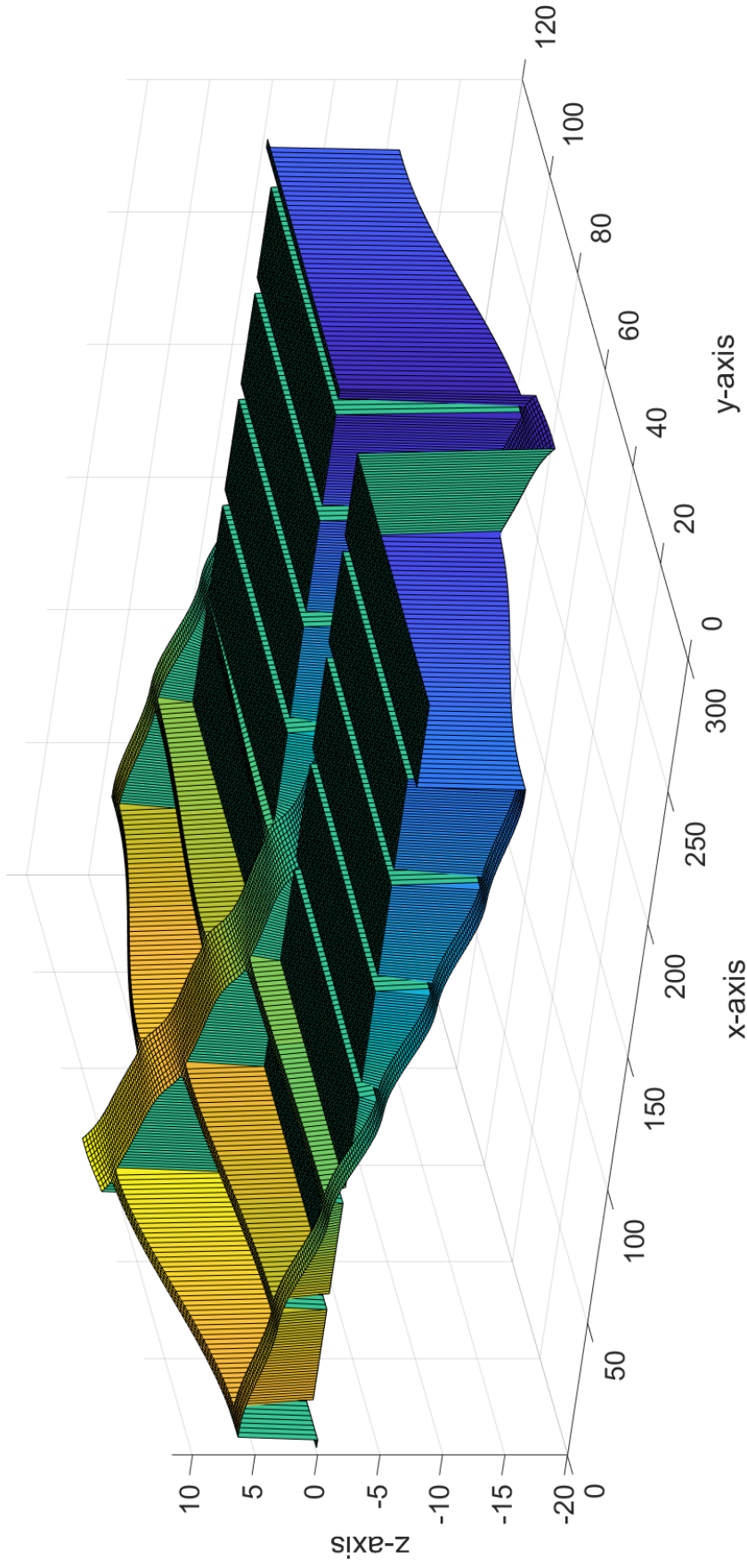


**Figure 6.11:** The figure shows the potential throughout the bipolar cell system with shunt currents, for a compilation of seven membrane cells. The x-axis represents the i-position. The y-axis represents the j-position. The vertical z-axis, represents the potential values to the given position.

### 6.3.2 Discharge by variations of shunt currents

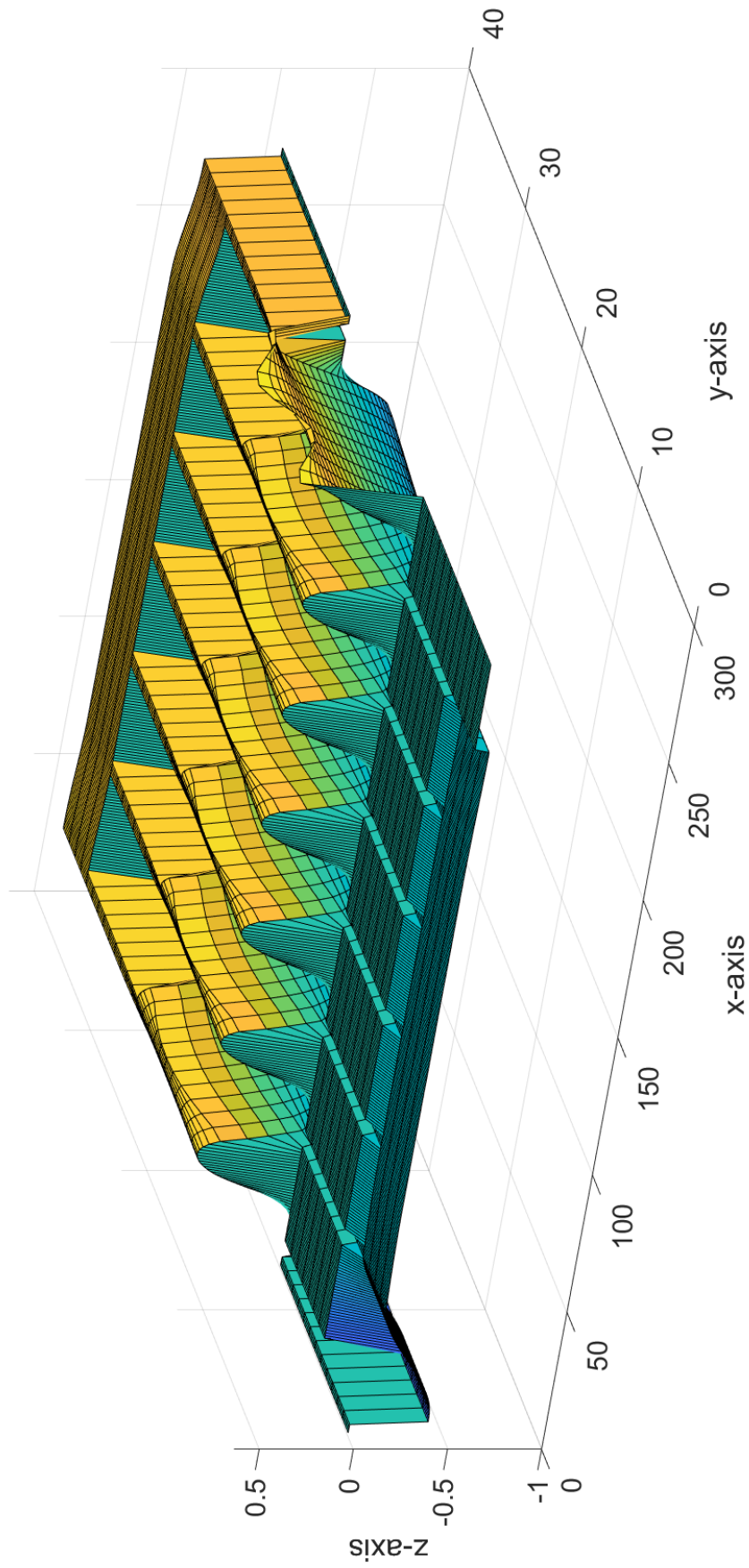
Figures 6.12, 6.13, 6.14, 6.15 and Figures 6.16, 6.17, 6.18, 6.19, shows the discharge simulation of the bipolar cell system with shunt currents for different time intervals. The simulation done in Figures 6.16 to 6.19 have three times longer anodic and cathodic inlet tubes, than for Figures 6.12 to 6.15. The time iteration steps,  $\Delta t$ , are respectively 0.001, 0.01, 0.1 and 1.

Figure 6.12 and 6.16 shows the simulation with the time iteration step 0.001. The simulation for Figure 6.16 have three times longer anodic and cathodic inlet tube length than Figure 6.12. From Figure 6.12 it can be seen that the bipolar cell system experiences a potential drop of 1.337 V. The potential drop through the anodic header and the cathodic header are respectively 0.337 V and 0.0888 V. From Figure 6.16, it can be seen that the potential drop through the bipolar cell system is 1.339 V. The potential drop through the anodic and cathodic headers are respectively 0.219 V and 0.065 V.

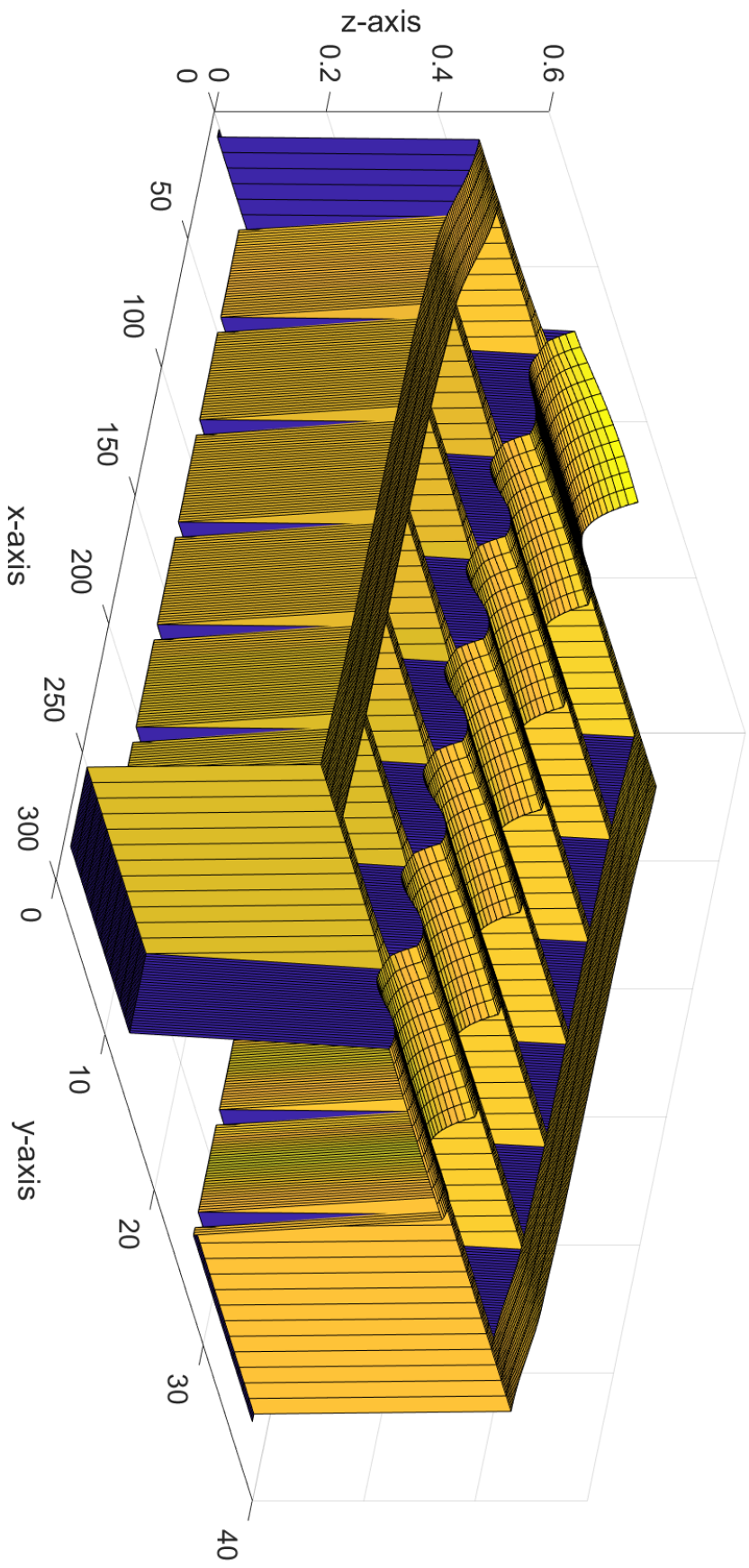
Figure 6.13 and 6.17 shows the simulation with the time iteration step 0.01. The simulation for Figure 6.17 have three times longer anodic and cathodic inlet tube length than Figure 6.13. From Figure 6.13 it can be seen that the bipolar cell system experiences a potential drop of 0.0841 V. The potential drop through the anodic header and the cathodic header are respectively 0.0521 V and 0.0181 V. From Figure 6.17, it can be seen that the potential drop through the bipolar cell system is 0.0879 V. The potential drop through the anodic and cathodic headers are respectively 0.0399 V and 0.0225 V.

Figure 6.14 and 6.18 shows the simulation with the time iteration step 0.1. The simulation for Figure 6.18 have three times longer anodic and cathodic inlet tube length than Figure 6.14. From Figure 6.14 it can be seen that the bipolar cell system experiences a potential drop of 0.0932 V. The potential drop through the anodic header and the cathodic header are respectively 0.0747 V and 0.076 V. From Figure 6.18, it can be seen that the potential drop through the bipolar cell system is 0.0961 V. The potential drop through the anodic and cathodic headers are respectively 0.0672 V and 0.0686 V.

Figure 6.15 and 6.19 shows the simulation with the time iteration step 1. The simulation for Figure 6.19 have three times longer anodic and cathodic inlet tube length than Figure 6.15. From Figure 6.15 it can be seen that the bipolar cell system experiences a potential drop of 0.0102 V. The potential drop through the anodic header and the cathodic header are respectively  $8.5 \times 10^{-3}$  V and  $8.5 \times 10^{-3}$  V. From Figure 6.19, it can be seen that the potential drop through the bipolar cell system is 0.0105 V. The potential drop through the anodic and cathodic headers are respectively  $7.6 \times 10^{-3}$  V and  $7.7 \times 10^{-3}$  V.



**Figure 6.12:** The figure shows the potentials throughout the bipolar cell system with shunt currents, for a compilation of seven membrane cells. The discharge simulation was done with the time iteration step of 0.001. The x-axis represents the i-position. The y-axis represents the j-position. The vertical z-axis, represents the potential values to the given position.



**Figure 6.13:** The figure shows the potentials throughout the bipolar cell system with shunt currents, for a compilation of seven membrane cells. The discharge simulation was done with the time iteration step of 0.01. The x-axis represents the i-position. The y-axis represents the j-position. The vertical z-axis, represents the potential values to the given position.

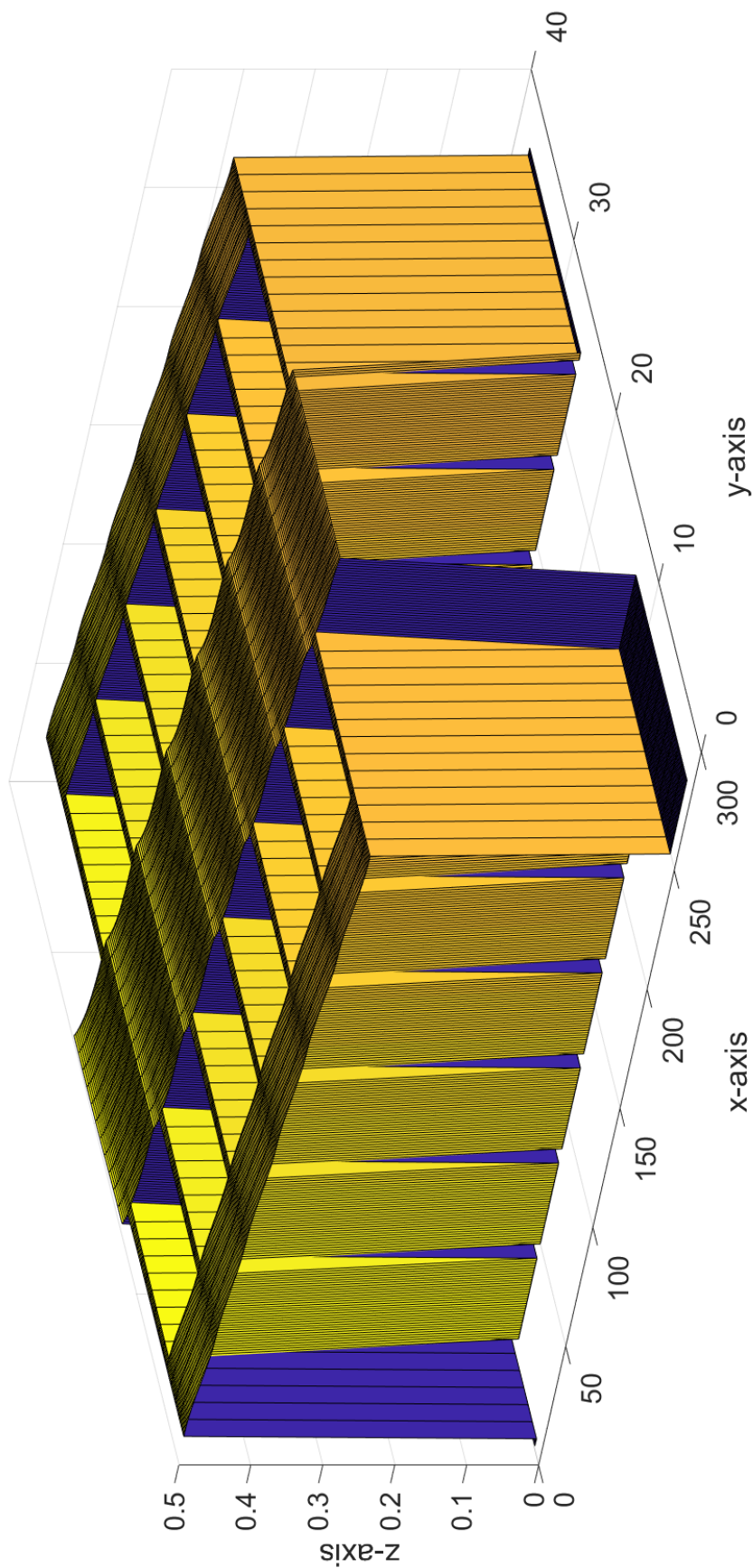


**Figure 6.14:** The figure shows the potentials throughout the bipolar cell system with shunt currents, for a compilation of seven membrane cells. The discharge simulation was done with the time iteration step of 0.1. The x-axis represents the i-position. The y-axis represents the j-position. The vertical z-axis, represents the potential values to the given position.

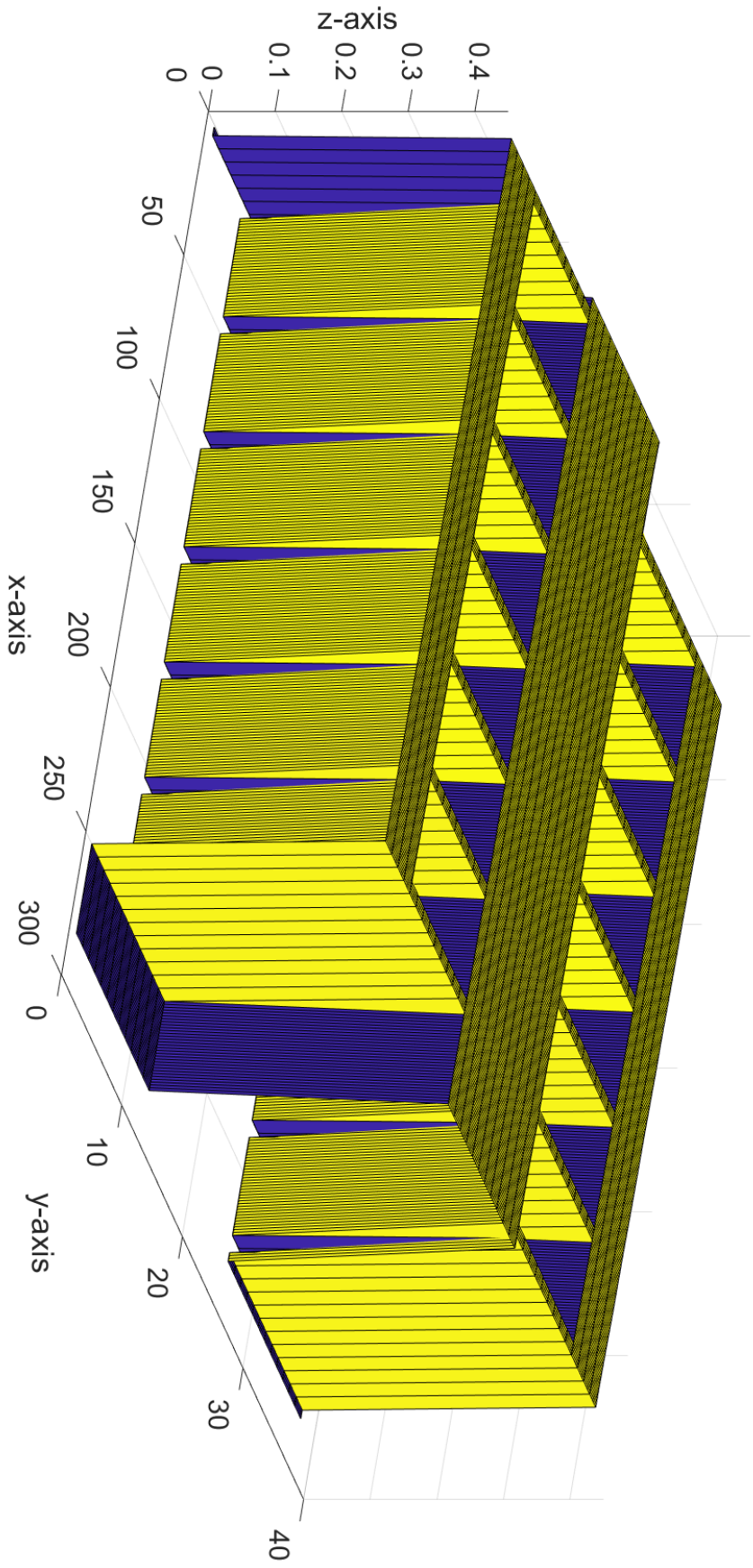


**Figure 6.15:** The figure shows the potentials throughout the bipolar cell system with shunt currents, for a compilation of seven membrane cells. The discharge simulation was done with the time iteration step of 1. The x-axis represents the i-position. The y-axis represents the j-position. The vertical z-axis, represents the potential values to the given position.

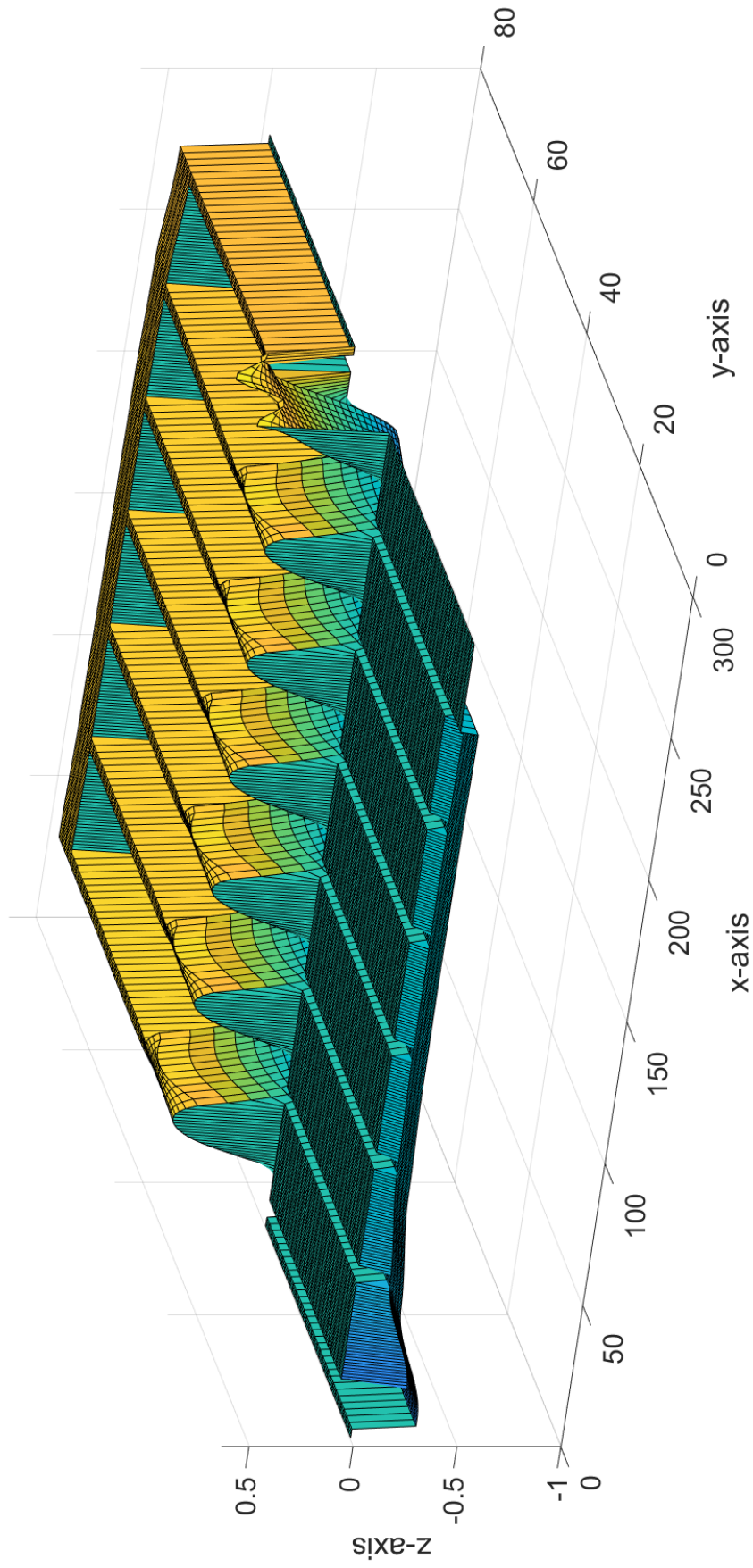


**Figure 6.16:** The figure shows the potentials throughout the bipolar cell system with shunt currents, for a compilation of seven membrane cells. The discharge simulation was done with the time iteration step of 0.001. The x-axis represents the i-position. The y-axis represents the j-position. The vertical z-axis, represents the potential values to the given position.





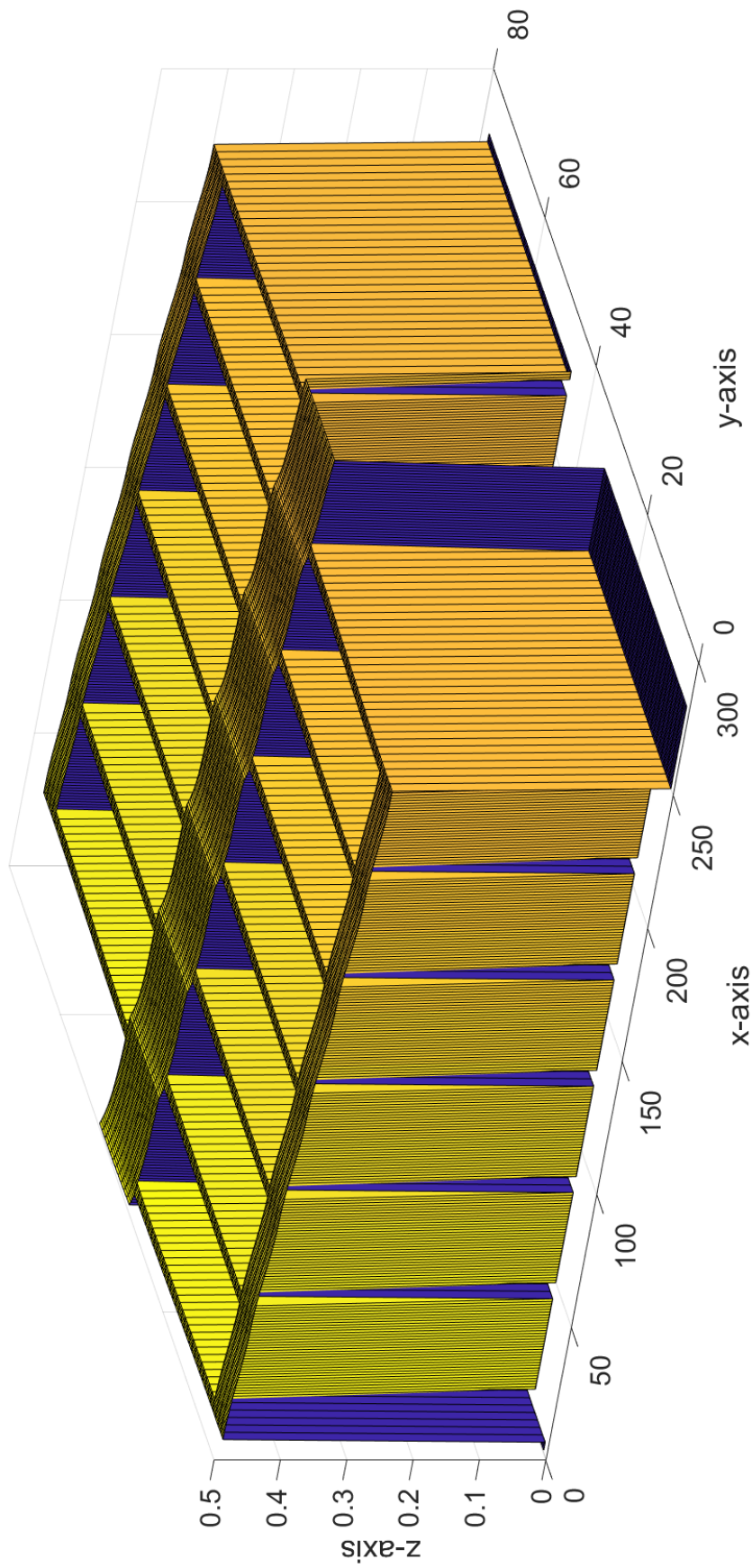


**Figure 6.18:** The figure shows the potentials throughout the bipolar cell system with shunt currents, for a compilation of seven membrane cells. The discharge simulation was done with the time iteration step of 0.1. The x-axis represents the i-position. The y-axis represents the j-position. The vertical z-axis, represents the potential values to the given position.

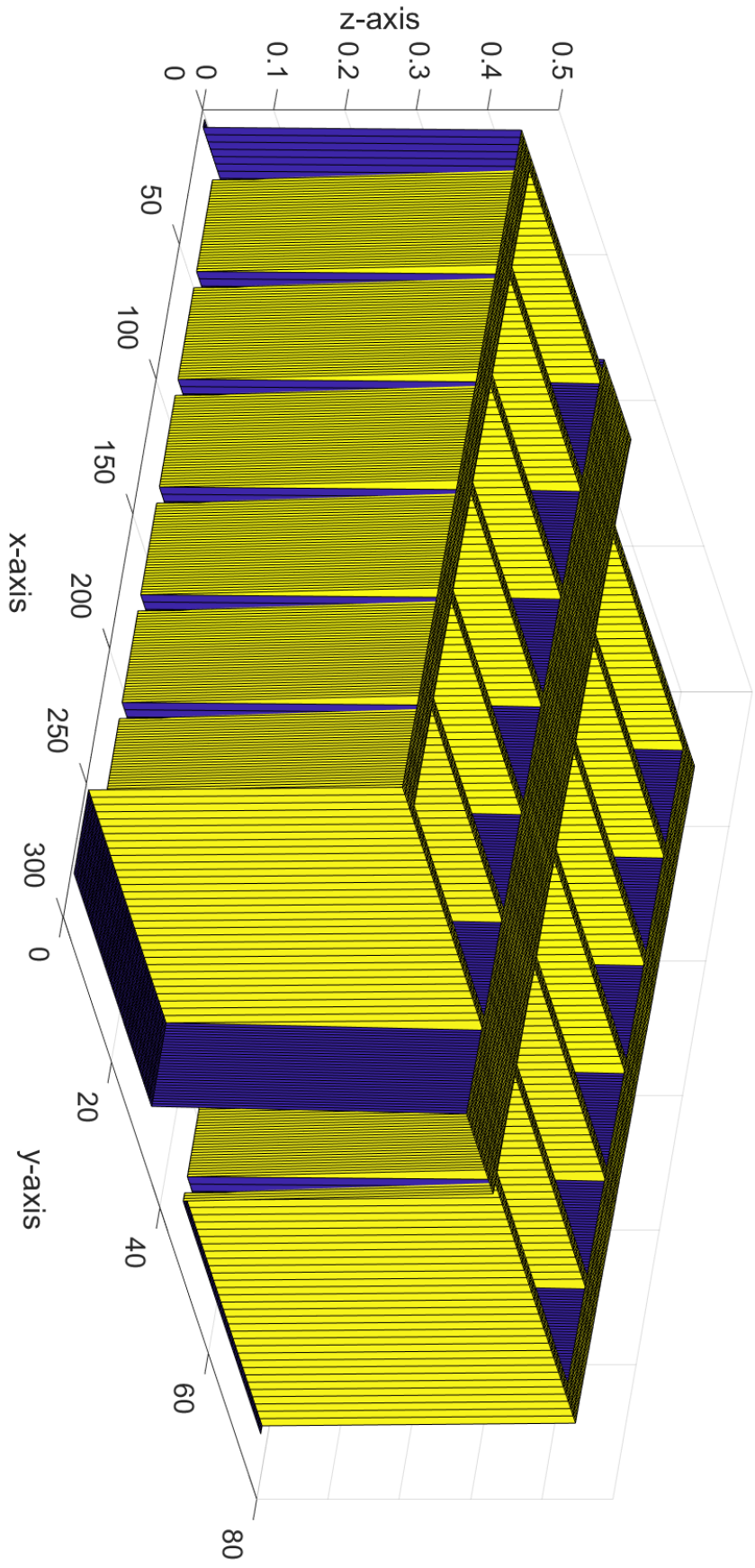


**Figure 6.19:** The figure shows the potentials throughout the bipolar cell system with shunt currents, for a compilation of seven membrane cells. The discharge simulation was done with the time iteration step of 1. The x-axis represents the  $i$ -position. The y-axis represents the  $j$ -position. The vertical z-axis, represents the potential values to the given position.

### 6.3.3 Discharge by variations of capacitance

Figures 6.20, 6.21, 6.22 and 6.23, shows the discharge simulations of the bipolar cell system with half the capacitance value for the anode and cathode, than for the simulations shown by Figures 6.12 through 6.19. The anodic and cathodic inlet tube lengths are of the same dimensions as the simulations shown by Figures 6.16 through 6.19. The iteration steps,  $\Delta t$ , are respectively 0.001, 0.01, 0.1 and 1.

Figure 6.20 shows the simulation with the time iteration step of 0.001. From the figure, it can be seen that the bipolar cell system experiences a potential drop of 1.0912 V. The potential drop through the anodic header and the cathodic header are respectively 0.3864 V and 0.0499 V. Figure 6.21 shows the simulation with the time iteration step of 0.01. From the figure, it can be seen that the bipolar cell system experiences a potential drop of 0.1699 V. The potential drop through the anodic header and the cathodic header are respectively 0.909 V and 0.0849 V. Figure 6.22 shows the simulation with the time iteration step of 0.1. From the figure, it can be seen that the bipolar cell system experiences a potential drop of 0.0512 V. The potential drop through the anodic header and the cathodic header are respectively 0.0366 V and 0.0371 V. Figure 6.23 shows the simulation with the time iteration step of 1. From the figure, it can be seen that the bipolar cell system experiences a potential drop of  $5.2 \times 10^{-3}$  V. The potential drop through the anodic header and the cathodic header are respectively  $3.8 \times 10^{-3}$  V and  $3.8 \times 10^{-3}$  V.

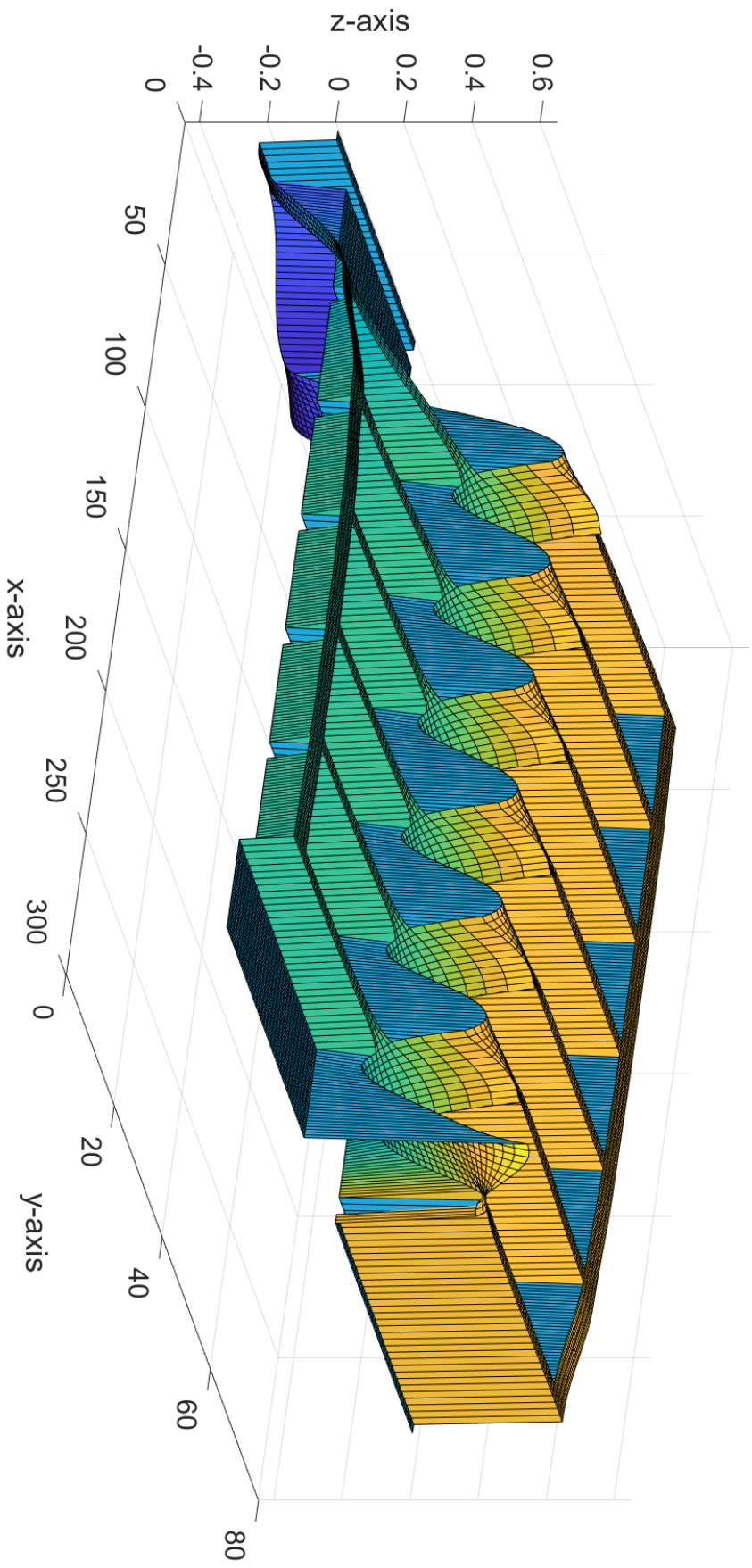


**Figure 6.20:** The figure shows the potentials throughout the bipolar cell system with shunt currents, for a compilation of seven membrane cells. The discharge simulation was done with the time iteration step of 0.001 and with half the capacitance value of the anode and cathode. The x-axis represents the i-position. The y-axis represents the j-position. The vertical z-axis, represents the potential values to the given position.

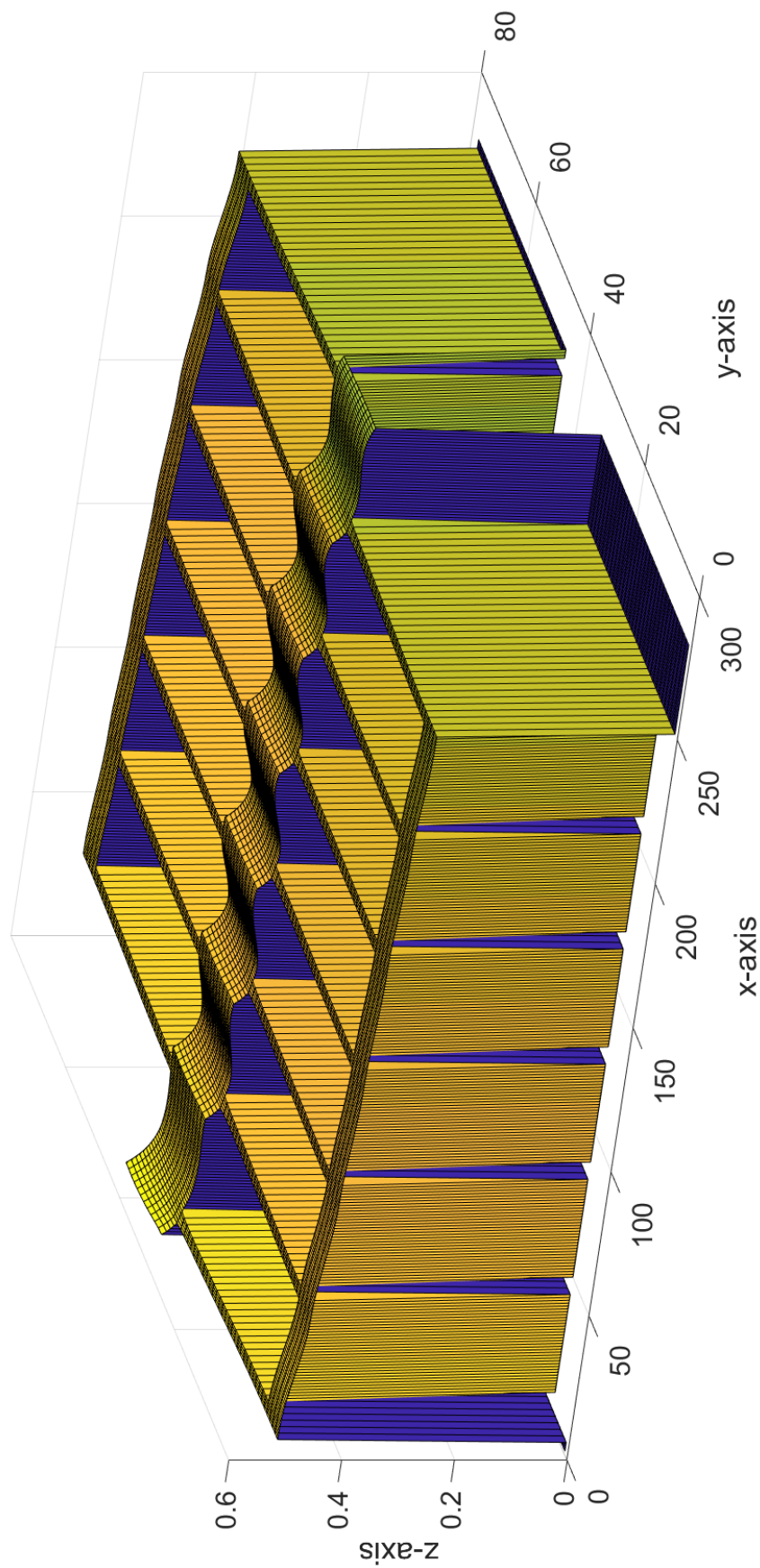


**Figure 6.21:** The figure shows the potentials throughout the bipolar cell system with shunt currents, for a compilation of seven membrane cells. The discharge simulation was done with the time iteration step of 0.01 and with half the capacitance value of the anode and cathode. The x-axis represents the  $i$ -position. The y-axis represents the  $j$ -position. The vertical z-axis, represents the potential values to the given position.

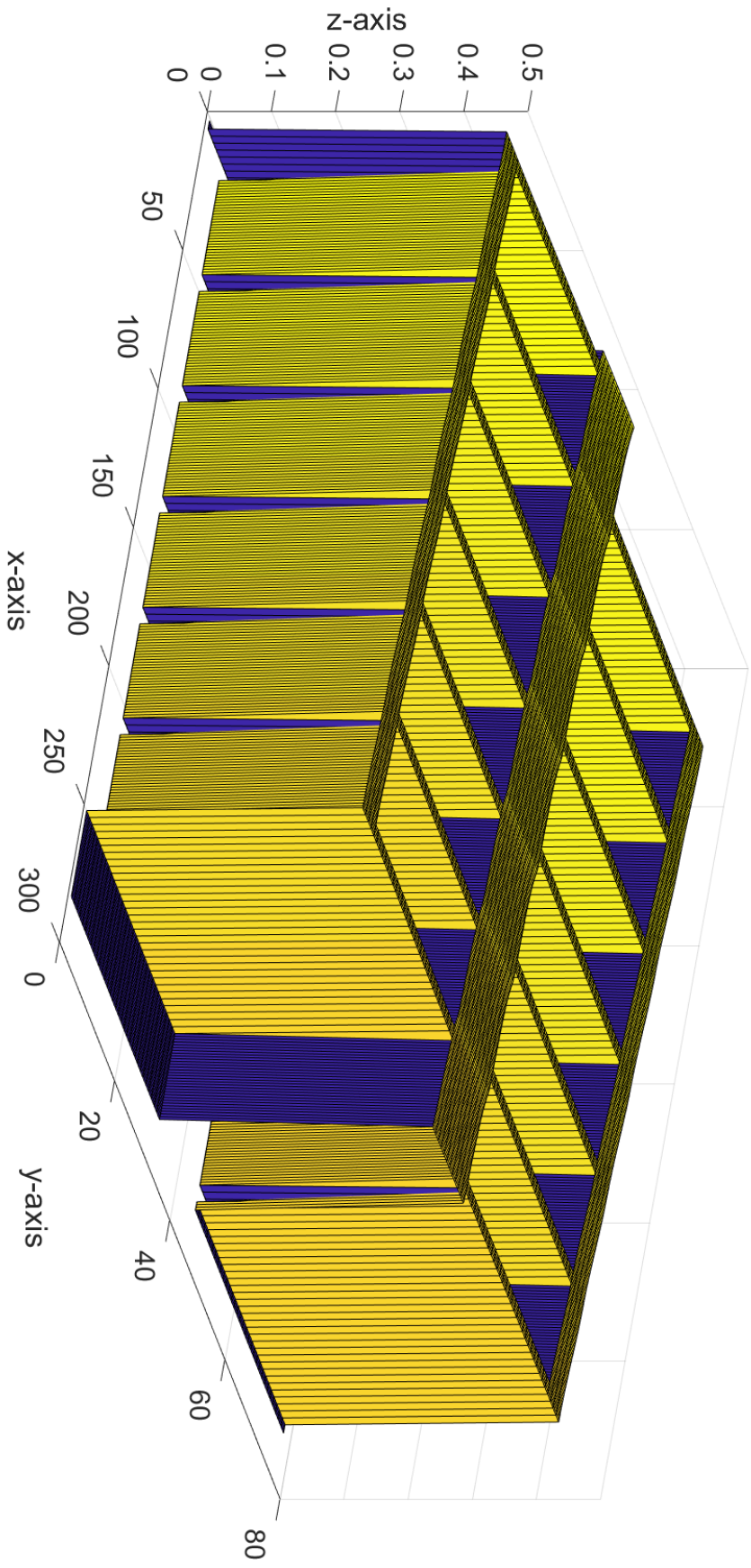


**Figure 6.22:** The figure shows the potentials throughout the bipolar cell system with shunt currents, for a compilation of seven membrane cells. The discharge simulation was done with the time iteration step of 0.1 and with half the capacitance value of the anode and cathode. The x-axis represents the i-position. The y-axis represents the j-position. The vertical z-axis, represents the potential values to the given position.

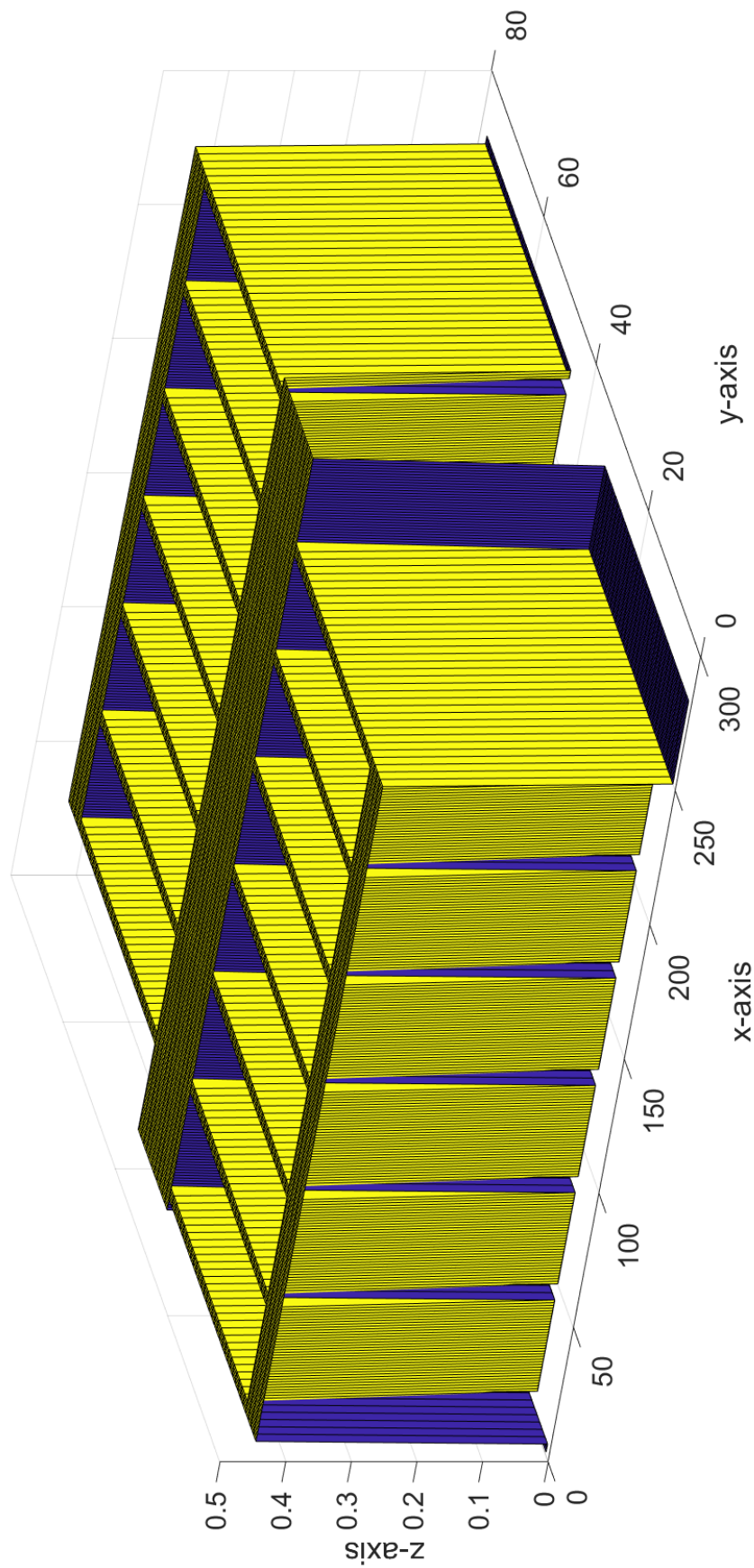


**Figure 6.23:** The figure shows the potentials throughout the bipolar cell system with shunt currents, for a compilation of seven membrane cells. The discharge simulation was done with the time iteration step of 1 and with half the capacitance value of the anode and cathode. The x-axis represents the  $i$ -position. The y-axis represents the  $j$ -position. The vertical z-axis, represents the potential values to the given position.





## 7 Discussion

The anode and the cathode were assumed to possess the properties of a capacitor. From the Figures 6.3 and 6.7, it can be seen that the phase angles, between the real and imaginary impedance components, are close to  $90^\circ$ . The deviation from the  $90^\circ$  can be caused by some small degree of diffusion of the reactants in the coatings or be caused by a non ideal current distribution during the EIS experiments. The phase angle of the anode is closer to  $90^\circ$  than that of the cathode. This may be because the coating made from nickel oxide and ruthenium oxide on the cathode, is more porous than the coating made of ruthenium oxide, iridium oxide and titanium oxide on the anode.

An important aspect of the model presented in Section 3 above is that it does not include other sources of potential differences in the system, but those related to ohmic drops in the electrolyte. Other sources of potential differences in bipolar cell systems may exist, such as those established by the Nernst equation,

$$E = E^0 - \frac{RT}{nF} \ln \frac{\prod_{\text{products}} a^\gamma}{\prod_{\text{reactants}} a^\gamma} \quad (7.1)$$

due to compositional differences between the anolyte and the catholyte. In addition to the reaction overpotentials. However, as the electrolyte along the cathode chain is electrically separated from the anode chain, we may assume that any potential difference resulting from differences in chemical composition according to Eq. (7.1) can simply be added to all the potentials on the anode side relative to those at the cathode side. This is applicable during the steady state operation of the bipolar cell system. For example, a reference electrode submerged at different points in the catholyte would sense the ohmic drops only with respect to other points in the catholyte. With respect to a similar reference electrode in the anolyte it would sense the potential according to Eq. (7.1) in addition. However, this assumption will break down if there are compositional differences *along* the cathode or anode chains.

Another way to describe why the Nernstian contributions on the cell potentials can be neglected, is as follows: Based on Figure 2.4, the cell potentials are given by Ohm's law, through the anodic and cathodic electrolyte and the membrane, and the Nernst equation between the anode and cathode. Since the bipolar cell system is composed of several membrane cells, the cathode from the left cell will be in contact with the anode from the right cell. So hypothetically, when moving in the *i*-position from left to right, the potential will experience a significant drop when reaching the cathode. But, when moving through the cathode and into the anode, the potential will experience an equivalent climb. Thus, the Nernstian contribution from the anode and the cathode will cancel each other out. What remains is then the potential change given by Ohm's law. The ability to disregard the Faradaic processes at the anode and the cathode is one of the strengths of this model.

At the discharge stage of the cell system, the Nernstian contributions may only be neglected for a short period of time after the cell system is released into open circuit. During the shutdown

of the cell system, a polarization rectifier is used to hold the cell potentials at around 1.4 V under the dechlorination stage. At this potential, the bipolar cell system will act as fuel cells, where oxygen gas is produced at the anodes and hydrogen gas is produced at the cathodes. When the polarization rectifier is turned off and the electrodes starts to discharge, there will be oxygen and hydrogen gas at the anode and the electrode surfaces. The activities of these gasses will influence the cell potentials. For a short time period into the discharge, the activities of the gasses can be assumed constant. For this time range, the electrodes will only experience capacitive discharge of the electrode coatings. The gasses would then rise to the top of the cells, which leads to the activities of the gasses at the electrode surfaces changes with time. Thus, it could be argued that the discharge stage contains two time intervals, shown by Figure 7.1, with different types of influences on the cell potentials. The developed model is valid for the first time interval where the electrodes experiences capacitive discharges.

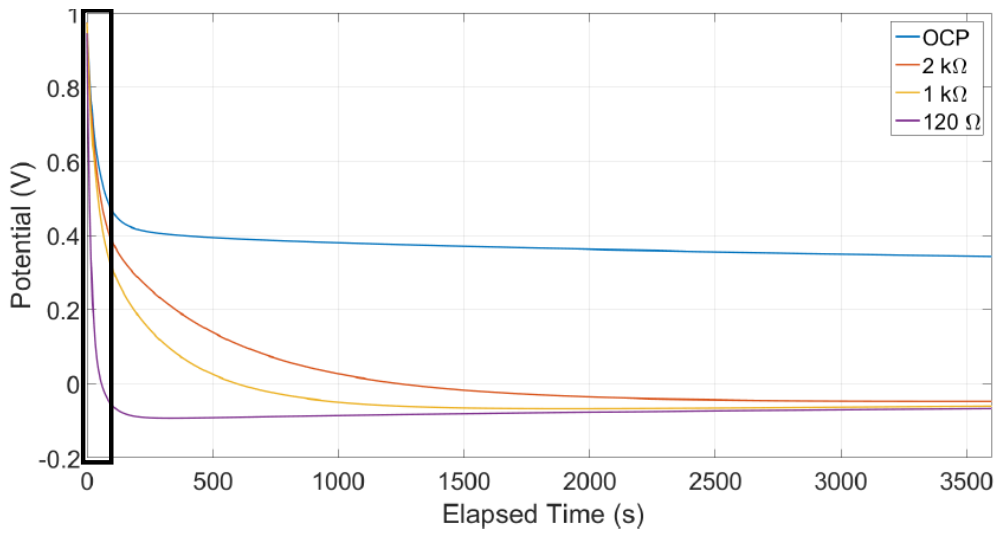


**Figure 7.1:** The figure shows the discharge plot of a anode sample, performed in the previous project thesis work [11]. The black box indicates the first time interval, where the electrodes undergoes only a capacitive discharge.

As expected, the length of the anodic and cathodic inlet tubes affects the current distribution throughout the bipolar cell system during operation. This can be seen by comparing Figures 6.10 and 6.11. By increasing the anodic and cathodic inlet tube lengths five times, the potential drop through the cell system increases by 2.36 V. This means that, with the equation,

$$\Delta U = R\Delta I \quad (7.2)$$

the current through the bipolar cell system increases with longer anodic and cathodic inlet tubes. The opposite happens in the headers. When increasing the inlet tubes by five times, the potential drop through the headers decreases by 5.99 V. Therefore, the amount of current going through the headers, decreases as the lengths of the anodic and cathodic inlet tube increases. The reason behind the changes of the current distribution, with respect to the inlet tube lengths, is because of the increase in the resistance through the longer tubes. It will be harder for the current to go through the inlet tubes and headers, so a larger amount of current will therefore go through the cell system instead. This leads to better current efficiency.

Even though the potential drop through the anodic and cathodic headers are of the same size, the amount of current going through them are not. The conductance of the anodic electrolyte is  $20.5344 \text{ Sm}^{-1}$  and the conductance of the cathodic electrolyte is  $32.25 \text{ Sm}^{-1}$ . Since the conductivity can be written as,

$$R_{electrolyte} = \frac{1}{\kappa} \quad (7.3)$$

the resistance through the anodic electrolyte is larger than for the cathodic electrolyte. This leads to a higher amount of current going through the cathodic electrolyte than through the anodic electrolyte, even though the potential drops are of the same value.

An increase of the anodic and cathodic inlet tube lengths by three times, will not notably change the potential drop through the cell system and the headers during the discharge stage. By comparing the potential drops shown by Figures 6.12 through 6.15 and 6.16 through 6.19, it can be seen that the potential drop trend from simulation of the steady state process continues. Though the effect of the inlet tube lengths on the potential drops are significantly smaller. To get a notable effect, the length of the inlet tube should be increased by a larger amount.

The changes in the capacitance of the anode and the cathode have significant effects on the potential drops during the discharge stage. By comparing the potential values from the simulations shown by Figures 6.16 through 6.19 and Figures 6.20 through 6.23, it can be seen that the potential drops happens faster for the simulations done with half the capacitance values for the anode and the cathode. This was to be expected, based on the discharge experiences done on the previous work during the project thesis [11]. By measuring the discharge rates based on the capacitance values and comparing the simulations to the real discharge data, it could be possible to assume the state of the electrodes. It is nevertheless a long way to go before this is possible.

The real natural discharge of the bipolar cell system, shown by Figure 2.3, shows a different picture than for the dynamically discharge simulation done in this master thesis. There may be several reasons for that. The most evident reason is that the simulation uses the same capacitance values for every anode and the same capacitance value for every cathode. The capacitance values from a real bipolar cell system that has been run in operation for a few years, will have lower capacitance values towards the middle of the cell stack. The results of the simulations done with different capacitance values, shows that it is clear that this will have a significant impact. The differences in the discharge speed of the anode sample based on the capacitance values, was also documented in the previous project thesis work [? ]. Another reason may be that, since this model only addresses the potential changes in the electrolyte, it will not capture changes in the cell voltages throughout the bipolar cell system. The natural discharge slopes shown by Figure 2.3, shows the cell voltage, while the simulations in this master thesis, shows the electrolytic potentials. It may be that the potential drops throughout the bipolar cell system during a natural discharge, would show similarities with the dynamically simulated potential drops, shown in the Result chapter.

The dimensions for the bipolar cell system used in the simulations, are too small. Normally a bipolar cell system for the chlor-alkali production may consist of around 120 to 160 membrane cells. In these simulation only seven membrane cells were used. In addition, the dimensions of the inlet tubes and the headers are smaller compared to the cells in real life than for the di-

mensions used in these simulations. The reason for the small dimensions used in the master thesis work, is the lack of computer capacity. The algorithm written in the `GeneratingMatrix-CreepCurrentDynamicSimulation` code requires a lot of processing power. The data generated, even though as sparse matrices, requires a huge amount of working memory. A normal portable computer would not have a chance to dynamically simulate the process with real dimensions. It is uncertain to what extent a fully dynamical simulation with real dimensions would differ in comparison to the dynamic simulations with limited dimensional parameters.

## 7.1 Further work

There are three main areas of which this work could be extended. The first one is to use a super computer to run the `GeneratingMatrixCreepCurrentDynamicSimulation` code, in order to be able to perform dynamical simulations with real life dimension parameters. The second, is to extend the two-dimensional model into a three dimensional one. This will make it possible to add the anodic and cathodic outlet tubes and their accompanying headers. The third one, is to compare and adjust the input parameters of the code, so that it is in accordance to a real chlor-alkali bipolar cell system.

## 8 Conclusion

The goal of programming a code that could dynamically simulate the bipolar cell system during operation and during the discharge stage was achieved. The length of the anodic and cathodic inlet tubes affected the amount of current going through the bipolar cell system during operation. Longer inlet tubes resulted in a larger amount of current through the cell system at the expense of the current going through the headers. A greater length of the anodic and cathodic inlet tubes, would therefore improve the current efficiency.

The impact of the length of the anodic and cathodic inlet tube during discharge, showed the same trends as during the operation, only to a much smaller degree. The differences in capacitance values for the anode and the cathode had a greater impact. A smaller capacitance value for the anodes and the cathodes, resulted in a faster discharge. The capacitance values for the anodes and the cathodes are dependent on the state of their coating. It can therefore be concluded that a poorer state of the electrode coatings will lead to a faster discharge. This conclusion also agrees with the results from the preceding project thesis work [11].

The simulations done with the `GeneratingMatrixCreepCurrentDynamicSimulation` code, could be used to predict the electrode residual coating in-situ. However, in order for that to be possible, further work may be required.



# References

- [1] Larry R. Faulkner Allen J. Bard. *Electrochemical Methods - Fundamentals and Applications*. Unated States of America, 1980. ISBN 0-471-05542-5.
- [2] Larry R. Faulkner Allen J. Bard. *Electrochemical Methods: Fundamentals and applications*. JOHN WILEY and SONS, INC., United States of America, 2nd ed. edition, 2001. ISBN 0-471-04372-9.
- [3] Bernard A. Boukamp. Electrochemical impedance spectroscopy. 2008. <http://www.lorentzcenter.nl/lc/web/2008/317/presentations/Boukamp.pdf>.
- [4] John F. Hamilton Bryant W. Rossiter. *Electrochemical Methods*, volume Volume 2 of *Physical Methods of Chemistry*. John Wiley and Sons, Inc., United states of America, Canada, second edition edition, 1986. ISBN 0-471-08027-6.
- [5] Wolf Vielstich Carl H. Hamann, Andrew Hamnett. *Electrochemistry*. WILEY-VCH Verlag GmbH and Co. KGaA, Weinheim, second edition, 2007. ISBN 978-3-527-31069-2.
- [6] The Essential ChemicalIndustry. Chemical process of a membrane cell. 2016. <http://www.essentialchemicalindustry.org/chemicals/chlorine.html>.
- [7] euro chlor. Industry review 2016-2017. Report, 2017. <http://fr.zone-secure.net/13451/398525/page=1>.
- [8] B. E. Conway. *Electrochemical Supercapacitors: Scientific Fundamentals and Technological Applications*, book section 16, pages 513–. Kluwe Academic/Plenum Publishers, New York, 1999. ISBN 0-306-45736-9.
- [9] National Research Council. *International Critical Tables of Numerical Data, Physics, Chemistry and Technology*, volume 6. The National Academies Press, Washington, DC, 1929. doi: doi:10.17226/20230.
- [10] Gamry Instruments. Basics of electrochemical impedance spectroscopy. 2017. <https://www.gamry.com/application-notes/EIS/basics-of-electrochemical-impedance-spectroscopy/>.
- [11] Per Sverre Iversen. *Diagnostis of chlorine electrolyzers based on self-discharge*. Thesis, 2017.
- [12] C. Montella J. P. Diard, B. Le Gorrec. Handbook of eletcrochemical impedance spectroscopy. 2013.
- [13] Karen E. Thomas-Alyea John Newman. *Electrochemical Systems*. Jhin Wiley and sons, Unated States of America, third edition, 2004. ISBN 0-471-47756-7.

- [14] Yanan Li, Jie Zhou, Yun Liu, Jian Tang, and Weihua Tang. Hierarchical nickel sulfide coated halloysite nanotubes for efficient energy storage. *Electrochimica Acta*, 245 (Supplement C):51–58, 2017. ISSN 0013-4686. doi: <https://doi.org/10.1016/j.electacta.2017.05.140>. URL <http://www.sciencedirect.com/science/article/pii/S0013468617311374>.
- [15] Organisation Intergouvernementale de la Convention du M<sup>Ã</sup>tre. *The International System of Units (SI)*. STEDI MEDIA, Paris, France., 8th edition edition, 2006. ISBN 92-822-2213-6.
- [16] Mark E. Orazem Pankaj Agarwal and Luis H. Garcia-Rubio. Measurement models for electrochemical impedance spectroscopy - demonstration of applicability. 1992.
- [17] H. S. Burney R. E. White, C. W. Walton and R. N. Beaver. Predicting shunt currents in stacks of bipolar plate cells. 1985.
- [18] Craig E. Banks Richard G. Compton. *Understanding Voltammetry*. World Scientific Publishing Co. Pte. Ltd., Singapore, 2007. ISBN 978-981-270-625-6.
- [19] Ahn Young Rack, Song Mi Yeon, Jo Seong Mu, Park Chong Rae, and Kim Dong Young. Electrochemical capacitors based on electrodeposited ruthenium oxide on nanofibre substrates. *Nanotechnology*, 17(12):2865, 2006. ISSN 0957-4484. <http://stacks.iop.org/0957-4484/17/i=12/a=007>.



# A Appendix

## A.1 Matlab code

```
% Written by Per Sverre Iversen, in the spring of 2018

function GeneratingMatrixCreepCurrentDynamicSimulation

%Step length
clear all

clc

t= input('Time(s)?')
deltat= input('Delta t(s)?')

%number of cells
Ncells=7;

%cell height, number of grid points in vertical directions
HeightCells=10;

%anodic chamber width oddetal hvis AnodicInletTubeWidth er odde

AnodicWidth=11;

%Membrane width

MembraneWidth=15;

%Kathodic chamber width

CathodicWidth=11;

%Cell width

CellWidth= (AnodicWidth+1) + (MembraneWidth+2) + (CathodicWidth+1) -1;
SystemWidth= (CellWidth*Ncells)+1
%%%%
%Creep current parameters
%anodic
AnodicInletTubeWidth=3;

AnodicInletTubeLength=30;
```

```
AnodicTubeWidth=3;

%cathodic

CathodicInletTubeWidth=3;

CathodicInletTubeLength=30;

CathodicTubeWidth=3;

%placement of the anodic creep current
ACC=((AnodicWidth-AnodicInletTubeWidth)/2)+2;
%round to the nearest integer
ACCI=round(ACC);
%correcting values for a in chambers
AA=AnodicInletTubeLength+AnodicTubeWidth+1;
%correcting values for a in anodic inlet tube
Aa=AnodicTubeWidth+1+ACCI;

%placement of the cathodic creep current
CCC=((CathodicWidth-CathodicInletTubeWidth)/2)+1;
%round to the nearest integer
CCCI=round(CCC);
%correcting values for a in chambers
CC=1+AnodicTubeWidth+AnodicInletTubeLength+HeightCells;
%correcting values for a in anodic inlet tube
Cc=(1+AnodicWidth)+(2+MembraneWidth)+CCCI;
%Cc=CathodicTubeWidth+1+CCCI

SystemHeight=(1+AnodicTubeWidth)+(AnodicInletTubeLength)+(HeightCells) ...
    +(CathodicInletTubeLength)+(CathodicTubeWidth+1)

%%

%A=zeros((HeightCells+2)*(CellWidth+1)*Ncells);

X=zeros(1);
%anodic chamber left
acl=-0.5;

%anodic chamber right
acr=-0.5;
%membrane left
ml=1.5;

%membrane right
mr=-1.5;

%cathodic chamber left
ccl=0.5;

%cathodic chamber right
ccr=0.5;
```

```

%anodic inlet tube left
aitl=0;

%anodic inlet tube right
aitr=0;

%dynamic for loop

%definere tidsskritt. Lavere lambda kortere tidsskritt
%anode %%%%%%%%%%%
%capacitance
%CapacitanceAnode=0.00354;

CapacitanceAnode=0.00177;
Conductancea=20.5344;

lambdaa=-((CapacitanceAnode*2)/(Conductancea*deltat))

%cathode %%%%%%%%%%%
%capacitance
%CapacitanceCathode=0.022257;
CapacitanceCathode=0.0111285;

Conductancec=32.25;

lambdaac=-((CapacitanceCathode*2)/(Conductancec*deltat))

    for tt=1:t
        A{tt}=zeros();
        b{tt}=zeros();
    jo=1;

%anodic chamber internal points

%-4diagonal for internal points in anode chamber
%%%%%%%%%%%%%%%%%%%%%%%%%%%%%%%%%%%%%%%%%%%%%%%%%%%%%%%%%%%%%%%%%%%%%%%%%%
j=jo;
z=0;

    for n=1:Ncells
        m=(AnodicInletTubeLength+(AnodicTubeWidth+1));
        a=AA+1;
        for k=1:HeightCells
            a=a+1;
            i=(m*CellWidth*Ncells)+a+(z*CellWidth);
            for l=1:AnodicWidth
                A{tt}(j,i)=4;
                i=i+1;
            end
        end
    end
end

```

```

        b{tt}(j,1)=0;
        j=j+1;
    end
    m=m+1;
end
z=z+1;
end

```

```

%%%%%%%%%%%%%%%%%%%%%%%%%%%%%%%%%%%%%%%%%%%%%%%%%%%%%%%%%%%%%%%%%%%%%%%%

```

```

%%%%%%%%%%%%%%%%%%%%%%%%%%%%%%%%%%%%%%%%%%%%%%%%%%%%%%%%%%%%%%%%%%%%%%%%

```

```

% -1 subdiagonal anodic chamber

```

```

j=j0;
z=0;

```

```

for n=1:Ncells
m=(AnodicInletTubeLength+(AnodicTubeWidth+1));
a=AA;
    for k=1:HeightCells
        a=a+1;
        i=(m*CellWidth*Ncells)+a+(z*CellWidth);
        for l=1:AnodicWidth
            A{tt}(j,i)=-1;
            i=i+1;
            j=j+1;
        end
        m=m+1;
    end
    z=z+1;
end

```

```

%%%%%%%%%%%%%%%%%%%%%%%%%%%%%%%%%%%%%%%%%%%%%%%%%%%%%%%%%%%%%%%%%%%%%%%%

```

```

%%%%%%%%%%%%%%%%%%%%%%%%%%%%%%%%%%%%%%%%%%%%%%%%%%%%%%%%%%%%%%%%%%%%%%%%

```

```

% -1 superdiagonal

```

```

j=j0;
z=0;

```

```

for n=1:Ncells
m=(AnodicInletTubeLength+(AnodicTubeWidth+1));
a=AA+2;
    for k=1:HeightCells
        a=a+1;
        i=(m*CellWidth*Ncells)+a+(z*CellWidth);
        for l=1:AnodicWidth
            A{tt}(j,i)=-1;
            i=i+1;
            j=j+1;
        end
        m=m+1;
    end
end

```





```

% -1 superdiagonal

j=jo;
z=0;
for n=1:Ncells
    m=(AnodicInletTubeLength+(AnodicTubeWidth+1)+0);
    a=AA+1;
    for k=1:HeightCells
        a=a+1;
        i=(AnodicWidth+2)+(m*CellWidth*Ncells)+a+(z*CellWidth);
        for l=1:MembraneWidth
            A{tt}(j,i)=-1;
            i=i+1;
            j=j+1;
        end
        m=m+1;
    end
    z=z+1;
end

```

```

%%%%%%%%%%%%%%%%%%%%%%%%%%%%%%%%%%%%%%%%%%%%%%%%%%%%%%%%%%%%%%%%%%%%%%%%

```

```

%%%%%%%%%%%%%%%%%%%%%%%%%%%%%%%%%%%%%%%%%%%%%%%%%%%%%%%%%%%%%%%%%%%%%%%%

```

```

% upper -1 diagonal

```

```

j=jo;
z=0;
for n=1:Ncells
    m=(AnodicInletTubeLength+(AnodicTubeWidth+1)+1);
    a=AA+1;
    for k=1:HeightCells
        a=a+1;
        i=(AnodicWidth+2)+(m*CellWidth*Ncells)+a+(z*CellWidth);
        for l=1:MembraneWidth
            A{tt}(j,i)=-1;
            i=i+1;
            j=j+1;
        end
        m=m+1;
    end
    z=z+1;
end

```

```

%%%%%%%%%%%%%%%%%%%%%%%%%%%%%%%%%%%%%%%%%%%%%%%%%%%%%%%%%%%%%%%%%%%%%%%%

```

```

%%%%%%%%%%%%%%%%%%%%%%%%%%%%%%%%%%%%%%%%%%%%%%%%%%%%%%%%%%%%%%%%%%%%%%%%

```

```

% lower -1 diagonals

```

```

j=jo;
z=0;
for n=1:Ncells
    m=(AnodicInletTubeLength+(AnodicTubeWidth+1)-1);
    a=AA-1;
    for k=1:HeightCells
        a=a+1;

```

```

        i=(AnodicWidth+2)+(m*CellWidth*Ncells)+a+(z*CellWidth);
        for l=1:MembraneWidth
            A{tt}(j,i)=-1;
            i=i+1;
            j=j+1;
        end
        m=m+1;
    end
    z=z+1;
end

jo=j;
%%%%%%%%%%%%%%%%%%%%%%%%%%%%%%%%%%%%%%%%%%%%%%%%%%%%%%%%%%%%%%%%%%%%%%%%
%test ok
%%%%%%%%%%%%%%%%%%%%%%%%%%%%%%%%%%%%%%%%%%%%%%%%%%%%%%%%%%%%%%%%%%%%%%%%

% Kathodic internal points
%%%%%%%%%%%%%%%%%%%%%%%%%%%%%%%%%%%%%%%%%%%%%%%%%%%%%%%%%%%%%%%%%%%%%%%%
%-4diagonal for internal points in cathodic chamber
%%%%%%%%%%%%%%%%%%%%%%%%%%%%%%%%%%%%%%%%%%%%%%%%%%%%%%%%%%%%%%%%%%%%%%%%

j=jo;
z=0;
    for n=1:Ncells
        m=(AnodicInletTubeLength+(AnodicTubeWidth+1)+0);
        a=AA+1;
        for k=1:HeightCells
            a=a+1;
            i=(AnodicWidth+MembraneWidth+2)+(m*CellWidth*Ncells)+a ...
                +(z*CellWidth);
            for l=1:CathodicWidth
                A{tt}(j,i)=4;
                i=i+1;
                b{tt}(j,l)=0;
                j=j+1;
            end
            m=m+1;
        end
        z=z+1;
    end

%%%%%%%%%%%%%%%%%%%%%%%%%%%%%%%%%%%%%%%%%%%%%%%%%%%%%%%%%%%%%%%%%%%%%%%%

%%%%%%%%%%%%%%%%%%%%%%%%%%%%%%%%%%%%%%%%%%%%%%%%%%%%%%%%%%%%%%%%%%%%%%%%
% -1 subdiagonal anodic chamber

j=jo;
z=0;

```



```

for n=1:Ncells
m=(AnodicInletTubeLength+(AnodicTubeWidth+1)+0);
a=AA+0;
for k=1:HeightCells
a=a+1;
i=(AnodicWidth+MembraneWidth+2)+(m*CellWidth*Ncells)+a+ ...
(z*CellWidth);
for l=1:CathodicWidth
A{tt}(j,i)=-1;
i=i+1;
j=j+1;
end
m=m+1;
end
z=z+1;
end

%%%%%%%%%%%%%%%%%%%%%%%%%%%%%%%%%%%%%%%%%%%%%%%%%%%%%%%%%%%%%%%%%%%%%%%%
%%%%%%%%%%%%%%%%%%%%%%%%%%%%%%%%%%%%%%%%%%%%%%%%%%%%%%%%%%%%%%%%%%%%%%%%
% -1 superdiagonal

j=j0;
z=0;
for n=1:Ncells
m=(AnodicInletTubeLength+(AnodicTubeWidth+1)+0);
a=AA+2;
for k=1:HeightCells
a=a+1;
i=(AnodicWidth+MembraneWidth+2)+(m*CellWidth*Ncells)+a+ ...
(z*CellWidth);
for l=1:CathodicWidth
A{tt}(j,i)=-1;
i=i+1;
j=j+1;
end
m=m+1;
end
z=z+1;
end

%%%%%%%%%%%%%%%%%%%%%%%%%%%%%%%%%%%%%%%%%%%%%%%%%%%%%%%%%%%%%%%%%%%%%%%%
%%%%%%%%%%%%%%%%%%%%%%%%%%%%%%%%%%%%%%%%%%%%%%%%%%%%%%%%%%%%%%%%%%%%%%%%
% upper -1 diagonal

j=j0;
z=0;
for n=1:Ncells
m=(AnodicInletTubeLength+(AnodicTubeWidth+1)+1);
a=AA+2;
for k=1:HeightCells
a=a+1;
i=(AnodicWidth+MembraneWidth+2)+(m*CellWidth*Ncells)+a+ ...

```



```

j=j0;
z=0;

for n=1:Ncells
m=(AnodicInletTubeLength+(AnodicTubeWidth+1)-1);
a=AA-1;
    for k=1:(HeightCells+2)
        a=a+1;
        i=(m*CellWidth*Ncells)+a+(z*CellWidth);
        % for l=1:AnodicWidth
        %     A(j,i)=-3;
        %     i=i+1;
        %     j=j+1;
        % end

        if tt==1
            A{tt}(j,i)=-3;
            b{tt}(j,1)=acl;
        else
            A{tt}(j,i)=-3-(lambdaa);
            b{tt}(j,1)=-(b{tt-1}(j,1))*(lambdaa);
        end
        i=i+1;
        j=j+1;
        m=m+1;
    end
    z=z+1;
end

```

```

j=j0;
z=0;

for n=1:Ncells
m=(AnodicInletTubeLength+(AnodicTubeWidth+1)-1);
a=AA+0;
    for k=1:(HeightCells+2)
        a=a+1;
        i=(m*CellWidth*Ncells)+a+(z*CellWidth);
        % for l=1:AnodicWidth
        %     A(j,i)=4;
        %     i=i+1;
        %     j=j+1;
        % end
        A{tt}(j,i)=4;
        i=i+1;
        j=j+1;
        m=m+1;
    end
    z=z+1;
end

```

```

j=j0;

```

```

z=0;

for n=1:Ncells
m=(AnodicInletTubeLength+(AnodicTubeWidth+1)-1);
a=AA+1;
    for k=1:(HeightCells+2)
        a=a+1;
        i=(m*CellWidth*Ncells)+a+(z*CellWidth);
        %for l=1:(AnodicWidth+1)
        %    A(j,i)=-1;
        %    i=i+1;
        %    j=j+1
        %end
        A{tt}(j,i)=-1;
        i=i+1;
        j=j+1;
        m=m+1;
    end
    z=z+1;
end
jo=j;
%%%%%%%%%%%%%%%%%%%%%%%%%%%%%%%%%%%%%%%%%%%%%%%%%%%%%%%%%%%%%%%%%%%%%%%%%%

%top
%%%%%%%%%%%%%%%%%%%%%%%%%%%%%%%%%%%%%%%%%%%%%%%%%%%%%%%%%%%%%%%%%%%%%%%%%%

j=jo;

z=0;

for n=1:Ncells
m=(AnodicInletTubeLength+(AnodicTubeWidth+1)+HeightCells);
a=AA+HeightCells+0;
    %for k=1:Ncells
        a=a+1;
        i=(m*CellWidth*Ncells)+a+(z*CellWidth);
        for l=1:AnodicWidth+1
            A{tt}(j,i)=-3;
            i=i+1;
            b{tt}(j,l)=0;
            j=j+1;
        end

        m=m+1;
    %end
    z=z+1;
end

j=jo;

z=0;

for n=1:Ncells
m=(AnodicInletTubeLength+(AnodicTubeWidth+1)+(HeightCells-1));
a=AA+HeightCells-1;
    %for k=1:Ncells

```

```

        a=a+1;
        i=(m*CellWidth*Ncells)+a+(z*CellWidth);
        for l=1:AnodicWidth+1
            A{tt}(j,i)=4;
            i=i+1;
            j=j+1;
        end

        m=m+1;
    %end
    z=z+1;
end

j=j0;

z=0;

for n=1:Ncells
    m=(AnodicInletTubeLength+(AnodicTubeWidth+1)+(HeightCells-2));
    a=AA+HeightCells-2;
    %for k=1:Ncells
        a=a+1;
        i=(m*CellWidth*Ncells)+a+(z*CellWidth);
        for l=1:AnodicWidth+1
            A{tt}(j,i)=-1;
            i=i+1;
            j=j+1;
        end

        m=m+1;
    %end
    z=z+1;
end
jo=j;
%%%%%%%%%%%%%%%%%%%%%%%%%%%%%%%%%%%%%%%%%%%%%%%%%%%%%%%%%%%%%%%%%%%%%%%%

%right

%%%%%%%%%%%%%%%%%%%%%%%%%%%%%%%%%%%%%%%%%%%%%%%%%%%%%%%%%%%%%%%%%%%%%%%%
%%%%%%%%%%%%%%%%%%%%%%%%%%%%%%%%%%%%%%%%%%%%%%%%%%%%%%%%%%%%%%%%%%%%%%%%

%Bottom
%%%%%%%%%%%%%%%%%%%%%%%%%%%%%%%%%%%%%%%%%%%%%%%%%%%%%%%%%%%%%%%%%%%%%%%%

j=j0;

z=0;

for n=1:Ncells
    m=(AnodicInletTubeLength+(AnodicTubeWidth+1)-1);
    a=AA-1;
    %for k=1:Ncells
        a=a+1;
        i=(m*CellWidth*Ncells)+a+(z*CellWidth);
        for l=1:(ACCI-1)

```

```

        A{tt}(j,i)=-3;
        i=i+1;
        b{tt}(j,1)=0;
        j=j+1;
    end
    for l=(ACCI):(ACCI)+AnodicInletTubeWidth-1
        A{tt}(j,i)=0;
        i=i+1;
        b{tt}(j,1)=0;
        j=j+1;
    end
    for l=(ACCI)+(AnodicInletTubeWidth):(AnodicWidth+1)
        A{tt}(j,i)=-3;
        i=i+1;
        b{tt}(j,1)=0;
        j=j+1;
    end

    m=m+1;
    %end
    z=z+1;
end

j=j0;

z=0;

for n=1:Ncells
    m=(AnodicInletTubeLength+(AnodicTubeWidth+1)+0);
    a=AA+0;
    %for k=1:Ncells
        a=a+1;
        i=(m*CellWidth*Ncells)+a+(z*CellWidth);
        for l=1:(((AnodicWidth-AnodicInletTubeWidth)/2)+1)
            A{tt}(j,i)=4;
            i=i+1;
            j=j+1;
        end
        for l=(((AnodicWidth-AnodicInletTubeWidth)/2)+2):...
            (((AnodicWidth-AnodicInletTubeWidth)/2)+1)+...
            AnodicInletTubeWidth)
            A{tt}(j,i)=0;
            i=i+1;
            j=j+1;
        end
        for l=(((AnodicWidth-AnodicInletTubeWidth)/2)+1)+...
            AnodicInletTubeWidth+1):(AnodicWidth+1)
            A{tt}(j,i)=4;
            i=i+1;
            j=j+1;
        end
    end

    m=m+1;
    %end
    z=z+1;
end

```

```

j=j0;

z=0;

for n=1:Ncells
m=(AnodicInletTubeLength+(AnodicTubeWidth+1)+1);
a=AA+1;
    %for k=1:Ncells
    a=a+1;
    i=(m*CellWidth*Ncells)+a+(z*CellWidth);
    for l=1:(((AnodicWidth-AnodicInletTubeWidth)/2)+1)
        A{tt}(j,i)=-1;
        i=i+1;
        j=j+1;
    end
    for l=(((AnodicWidth-AnodicInletTubeWidth)/2)+2): ...
        (((AnodicWidth-AnodicInletTubeWidth)/2)+1)+ ...
        AnodicInletTubeWidth)
        A{tt}(j,i)=0;
        i=i+1;
        j=j+1;
    end
    for l=(((AnodicWidth-AnodicInletTubeWidth)/2)+1) ...
        +AnodicInletTubeWidth+1):(AnodicWidth+1)
        A{tt}(j,i)=-1;
        i=i+1;
        j=j+1;
    end

    m=m+1;
    %end
    z=z+1;
end
j0=j;
%%%%%%%%%%%%%%%%%%%%%%%%%%%%%%%%%%%%%%%%%%%%%%%%%%%%%%%%%%%%%%%%%%%%%%%%

%Membrane
%%%%%%%%%%%%%%%%%%%%%%%%%%%%%%%%%%%%%%%%%%%%%%%%%%%%%%%%%%%%%%%%%%%%%%%%
%Left
%%%%%%%%%%%%%%%%%%%%%%%%%%%%%%%%%%%%%%%%%%%%%%%%%%%%%%%%%%%%%%%%%%%%%%%%

j=j0;
z=0;

for n=1:Ncells
m=(AnodicInletTubeLength+(AnodicTubeWidth+1)-1);
a=AA-1;
    for k=1:(HeightCells+2)
        a=a+1;
        i=(m*CellWidth*Ncells)+a+(z*CellWidth)+(AnodicWidth+1);
        % for l=1:AnodicWidth

```

```
        %      A(j,i)=-3;
        %      i=i+1;
        %      j=j+1;
        % end
        A{tt}(j,i)=-6;
        i=i+1;
        b{tt}(j,1)=0;
        j=j+1;
        m=m+1;
    end
    z=z+1;
end
```

```
j=jo;
z=0;
```

```
for n=1:Ncells
m=(AnodicInletTubeLength+(AnodicTubeWidth+1)-1);
a=AA+0;
    for k=1:(HeightCells+2)
        a=a+1;
        i=(m*CellWidth*Ncells)+a+(z*CellWidth)+(AnodicWidth+1);
        % for l=1:AnodicWidth
        %      A(j,i)=4;
        %      i=i+1;
        %      j=j+1;
        % end
        A{tt}(j,i)=4;
        i=i+1;
        j=j+1;
        m=m+1;
    end
    z=z+1;
end
```

```
j=jo;
z=0;
```

```
for n=1:Ncells
m=(AnodicInletTubeLength+(AnodicTubeWidth+1)-1);
a=AA+1;
    for k=1:(HeightCells+2)
        a=a+1;
        i=(m*CellWidth*Ncells)+a+(z*CellWidth)+(AnodicWidth+1);
        %for l=1:(AnodicWidth+1)
        %      A(j,i)=-1;
        %      i=i+1;
        %      j=j+1
        %end
        A{tt}(j,i)=-1;
        i=i+1;
        j=j+1;
        m=m+1;
    end
end
```





```
j=j0;
```

```
z=0;
```

```
for n=1:Ncells
m=(AnodicInletTubeLength+(AnodicTubeWidth+1)+(HeightCells+0));
a=AA+HeightCells+0;
    %for k=1:Ncells
        a=a+1;
        i=(m*CellWidth*Ncells)+a+(z*CellWidth)+(AnodicWidth+1);
        for l=1:MembraneWidth+2
            A{tt}(j,i)=-3;
            i=i+1;
            b{tt}(j,l)=0;
            j=j+1;
        end

        m=m+1;
    %end
    z=z+1;
end
```

```
j=j0;
```

```
z=0;
```

```
for n=1:Ncells
m=(AnodicInletTubeLength+(AnodicTubeWidth+1)+(HeightCells-1));
a=AA+HeightCells-1;
    %for k=1:Ncells
        a=a+1;
        i=(m*CellWidth*Ncells)+a+(z*CellWidth)+(AnodicWidth+1);
        for l=1:MembraneWidth+2
            A{tt}(j,i)=4;
            i=i+1;
            j=j+1;
        end

        m=m+1;
    %end
    z=z+1;
end
```

```
j=j0;
```

```
z=0;
```

```
for n=1:Ncells
m=(AnodicInletTubeLength+(AnodicTubeWidth+1)+(HeightCells-2));
a=AA+HeightCells-2;
    %for k=1:Ncells
        a=a+1;
        i=(m*CellWidth*Ncells)+a+(z*CellWidth)+(AnodicWidth+1);
        for l=1:MembraneWidth+2
            A{tt}(j,i)=-1;
```

```

        i=i+1;
        j=j+1;
    end

    m=m+1;
%end
    z=z+1;
end

jo=j;
%%%%%%%%%%%%%%%%%%%%%%%%%%%%%%%%%%%%%%%%%%%%%%%%%%%%%%%%%%%%%%%%%%%%%%%%

%right
%%%%%%%%%%%%%%%%%%%%%%%%%%%%%%%%%%%%%%%%%%%%%%%%%%%%%%%%%%%%%%%%%%%%%%%%

j=jo;
z=0;

for n=1:Ncells
m=(AnodicInletTubeLength+(AnodicTubeWidth+1)-1);
a=AA-1;
    for k=1:(HeightCells+2)
        a=a+1;
        i=(m*CellWidth*Ncells)+a+(z*CellWidth)+(AnodicWidth+1) ...
            +(MembraneWidth+1);
        % for l=1:AnodicWidth
        %     A(j,i)=-3;
        %     i=i+1;
        %     j=j+1;
        % end
        A{tt}(j,i)=-6;
        i=i+1;
        b{tt}(j,1)=0;
        j=j+1;
        m=m+1;
    end
    z=z+1;
end

j=jo;
z=0;

for n=1:Ncells
m=(AnodicInletTubeLength+(AnodicTubeWidth+1)-1);
a=AA-2;
    for k=1:(HeightCells+2)
        a=a+1;
        i=(m*CellWidth*Ncells)+a+(z*CellWidth)+(AnodicWidth+1) ...
            +(MembraneWidth+1);
        % for l=1:AnodicWidth
        %     A(j,i)=4;
        %     i=i+1;
        %     j=j+1;
        % end

```

```
        A{tt}(j,i)=4;
        i=i+1;
        j=j+1;
        m=m+1;
    end
    z=z+1;
end
```

```
j=jo;
z=0;
```

```
for n=1:Ncells
m=(AnodicInletTubeLength+(AnodicTubeWidth+1)-1);
a=AA-3;
    for k=1:(HeightCells+2)
        a=a+1;
        i=(m*CellWidth*Ncells)+a+(z*CellWidth)+(AnodicWidth+1) ...
            +(MembraneWidth+1);
        % for l=1:AnodicWidth
        %     A(j,i)=-1;
        %     i=i+1;
        %     j=j+1;
        % end
        A{tt}(j,i)=-1;
        i=i+1;
        j=j+1;
        m=m+1;
    end
    z=z+1;
end
```

```
j=jo;
z=0;
```

```
for n=1:Ncells
m=(AnodicInletTubeLength+(AnodicTubeWidth+1)-1);
a=AA+0;
    for k=1:(HeightCells+2)
        a=a+1;
        i=(m*CellWidth*Ncells)+a+(z*CellWidth)+(AnodicWidth+1) ...
            +(MembraneWidth+1);
        % for l=1:AnodicWidth
        %     A(j,i)=-1;
        %     i=i+1;
        %     j=j+1;
        % end
        A{tt}(j,i)=4;
        i=i+1;
        j=j+1;
        m=m+1;
    end
    z=z+1;
```

```

end

j=j0;
z=0;

for n=1:Ncells
m=(AnodicInletTubeLength+(AnodicTubeWidth+1)-1);
a=AA+1;
    for k=1:(HeightCells+2)
        a=a+1;
        i=(m*CellWidth*Ncells)+a+(z*CellWidth)+(AnodicWidth+1) ...
            +(MembraneWidth+1);
        % for l=1:AnodicWidth
        %     A(j,i)=-1;
        %     i=i+1;
        %     j=j+1;
        % end
        A{tt}(j,i)=-1;
        i=i+1;
        j=j+1;
        m=m+1;
    end
    z=z+1;
end

j0=j;

%%%%%%%%%%%%%%%%%%%%%%%%%%%%%%%%%%%%%%%%%%%%%%%%%%%%%%%%%%%%%%%%%%%%%%%%

%bottom
%%%%%%%%%%%%%%%%%%%%%%%%%%%%%%%%%%%%%%%%%%%%%%%%%%%%%%%%%%%%%%%%%%%%%%%%

j=j0;
z=0;

for n=1:Ncells
m=(AnodicInletTubeLength+(AnodicTubeWidth+1)-1);
a=AA-1;
    %for k=1:Ncells
    a=a+1;
    i=(m*CellWidth*Ncells)+a+(z*CellWidth)+(AnodicWidth+1);
    for l=1:MembraneWidth+2
        A{tt}(j,i)=-3;
        i=i+1;
        b{tt}(j,1)=0;
        j=j+1;
    end

    m=m+1;
%end

```



```
%%%%%%%%%%%%%%%%%%%%%%%%%%%%%%%%%%%%%%%%%%%%%%%%%%%%%%%%%%%%%%%%%%%%%%%%%
```

```
j=j0;
```

```
z=0;
```

```

for n=1:Ncells
m=(AnodicInletTubeLength+(AnodicTubeWidth+1)+(HeightCells+0));
a=AA+HeightCells+0;
  %for k=1:Ncells
    a=a+1;
    i=(m*CellWidth*Ncells)+a+(z*CellWidth)+(AnodicWidth+1)+ ...
      (MembraneWidth+2);
    for l=1:(CathodicWidth+1)-(CathodicInletTubeWidth+CCCI-1)-1
      A{tt}(j,i)=-3;
      i=i+1;
      b{tt}(j,1)=0;
      j=j+1;
    end
    for l=(CathodicWidth+1)-(CathodicInletTubeWidth+CCCI-1): ...
      ((CathodicWidth+1)-CCCI)
      A{tt}(j,i)=0;
      i=i+1;
      b{tt}(j,1)=0;
      j=j+1;
    end
    for l=((CathodicWidth+1)-CCCI)+1:(CathodicWidth+1)
      A{tt}(j,i)=-3;
      i=i+1;
      b{tt}(j,1)=0;
      j=j+1;
    end
    m=m+1;
  %end
  z=z+1;
end
```

```
j=j0;
```

```
z=0;
```

```

for n=1:Ncells
m=(AnodicInletTubeLength+(AnodicTubeWidth+1)+(HeightCells-1));
a=AA+HeightCells-1;
  %for k=1:Ncells
    a=a+1;
    i=(m*CellWidth*Ncells)+a+(z*CellWidth)+(AnodicWidth+1)+ ...
      (MembraneWidth+2);
    for l=1:(CathodicWidth+1)-(CathodicInletTubeWidth+CCCI-1)-1
      A{tt}(j,i)=4;
      i=i+1;
      b{tt}(j,1)=0;
      j=j+1;
    end
    for l=(CathodicWidth+1)-(CathodicInletTubeWidth+CCCI-1): ...
```

```

        ((CathodicWidth+1)-CCCI)
        A{tt}(j,i)=0;
        i=i+1;
        b{tt}(j,1)=0;
        j=j+1;
    end
    for l=(CathodicWidth+1)-CCCI+1:(CathodicWidth+1)
        A{tt}(j,i)=4;
        i=i+1;
        b{tt}(j,1)=0;
        j=j+1;
    end

    m=m+1;
%end
    z=z+1;
end

j=j0;

z=0;

for n=1:Ncells
    m=(AnodicInletTubeLength+(AnodicTubeWidth+1)+(HeightCells-2));
    a=AA+HeightCells-2;
    %for k=1:Ncells
        a=a+1;
        i=(m*CellWidth*Ncells)+a+(z*CellWidth)+(AnodicWidth+1) ...
            +(MembraneWidth+2);
        for l=1:(CathodicWidth+1)-(CathodicInletTubeWidth+CCCI-1)-1
            A{tt}(j,i)=-1;
            i=i+1;
            b{tt}(j,1)=0;
            j=j+1;
        end
        for l=(CathodicWidth+1)-(CathodicInletTubeWidth+CCCI-1): ...
            ((CathodicWidth+1)-CCCI)
            A{tt}(j,i)=0;
            i=i+1;
            b{tt}(j,1)=0;
            j=j+1;
        end
        for l=((CathodicWidth+1)-CCCI)+1:(CathodicWidth+1)
            A{tt}(j,i)=-1;
            i=i+1;
            b{tt}(j,1)=0;
            j=j+1;
        end
    end

    m=m+1;
%end
    z=z+1;
end

j0=j;

```



```

%%%%%%%%%%%%%%%%%%%%%%%%%%%%%%%%%%%%%%%%%%%%%%%%%%%%%%%%%%%%%%%%%%%%%%%%
%right
%%%%%%%%%%%%%%%%%%%%%%%%%%%%%%%%%%%%%%%%%%%%%%%%%%%%%%%%%%%%%%%%%%%%%%%%

j=j0;
z=0;

for n=1:Ncells
m=(AnodicInletTubeLength+(AnodicTubeWidth+1)-1);
a=AA-1;
    for k=1:(HeightCells+2)
        a=a+1;
        i=(m*CellWidth*Ncells)+a+(z*CellWidth)+(AnodicWidth+1) ...
            +(MembraneWidth+1)+(CathodicWidth+1);
        % for l=1:AnodicWidth
        %     A(j,i)=-3;
        %     i=i+1;
        %     j=j+1;
        % end

        if tt==1
            A{tt}(j,i)=-3;
            b{tt}(j,1)=ccr;
        else
            A{tt}(j,i)=-3-(lambdac);
            b{tt}(j,1)=-(b{tt-1}(j,1))*(lambdac);
        end
        %     A{tt}(j,i)=-3;
        %     b{tt}(j,1)=ccr;

        i=i+1;
        j=j+1;
        m=m+1;
    end
    z=z+1;
end

j=j0;
z=0;

for n=1:Ncells
m=(AnodicInletTubeLength+(AnodicTubeWidth+1)-1);
a=AA-2;
    for k=1:(HeightCells+2)
        a=a+1;
        i=(m*CellWidth*Ncells)+a+(z*CellWidth)+(AnodicWidth+1) ...
            +(MembraneWidth+1)+(CathodicWidth+1);
        % for l=1:AnodicWidth
        %     A(j,i)=4;
        %     i=i+1;

```

```

        %     j=j+1;
    % end
    A{tt}(j,i)=4;
    i=i+1;
    j=j+1;
    m=m+1;
end
z=z+1;
end

```

```

j=j0;
z=0;

```

```

for n=1:Ncells
m=(AnodicInletTubeLength+(AnodicTubeWidth+1)-1);
a=AA-3;
    for k=1:(HeightCells+2)
        a=a+1;
        i=(m*CellWidth*Ncells)+a+(z*CellWidth)+(AnodicWidth+1) ...
            +(MembraneWidth+1)+(CathodicWidth+1);
        % for l=1:AnodicWidth
        %     A(j,i)=-1;
        %     i=i+1;
        %     j=j+1;
        % end
        A{tt}(j,i)=-1;
        i=i+1;
        j=j+1;
        m=m+1;
    end
    z=z+1;
end
end

```

```

j0=j;

```

```

%%%%%%%%%%%%%%%%%%%%%%%%%%%%%%%%%%%%%%%%%%%%%%%%%%%%%%%%%%%%%%%%%%%%%%%%

```

```

%bottom

```

```

%%%%%%%%%%%%%%%%%%%%%%%%%%%%%%%%%%%%%%%%%%%%%%%%%%%%%%%%%%%%%%%%%%%%%%%%

```

```

j=j0;
z=0;

```

```

for n=1:Ncells
m=(AnodicInletTubeLength+(AnodicTubeWidth+1)-1);
a=AA-1;
    %for k=1:Ncells
        a=a+1;
        i=(m*CellWidth*Ncells)+a+(z*CellWidth)+(AnodicWidth+1) ...
            +(MembraneWidth+2);
        for l=1:CathodicWidth+1
            A{tt}(j,i)=-3;

```





```

j=j0;
z=0;

for n=1:Ncells
m=AnodicTubeWidth+1;
a=Aa+0;
    for k=1:AnodicInletTubeLength
        a=a+1;
        i=(m*CellWidth*Ncells)+a+(z*CellWidth);
        for l=1:AnodicInletTubeWidth
            A{tt}(j,i)=-1;
            i=i+1;
            j=j+1;
        end
        m=m+1;
    end
    z=z+1;
end

%%%%%%%%%%%%%%%%%%%%%%%%%%%%%%%%%%%%%%%%%%%%%%%%%%%%%%%%%%%%%%%%%%%%%%%%
%%%%%%%%%%%%%%%%%%%%%%%%%%%%%%%%%%%%%%%%%%%%%%%%%%%%%%%%%%%%%%%%%%%%%%%%
% upper -1 diagonal

j=j0;
z=0;

for n=1:Ncells
m=AnodicTubeWidth+2;
a=Aa+0;
    for k=1:AnodicInletTubeLength
        a=a+1;
        i=(m*CellWidth*Ncells)+a+(z*CellWidth);
        for l=1:AnodicInletTubeWidth
            A{tt}(j,i)=-1;
            i=i+1;
            j=j+1;
        end
        m=m+1;
    end
    z=z+1;
end

%%%%%%%%%%%%%%%%%%%%%%%%%%%%%%%%%%%%%%%%%%%%%%%%%%%%%%%%%%%%%%%%%%%%%%%%
%%%%%%%%%%%%%%%%%%%%%%%%%%%%%%%%%%%%%%%%%%%%%%%%%%%%%%%%%%%%%%%%%%%%%%%%
% lower -1 diagonals

j=j0;
z=0;

for n=1:Ncells
m=AnodicTubeWidth+0;
a=Aa-2;
    for k=1:AnodicInletTubeLength

```

```

        a=a+1;
        i=(m*CellWidth*Ncells)+a+(z*CellWidth);
        for l=1:AnodicInletTubeWidth
            A{tt}(j,i)=-1;
            i=i+1;
            j=j+1;
        end
        m=m+1;
    end
    z=z+1;
end

j=j;
%%%%%%%%%%%%%%%%%%%%%%%%%%%%%%%%%%%%%%%%%%%%%%%%%%%%%%%%%%%%%%%%%%%%%%%%

%%%%%%%%%%%%%%%%%%%%%%%%%%%%%%%%%%%%%%%%%%%%%%%%%%%%%%%%%%%%%%%%%%%%%%%%

% edge point boundaries
% AnodicInletTube
%%%%%%%%%%%%%%%%%%%%%%%%%%%%%%%%%%%%%%%%%%%%%%%%%%%%%%%%%%%%%%%%%%%%%%%%

% Left
%%%%%%%%%%%%%%%%%%%%%%%%%%%%%%%%%%%%%%%%%%%%%%%%%%%%%%%%%%%%%%%%%%%%%%%%
j=j;
z=0;

for n=1:Ncells
    m=(AnodicTubeWidth+1);
    a=Aa-2;
    for k=1:AnodicInletTubeLength
        a=a+1;
        i=(m*CellWidth*Ncells)+a+(z*CellWidth);
        % for l=1:AnodicWidth
        %     A(j,i)=-3;
        %     i=i+1;
        %     j=j+1;
        % end
        A{tt}(j,i)=-3;
        i=i+1;
        b{tt}(j,l)=aitl;
        j=j+1;
        m=m+1;
    end
    z=z+1;
end

j=j;
z=0;

```

```

for n=1:Ncells
m=(AnodicTubeWidth+1);
a=Aa-1;
    for k=1:AnodicInletTubeLength
        a=a+1;
        i=(m*CellWidth*Ncells)+a+(z*CellWidth);
        % for l=1:AnodicWidth
        %     A(j,i)=4;
        %     i=i+1;
        %     j=j+1;
        % end
        A{tt}(j,i)=4;
        i=i+1;
        j=j+1;
        m=m+1;
    end
    z=z+1;
end

j=j0;
z=0;

for n=1:Ncells
m=(AnodicTubeWidth+1);
a=Aa+0;
    for k=1:AnodicInletTubeLength
        a=a+1;
        i=(m*CellWidth*Ncells)+a+(z*CellWidth);
        %for l=1:(AnodicWidth+1)
        %     A(j,i)=-1;
        %     i=i+1;
        %     j=j+1
        %end
        A{tt}(j,i)=-1;
        i=i+1;
        j=j+1;
        m=m+1;
    end
    z=z+1;
end
j0=j;
%%%%%%%%%%%%%%%%%%%%%%%%%%%%%%%%%%%%%%%%%%%%%%%%%%%%%%%%%%%%%%%%%%%%%%%%

%right
%%%%%%%%%%%%%%%%%%%%%%%%%%%%%%%%%%%%%%%%%%%%%%%%%%%%%%%%%%%%%%%%%%%%%%%%

j=j0;
z=0;

for n=1:Ncells
m=(AnodicTubeWidth+1);
a=Aa-1;
    for k=1:AnodicInletTubeLength
        a=a+1;

```

```
        i=(m*CellWidth*Ncells)+a+(z*CellWidth)+AnodicInletTubeWidth;
    % for l=1:AnodicWidth
    %     A(j,i)=-3;
    %     i=i+1;
    %     j=j+1;
    % end
    A{tt}(j,i)=-3;
    i=i+1;
    b{tt}(j,1)=aitr;
    j=j+1;
    m=m+1;
end
z=z+1;
end
```

```
j=jo;
z=0;
```

```
for n=1:Ncells
m=(AnodicTubeWidth+1);
a=Aa-2;
    for k=1:AnodicInletTubeLength
        a=a+1;
        i=(m*CellWidth*Ncells)+a+(z*CellWidth)+AnodicInletTubeWidth;
        % for l=1:AnodicWidth
        %     A(j,i)=4;
        %     i=i+1;
        %     j=j+1;
        % end
        A{tt}(j,i)=4;
        i=i+1;
        j=j+1;
        m=m+1;
    end
    z=z+1;
end
```

```
j=jo;
z=0;
```

```
for n=1:Ncells
m=(AnodicTubeWidth+1);
a=Aa-3;
    for k=1:AnodicInletTubeLength
        a=a+1;
        i=(m*CellWidth*Ncells)+a+(z*CellWidth)+AnodicInletTubeWidth;
        % for l=1:AnodicWidth
        %     A(j,i)=-1;
        %     i=i+1;
        %     j=j+1;
        % end
        A{tt}(j,i)=-1;
        i=i+1;
    end
end
```



```

        j=j+1;
        m=m+1;
    end
    z=z+1;
end

jo=j;

%%%%%%%%%%%%%%%%%%%%%%%%%%%%%%%%%%%%%%%%%%%%%%%%%%%%%%%%%%%%%%%%%%%%%%%%
%%%%%%%%%%%%%%%%%%%%%%%%%%%%%%%%%%%%%%%%%%%%%%%%%%%%%%%%%%%%%%%%%%%%%%%%

%internal points anodic tube

%-4diagonal for internal points for anodic tube
%%%%%%%%%%%%%%%%%%%%%%%%%%%%%%%%%%%%%%%%%%%%%%%%%%%%%%%%%%%%%%%%%%%%%%%%
j=jo;
z=0;

m=1;
a=ACCI+0;
    for k=1:AnodicTubeWidth
        a=a+1;
        i=(m*CellWidth*Ncells)+a+(z*CellWidth);
        for l=1:(((Ncells*CellWidth)+1)-((ACCI-1)+((AnodicWidth+2) ...
            -(ACCI-1)+AnodicInletTubeWidth))- (MembraneWidth+1) ...
            -(CathodicWidth+1))
            A{tt}(j,i)=4;
            i=i+1;
            b{tt}(j,l)=0;
            j=j+1;
        end
        m=m+1;
    end
end

%%%%%%%%%%%%%%%%%%%%%%%%%%%%%%%%%%%%%%%%%%%%%%%%%%%%%%%%%%%%%%%%%%%%%%%%

%%%%%%%%%%%%%%%%%%%%%%%%%%%%%%%%%%%%%%%%%%%%%%%%%%%%%%%%%%%%%%%%%%%%%%%%
% -1 subdiagonal anodic chamber

j=jo;
z=0;

m=1;
a=ACCI-1;
    for k=1:AnodicTubeWidth
        a=a+1;
        i=(m*CellWidth*Ncells)+a+(z*CellWidth);
        for l=1:(((Ncells*CellWidth)+1)-((ACCI-1)+((AnodicWidth+2) ...
            -(ACCI-1)+AnodicInletTubeWidth))- (MembraneWidth+1) ...
            -(CathodicWidth+1))
            A{tt}(j,i)=-1;

```

```

        i=i+1;
        j=j+1;
    end
    m=m+1;
end

%%%%%%%%%%%%%%%%%%%%%%%%%%%%%%%%%%%%%%%%%%%%%%%%%%%%%%%%%%%%%%%%%%%%%%%%

%%%%%%%%%%%%%%%%%%%%%%%%%%%%%%%%%%%%%%%%%%%%%%%%%%%%%%%%%%%%%%%%%%%%%%%%
% -1 superdiagonal

j=jo;
z=0;

    m=1;
    a=ACCI+1;
    for k=1:AnodicTubeWidth
        a=a+1;
        i=(m*CellWidth*Ncells)+a+(z*CellWidth);
        for l=1:((Ncells*CellWidth)+1)-(ACCI-1)+(AnodicWidth+2) ...
            -((ACCI-1)+AnodicInletTubeWidth))- (MembraneWidth+1) ...
            - (CathodicWidth+1)
            A{tt}(j,i)=-1;
            i=i+1;
            j=j+1;
        end
        m=m+1;
    end
end

%%%%%%%%%%%%%%%%%%%%%%%%%%%%%%%%%%%%%%%%%%%%%%%%%%%%%%%%%%%%%%%%%%%%%%%%

%%%%%%%%%%%%%%%%%%%%%%%%%%%%%%%%%%%%%%%%%%%%%%%%%%%%%%%%%%%%%%%%%%%%%%%%
% upper -1 diagonal

j=jo;
z=0;

    m=2;
    a=ACCI+1;
    for k=1:AnodicTubeWidth
        a=a+1;
        i=(m*CellWidth*Ncells)+a+(z*CellWidth);
        for l=1:((Ncells*CellWidth)+1)-(ACCI-1)+(AnodicWidth+2) ...
            -((ACCI-1)+AnodicInletTubeWidth))- (MembraneWidth+1) ...
            - (CathodicWidth+1)
            A{tt}(j,i)=-1;
            i=i+1;
            j=j+1;
        end
        m=m+1;
    end
end

```

```

%%%%%%%%%%%%%%%%%%%%%%%%%%%%%%%%%%%%%%%%%%%%%%%%%%%%%%%%%%%%%%%%%%%%%%%%
%%%%%%%%%%%%%%%%%%%%%%%%%%%%%%%%%%%%%%%%%%%%%%%%%%%%%%%%%%%%%%%%%%%%%%%%
% lower -1 diagonals

j=j0;
z=0;

    m=0;
    a=ACCI-1;
    for k=1:AnodicTubeWidth
        a=a+1;
        i=(m*CellWidth*Ncells)+a+(z*CellWidth);
        for l=1:(((Ncells*CellWidth)+1)-((ACCI-1)+(AnodicWidth+2) ...
            -(ACCI-1)+AnodicInletTubeWidth))- (MembraneWidth+1) ...
            -(CathodicWidth+1))
            A{tt}(j,i)=-1;
            i=i+1;
            j=j+1;
        end
        m=m+1;
    end

j0=j;
%%%%%%%%%%%%%%%%%%%%%%%%%%%%%%%%%%%%%%%%%%%%%%%%%%%%%%%%%%%%%%%%%%%%%%%%

%edge point boundaries
%for anodic tube
%%%%%%%%%%%%%%%%%%%%%%%%%%%%%%%%%%%%%%%%%%%%%%%%%%%%%%%%%%%%%%%%%%%%%%%%
% Left
%%%%%%%%%%%%%%%%%%%%%%%%%%%%%%%%%%%%%%%%%%%%%%%%%%%%%%%%%%%%%%%%%%%%%%%%
j=j0;
z=0;

%   for n=1:Ncells
    m=0;
    a=ACCI-2;
    for k=1:(AnodicTubeWidth+1)
        a=a+1;
        i=(m*CellWidth*Ncells)+a+(z*CellWidth);
        % for l=1:AnodicWidth
        %   A(j,i)=-3;
        %   i=i+1;
        %   j=j+1;
        % end
        A{tt}(j,i)=-3;
        i=i+1;
        b{tt}(j,1)=0;
        j=j+1;
        m=m+1;
    end
    z=z+1;
%   end

```

```

j=j0;
z=0;

%   for n=1:Ncells
m=0;
a=ACCI-1;
    for k=1:(AnodicTubeWidth+1)
        a=a+1;
        i=(m*CellWidth*Ncells)+a+(z*CellWidth);
        % for l=1:AnodicWidth
        %     A(j,i)=4;
        %     i=i+1;
        %     j=j+1;
        % end
        A{tt}(j,i)=4;
        i=i+1;
        j=j+1;
        m=m+1;
    end
    z=z+1;
%   end

j=j0;
z=0;

%   for n=1:Ncells
m=0;
a=ACCI+0;
    for k=1:(AnodicTubeWidth+1)
        a=a+1;
        i=(m*CellWidth*Ncells)+a+(z*CellWidth);
        %for l=1:(AnodicWidth+1)
        %     A(j,i)=-1;
        %     i=i+1;
        %     j=j+1;
        %end
        A{tt}(j,i)=-1;
        i=i+1;
        j=j+1;
        m=m+1;
    end
    z=z+1;
%   end
j0=j;
%%%%%%%%%%%%%%%%%%%%%%%%%%%%%%%%%%%%%%%%%%%%%%%%%%%%%%%%%%%%%%%%%%%%%%%%
%top
%%%%%%%%%%%%%%%%%%%%%%%%%%%%%%%%%%%%%%%%%%%%%%%%%%%%%%%%%%%%%%%%%%%%%%%%
j=j0;
corra=((AnodicWidth-7)/2)+1;
z=0;
zz=0;
    for n=1:(Ncells-1)
        m=(AnodicTubeWidth+1);

```

```

a=AnodicTubeWidth+AnodicInletTubeWidth+ACCI;
  %for k=1:Ncells
  a=a+1;
  i=((zz*(AnodicInletTubeWidth-1))+(m*CellWidth*Ncells)+a ...
    +(z*(AnodicInletTubeWidth+ ...
      (CathodicWidth+1+MembraneWidth+2+AnodicWidth+1) ...
      -(ACCI-corra)+AnodicInletTubeWidth)))));
  for l=1:(CathodicWidth+1+MembraneWidth+2+AnodicWidth+1) ...
    -(AnodicInletTubeWidth+1)
    A{tt}(j,i)=-3;
    i=i+1;
    b{tt}(j,l)=0;
    j=j+1;
  end

  m=m+1;
%end
z=z+1;
zz=zz+1;
end

j=j0;

z=0;
zz=0;
for n=1:(Ncells-1)
m=(AnodicTubeWidth+0);
a=AnodicTubeWidth+AnodicInletTubeWidth+ACCI-1;
  %for k=1:Ncells
  a=a+1;
  i=((zz*(AnodicInletTubeWidth-1))+(m*CellWidth*Ncells) ...
    +a+(z*(AnodicInletTubeWidth+(CathodicWidth ...
      +1+MembraneWidth+2+AnodicWidth+1) ...
      -(ACCI-corra)+AnodicInletTubeWidth)))));
  for l=1:(CathodicWidth+1+MembraneWidth+2+AnodicWidth+1) ...
    -(AnodicInletTubeWidth+1)
    A{tt}(j,i)=4;
    i=i+1;
    j=j+1;
  end

  m=m+1;
%end
z=z+1;
zz=zz+1;
end

j=j0;

z=0;
zz=0;
for n=1:(Ncells-1)
m=(AnodicTubeWidth-1);
a=AnodicTubeWidth+AnodicInletTubeWidth+ACCI-2;
  %for k=1:Ncells

```

```

a=a+1;
i=((zz*(AnodicInletTubeWidth-1))+(m*CellWidth*Ncells) ...
+a+(z*(AnodicInletTubeWidth+((CathodicWidth ...
+1+MembraneWidth+2+AnodicWidth+1) ...
-((ACCI-corra)+AnodicInletTubeWidth)))));
for l=1:(CathodicWidth+1+MembraneWidth+2+AnodicWidth+1) ...
-(AnodicInletTubeWidth+1)
A{tt}(j,i)=-1;
i=i+1;
j=j+1;
end

m=m+1;
%end
z=z+1;
zz=zz+1;
end

jo=j;
%%%%%%%%%%%%%%%%%%%%%%%%%%%%%%%%%%%%%%%%%%%%%%%%%%%%%%%%%%%%%%%%%%%%%%%%
%right
%%%%%%%%%%%%%%%%%%%%%%%%%%%%%%%%%%%%%%%%%%%%%%%%%%%%%%%%%%%%%%%%%%%%%%%%
j=jo;
z=0;

% for n=1:(Ncells-1)
m=0;
a=((Ncells*CellWidth)+1)-(MembraneWidth+2)-(CathodicWidth+1) ...
-((AnodicWidth+1)-(ACCI+AnodicInletTubeWidth))-1);
for k=1:(AnodicTubeWidth+1)
a=a+1;
i=(m*CellWidth*Ncells)+a+(z*CellWidth);
% for l=1:AnodicWidth
% A(j,i)=-3;
% i=i+1;
% j=j+1;
% end
A{tt}(j,i)=-3;
i=i+1;
b{tt}(j,1)=0;
j=j+1;
m=m+1;
end
z=z+1;
% end

j=jo;
z=0;

% for n=1:(Ncells-1)
m=0;
a=((Ncells*CellWidth)+1)-(MembraneWidth+2)-(CathodicWidth+1) ...
-((AnodicWidth+1)-(ACCI+AnodicInletTubeWidth))-2);
for k=1:(AnodicTubeWidth+1)
a=a+1;
i=(m*CellWidth*Ncells)+a+(z*CellWidth);

```

```

        % for l=1:AnodicWidth
        %     A(j,i)=4;
        %     i=i+1;
        %     j=j+1;
        % end
        A{tt}(j,i)=4;
        i=i+1;
        j=j+1;
        m=m+1;
    end
    z=z+1;
% end

j=j0;
z=0;

% for n=1:(Ncells-1)
m=0;
a=((Ncells*CellWidth)+1)-(MembraneWidth+2)-(CathodicWidth+1) ...
-(AnodicWidth+1)-(ACCI+AnodicInletTubeWidth)-3);
for k=1:(AnodicTubeWidth+1)
    a=a+1;
    i=(m*CellWidth*Ncells)+a+(z*CellWidth);
    % for l=1:AnodicWidth
    %     A(j,i)=-1;
    %     i=i+1;
    %     j=j+1;
    % end
    A{tt}(j,i)=-1;
    i=i+1;
    j=j+1;
    m=m+1;
end
z=z+1;
% end

j0=j;

%%%%%%%%%%%%%%%%%%%%%%%%%%%%%%%%%%%%%%%%%%%%%%%%%%%%%%%%%%%%%%%%%%%%%%%%
%bottom
%%%%%%%%%%%%%%%%%%%%%%%%%%%%%%%%%%%%%%%%%%%%%%%%%%%%%%%%%%%%%%%%%%%%%%%%
j=j0;
z=0;

% for n=1:Ncells
m=0;
a=ACCI-2;
%for k=1:Ncells
a=a+1;
i=(m*CellWidth*Ncells)+a+(z*CellWidth);
for l=1:(((Ncells*CellWidth)+1)-(ACCI-2)-((AnodicWidth+1) ...
-(AnodicInletTubeWidth+(ACCI)))-(MembraneWidth+2) ...
-(CathodicWidth+1))
A{tt}(j,i)=-3;

```







```
%%%%%%%%%%%%%%%%%%%%%%%%%%%%%%%%%%%%%%%%%%%%%%%%%%%%%%%%%%%%%%%%%%%%%%%%%
```

```
% -1 superdiagonal
```

```
j=jo;
```

```
z=0;
```

```
for n=1:Ncells
```

```
  m=CC;
```

```
  a=Cc+1;
```

```
    for k=1:CatholicInletTubeLength
```

```
  %
```

```
    a=a+1;
```

```
    i=(m*SystemWidth)+a+(z*CellWidth);
```

```
    for l=1:CatholicInletTubeWidth
```

```
      A{tt}(j,i)=-1;
```

```
      i=i+1;
```

```
      j=j+1;
```

```
    end
```

```
    m=m+1;
```

```
  end
```

```
  z=z+1;
```

```
end
```

```
%%%%%%%%%%%%%%%%%%%%%%%%%%%%%%%%%%%%%%%%%%%%%%%%%%%%%%%%%%%%%%%%%%%%%%%%%
```

```
%%%%%%%%%%%%%%%%%%%%%%%%%%%%%%%%%%%%%%%%%%%%%%%%%%%%%%%%%%%%%%%%%%%%%%%%%
```

```
% upper -1 diagonal
```

```
j=jo;
```

```
z=0;
```

```
for n=1:Ncells
```

```
  m=CC+1;
```

```
  a=Cc;
```

```
    for k=1:CatholicInletTubeLength
```

```
  %
```

```
    a=a+1;
```

```
    i=(m*SystemWidth)+a+(z*CellWidth);
```

```
    for l=1:CatholicInletTubeWidth
```

```
      A{tt}(j,i)=-1;
```

```
      i=i+1;
```

```
      j=j+1;
```

```
    end
```

```
    m=m+1;
```

```
  end
```

```
  z=z+1;
```

```
end
```

```
%%%%%%%%%%%%%%%%%%%%%%%%%%%%%%%%%%%%%%%%%%%%%%%%%%%%%%%%%%%%%%%%%%%%%%%%%
```

```
%%%%%%%%%%%%%%%%%%%%%%%%%%%%%%%%%%%%%%%%%%%%%%%%%%%%%%%%%%%%%%%%%%%%%%%%%
```

```
% lower -1 diagonals
```

```
j=jo;
```

```
z=0;
```

```
for n=1:Ncells
```

```

m=CC-1;
a=Cc;
for k=1:CathodicInletTubeLength
%
    a=a+1;
    i=(m*SystemWidth)+a+(z*CellWidth);
    for l=1:CathodicInletTubeWidth
        A{tt}(j,i)=-1;
        i=i+1;
        j=j+1;
    end
    m=m+1;
end
z=z+1;
end

jo=j;
%%%%%%%%%%%%%%%%%%%%%%%%%%%%%%%%%%%%%%%%%%%%%%%%%%%%%%%%%%%%%%%%%%%%%%%%

% edge point boundaries
% CathodicInletTube
%%%%%%%%%%%%%%%%%%%%%%%%%%%%%%%%%%%%%%%%%%%%%%%%%%%%%%%%%%%%%%%%%%%%%%%%

% Left
%%%%%%%%%%%%%%%%%%%%%%%%%%%%%%%%%%%%%%%%%%%%%%%%%%%%%%%%%%%%%%%%%%%%%%%%
j=jo;
z=0;

for n=1:Ncells
m=CC;
a=Cc-1;
for k=1:CathodicInletTubeLength
%
    a=a+1;
    i=(m*SystemWidth)+a+(z*CellWidth);
    % for l=1:AnodicWidth
    %     A(j,i)=-3;
    %     i=i+1;
    %     j=j+1;
    % end
    A{tt}(j,i)=-3;
    i=i+1;
    b{tt}(j,1)=0;
    j=j+1;
    m=m+1;
end
z=z+1;
end

j=jo;
z=0;

for n=1:Ncells
m=CC;
a=Cc;
for k=1:CathodicInletTubeLength

```

```

%         a=a+1;
         i=(m*SystemWidth)+a+(z*CellWidth);
%     for l=1:AnodicWidth
%         A(j,i)=4;
%         i=i+1;
%         j=j+1;
%     end
         A{tt}(j,i)=4;
         i=i+1;
         j=j+1;
         m=m+1;
     end
     z=z+1;
end

j=j0;
z=0;

for n=1:Ncells
m=CC;
a=Cc+1;
    for k=1:CathodicInletTubeLength
%         a=a+1;
         i=(m*SystemWidth)+a+(z*CellWidth);
%     for l=1:(AnodicWidth+1)
%         A(j,i)=-1;
%         i=i+1;
%         j=j+1;
%     end
         A{tt}(j,i)=-1;
         i=i+1;
         j=j+1;
         m=m+1;
    end
    z=z+1;
end

j0=j;
%%%%%%%%%%%%%%%%%%%%%%%%%%%%%%%%%%%%%%%%%%%%%%%%%%%%%%%%%%%%%%%%%%%%%%%%

%right
%%%%%%%%%%%%%%%%%%%%%%%%%%%%%%%%%%%%%%%%%%%%%%%%%%%%%%%%%%%%%%%%%%%%%%%%
j=j0;
z=0;

for n=1:Ncells
m=CC;
a=Cc+CathodicInletTubeWidth;
    for k=1:CathodicInletTubeLength
%         a=a+1;
         i=(m*SystemWidth)+a+(z*CellWidth);
%     for l=1:AnodicWidth
%         A(j,i)=-3;
%         i=i+1;

```

```

        %     j=j+1;
        % end
        A{tt}(j,i)=-3;
        i=i+1;
        b{tt}(j,1)=0;
        j=j+1;
        m=m+1;
    end
    z=z+1;
end

j=j0;
z=0;

for n=1:Ncells
    m=CC;
    a=Cc+CathodicInletTubeWidth-1;
    for k=1:CathodicInletTubeLength
        %     a=a+1;
        i=(m*SystemWidth)+a+(z*CellWidth);
        % for l=1:AnodicWidth
        %     A(j,i)=4;
        %     i=i+1;
        %     j=j+1;
        % end
        A{tt}(j,i)=4;
        i=i+1;
        j=j+1;
        m=m+1;
    end
    z=z+1;
end

j=j0;
z=0;

for n=1:Ncells
    m=CC;
    a=Cc+CathodicInletTubeWidth-2;
    for k=1:CathodicInletTubeLength
        %     a=a+1;
        i=(m*SystemWidth)+a+(z*CellWidth);
        % for l=1:AnodicWidth
        %     A(j,i)=-1;
        %     i=i+1;
        %     j=j+1;
        % end
        A{tt}(j,i)=-1;
        i=i+1;
        j=j+1;
        m=m+1;
    end
    z=z+1;
end

```

```

end

jo=j;

%%%%%%%%%%%%%%%%%%%%%%%%%%%%%%%%%%%%%%%%%%%%%%%%%%%%%%%%%%%%%%%%%%%%%%%%

%internal points cathodic tube

%-4diagonal for internal points for cathodic tube
%%%%%%%%%%%%%%%%%%%%%%%%%%%%%%%%%%%%%%%%%%%%%%%%%%%%%%%%%%%%%%%%%%%%%%%%
j=jo;
z=0;

m=CC+CathodicInletTubeLength;
a=Cc;
for k=1:CathodicTubeWidth
%   a=a+1;
   i=(m*SystemWidth)+a+(z*CellWidth);
   for l=1:SystemWidth-(1+AnodicWidth)-(2+MembraneWidth) ...
       -(CCCI-1)-CCCI
       A{tt}(j,i)=4;
       i=i+1;
       b{tt}(j,l)=0;
       j=j+1;
   end
   m=m+1;
end

%%%%%%%%%%%%%%%%%%%%%%%%%%%%%%%%%%%%%%%%%%%%%%%%%%%%%%%%%%%%%%%%%%%%%%%%

%%%%%%%%%%%%%%%%%%%%%%%%%%%%%%%%%%%%%%%%%%%%%%%%%%%%%%%%%%%%%%%%%%%%%%%%
% -1 subdiagonal anodic chamber

j=jo;
z=0;

m=CC+CathodicInletTubeLength;
a=Cc-1;
for k=1:CathodicTubeWidth
%   a=a+1;
   i=(m*SystemWidth)+a+(z*CellWidth);
   for l=1:SystemWidth-(1+AnodicWidth)-(2+MembraneWidth) ...
       -(CCCI-1)-CCCI
       A{tt}(j,i)=-1;
       i=i+1;
       j=j+1;
   end
   m=m+1;
end

```

```

%%%%%%%%%%%%%%%%%%%%%%%%%%%%%%%%%%%%%%%%%%%%%%%%%%%%%%%%%%%%%%%%%%%%%%%%
%%%%%%%%%%%%%%%%%%%%%%%%%%%%%%%%%%%%%%%%%%%%%%%%%%%%%%%%%%%%%%%%%%%%%%%%
% -1 superdiagonal

j=j0;
z=0;

m=CC+CathodicInletTubeLength;
a=Cc+1;
for k=1:CathodicTubeWidth
%
    a=a+1;
    i=(m*SystemWidth)+a+(z*CellWidth);
    for l=1:SystemWidth-(1+AnodicWidth)-(2+MembraneWidth) ...
        -(CCCI-1)-CCCI
        A{tt}(j,i)=-1;
        i=i+1;
        j=j+1;
    end
    m=m+1;
end

%%%%%%%%%%%%%%%%%%%%%%%%%%%%%%%%%%%%%%%%%%%%%%%%%%%%%%%%%%%%%%%%%%%%%%%%
%%%%%%%%%%%%%%%%%%%%%%%%%%%%%%%%%%%%%%%%%%%%%%%%%%%%%%%%%%%%%%%%%%%%%%%%
% upper -1 diagonal

j=j0;
z=0;

m=CC+CathodicInletTubeLength+1;
a=Cc;
for k=1:CathodicTubeWidth
%
    a=a+1;
    i=(m*SystemWidth)+a+(z*CellWidth);
    for l=1:SystemWidth-(1+AnodicWidth)-(2+MembraneWidth) ...
        -(CCCI-1)-CCCI
        A{tt}(j,i)=-1;
        i=i+1;
        j=j+1;
    end
    m=m+1;
end

%%%%%%%%%%%%%%%%%%%%%%%%%%%%%%%%%%%%%%%%%%%%%%%%%%%%%%%%%%%%%%%%%%%%%%%%
%%%%%%%%%%%%%%%%%%%%%%%%%%%%%%%%%%%%%%%%%%%%%%%%%%%%%%%%%%%%%%%%%%%%%%%%
% lower -1 diagonals

j=j0;
z=0;

m=CC+CathodicInletTubeLength-1;

```

```

a=Cc;
  for k=1:CathodicTubeWidth
%     a=a+1;
    i=(m*SystemWidth)+a+(z*CellWidth);
    for l=1:SystemWidth-(1+AnodicWidth)-(2+MembraneWidth) ...
      - (CCCI-1) -CCCI
      A{tt}(j,i)=-1;
      i=i+1;
      j=j+1;
    end
    m=m+1;
  end
end

jo=j;
%%%%%%%%%%%%%%%%%%%%%%%%%%%%%%%%%%%%%%%%%%%%%%%%%%%%%%%%%%%%%%%%%%%%%%%%

%edge point boundaries
%for cathodic tube
%%%%%%%%%%%%%%%%%%%%%%%%%%%%%%%%%%%%%%%%%%%%%%%%%%%%%%%%%%%%%%%%%%%%%%%%
% Left
%%%%%%%%%%%%%%%%%%%%%%%%%%%%%%%%%%%%%%%%%%%%%%%%%%%%%%%%%%%%%%%%%%%%%%%%
j=jo;
z=0;

%   for n=1:Ncells
m=CC+CathodicInletTubeLength;
a=Cc-1;
  for k=1:(CathodicTubeWidth+1)
%     a=a+1;
    i=(m*SystemWidth)+a+(z*CellWidth);
    % for l=1:AnodicWidth
    %   A(j,i)=-3;
    %   i=i+1;
    %   j=j+1;
    % end
    A{tt}(j,i)=-3;
    i=i+1;
    b{tt}(j,1)=0;
    j=j+1;
    m=m+1;
  end
  z=z+1;
%   end

j=jo;
z=0;

%   for n=1:Ncells
m=CC+CathodicInletTubeLength;
a=Cc;
  for k=1:(CathodicTubeWidth+1)
%     a=a+1;
    i=(m*SystemWidth)+a+(z*CellWidth);
    % for l=1:AnodicWidth

```



```

        %     A(j,i)=4;
        %     i=i+1;
        %     j=j+1;
        % end
        A{tt}(j,i)=4;
        i=i+1;
        j=j+1;
        m=m+1;
    end
    z=z+1;
%     end

j=j0;
z=0;

%     for n=1:Ncells
m=CC+CathodicInletTubeLength;
a=Cc+1;
    for k=1:(CathodicTubeWidth+1)
%
        a=a+1;
        i=(m*SystemWidth)+a+(z*CellWidth);
        %for l=1:(AnodicWidth+1)
        %     A(j,i)=-1;
        %     i=i+1;
        %     j=j+1
        %end
        A{tt}(j,i)=-1;
        i=i+1;
        j=j+1;
        m=m+1;
    end
    z=z+1;
%     end
j0=j;
%%%%%%%%%%%%%%%%%%%%%%%%%%%%%%%%%%%%%%%%%%%%%%%%%%%%%%%%%%%%%%%%%%%%%%%%%%%%%%
%top
%%%%%%%%%%%%%%%%%%%%%%%%%%%%%%%%%%%%%%%%%%%%%%%%%%%%%%%%%%%%%%%%%%%%%%%%%%%%%%
j=j0;
z=0;

%     for n=1:Ncells
m=CC+CathodicInletTubeLength+CathodicTubeWidth;
a=Cc-1;
    %for k=1:Ncells
%
        a=a+1;
        i=(m*SystemWidth)+a+(z*CellWidth);
        for l=1:SystemWidth-(1+AnodicWidth)-(2+MembraneWidth) ...
            -(CCCI-2)-(CathodicWidth-(CCCI-1)-CathodicInletTubeWidth)
            A{tt}(j,i)=-3;
            i=i+1;
            b{tt}(j,1)=0;
            j=j+1;
        end
    end

```

```

        m=m+1;
    %end
    z=z+1;
%    end

j=jo;
z=0;

%    for n=1:Ncells
m=CC+CathodicInletTubeLength+CathodicTubeWidth-1;
a=Cc-1;
    %for k=1:Ncells
%
        a=a+1;
        i=(m*SystemWidth)+a+(z*CellWidth);
        for l=1:SystemWidth-(1+AnodicWidth)-(2+MembraneWidth) ...
            -(CCCI-2)-(CathodicWidth-(CCCI-1) -CathodicInletTubeWidth)
            A{tt}(j,i)=4;
            i=i+1;
            j=j+1;
        end

        m=m+1;
    %end
    z=z+1;
%    end

j=jo;
z=0;

%    for n=1:Ncells
m=CC+CathodicInletTubeLength+CathodicTubeWidth-2;
a=Cc-1;
    %for k=1:Ncells
%
        a=a+1;
        i=(m*SystemWidth)+a+(z*CellWidth);
        for l=1:SystemWidth-(1+AnodicWidth)-(2+MembraneWidth) ...
            -(CCCI-2)-(CathodicWidth-(CCCI-1) -CathodicInletTubeWidth)
            A{tt}(j,i)=-1;
            i=i+1;
            j=j+1;
        end

        m=m+1;
    %end
    z=z+1;
%    end
jo=j;

%%%%%%%%%%%%%%%%%%%%%%%%%%%%%%%%%%%%%%%%%%%%%%%%%%%%%%%%%%%%%%%%%%%%%%%%%%
%right
%%%%%%%%%%%%%%%%%%%%%%%%%%%%%%%%%%%%%%%%%%%%%%%%%%%%%%%%%%%%%%%%%%%%%%%%%%
j=jo;
z=0;

%    for n=1:(Ncells-1)
m=CC+CathodicInletTubeLength;

```

```

a=SystemWidth-CathodicWidth+CCCI+CathodicInletTubeWidth-1;
for k=1:(CathodicTubeWidth+1)
%   a=a+1;   CathodicWidth
      i=(m*SystemWidth)+a+(z*CellWidth);
      % for l=1:AnodicWidth
      %   A(j,i)=-3;
      %   i=i+1;
      %   j=j+1;
      % end
      A{tt}(j,i)=-3;
      i=i+1;
      b{tt}(j,1)=0;
      j=j+1;
      m=m+1;
end
z=z+1;
% end

j=j0;
z=0;

%   for n=1:(Ncells-1)
m=CC+CathodicInletTubeLength;
a=SystemWidth-CathodicWidth+CCCI+CathodicInletTubeWidth-2;

%   a=SystemWidth-(CCCI-1)-1;
for k=1:(CathodicTubeWidth+1)
%   a=a+1;
      i=(m*SystemWidth)+a+(z*CellWidth);
      % for l=1:AnodicWidth
      %   A(j,i)=4;
      %   i=i+1;
      %   j=j+1;
      % end
      A{tt}(j,i)=4;
      i=i+1;
      j=j+1;
      m=m+1;
end
z=z+1;
% end

j=j0;
z=0;

%   for n=1:(Ncells-1)
m=CC+CathodicInletTubeLength;
a=SystemWidth-CathodicWidth+CCCI+CathodicInletTubeWidth-3;
%   a=SystemWidth-(CCCI-1)-2;
for k=1:(CathodicTubeWidth+1)
%   a=a+1;
      i=(m*SystemWidth)+a+(z*CellWidth);
      % for l=1:AnodicWidth

```

```

        %     A(j,i)=-1;
        %     i=i+1;
        %     j=j+1;
        % end
        A{tt}(j,i)=-1;
        i=i+1;
        j=j+1;
        m=m+1;
    end
    z=z+1;
%     end

jo=j;

%%%%%%%%%%%%%%%%%%%%%%%%%%%%%%%%%%%%%%%%%%%%%%%%%%%%%%%%%%%%%%%%%%%%%%%%
%bottom
%%%%%%%%%%%%%%%%%%%%%%%%%%%%%%%%%%%%%%%%%%%%%%%%%%%%%%%%%%%%%%%%%%%%%%%%
j=jo;
corrc=(CathodicWidth-7)/2+1;
z=0;
zz=0;
    for n=1:(Ncells-1)
        m=CC+CathodicInletTubeLength-1;
        a=Cc+CathodicInletTubeWidth;
        %for k=1:Ncells
        %     a=a+1;
        %
        %         i=(zz*(CathodicInletTubeWidth-1)+(m*SystemWidth)+a ...
+ (z*(CathodicInletTubeWidth+(CathodicWidth ...
+1+MembraneWidth+2+AnodicWidth+1)-(CCCI+AnodicInletTubeWidth)))));
        i=(m*SystemWidth)+a+(z*CellWidth);
        for l=1:(CathodicWidth+1+MembraneWidth+2+AnodicWidth+1) ...
            -(CathodicInletTubeWidth+1)
            A{tt}(j,i)=-3;
            i=i+1;
            b{tt}(j,l)=0;
            j=j+1;
        end

        %         m=m+1;
        %end
        z=z+1;
        zz=zz+1;
    end

j=jo;

z=0;
zz=0;
    for n=1:(Ncells-1)
        m=CC+CathodicInletTubeLength;
        a=Cc+CathodicInletTubeWidth;
        %for k=1:Ncells
        %     a=a+1;
        %         i=(zz*(CathodicInletTubeWidth-1)+(m*SystemWidth) ...
+ a+(z*(CathodicInletTubeWidth+(CathodicWidth ...

```

```

+1+MembraneWidth+2+AnodicWidth+1) ...
-(CCCI-corrC+AnodicInletTubeWidth)))));
    i=(m*SystemWidth)+a+(z*CellWidth);
    for l=1:((CathodicWidth+1+MembraneWidth+2+AnodicWidth+1) ...
      -(CathodicInletTubeWidth+1))
      A{tt}(j,i)=4;
      i=i+1;
      j=j+1;
    end

%           m=m+1;
%end
z=z+1;
zz=zz+1;
end

j=j0;

z=0;
zz=0;
for n=1:(Ncells-1)
  m=CC+CathodicInletTubeLength+1;
  a=Cc+CathodicInletTubeWidth;
  %for k=1:Ncells
%           a=a+1;
%           i=((zz*(CathodicInletTubeWidth-1))+(m*SystemWidth) ...
+a+(z*(CathodicInletTubeWidth+(CathodicWidth ...
+1+MembraneWidth+2+AnodicWidth+1) ...
-(CCCI-corrC+AnodicInletTubeWidth)))));
    i=(m*SystemWidth)+a+(z*CellWidth);
    for l=1:((CathodicWidth+1+MembraneWidth+2+AnodicWidth+1) ...
      -(CathodicInletTubeWidth+1))
      A{tt}(j,i)=-1;
      i=i+1;
      j=j+1;
    end

%           m=m+1;
%end
z=z+1;
zz=zz+1;
end
jo=j;
%%%%%%%%%%%%%%%%%%%%%%%%%%%%%%%%%%%%%%%%%%%%%%%%%%%%%%%%%%%%%%%%%%%%%%%%
end

%%%%%%%%%%%%%%%%%%%%%%%%%%%%%%%%%%%%%%%%%%%%%%%%%%%%%%%%%%%%%%%%%%%%%%%%

%A{2}
% A and b must be in the same time
SA = sparse(A{2});
Sb = sparse(b{2});

figure(1)
%   spy(A)

```

```
spy(SA)

figure(2)
spy(Sb)
% A1 = A(:,1:end-((Ncells-1)*(HeightCells+2)));
% S1 = S(:,1:end-((Ncells-1)*(HeightCells+2)));

% u=A1\X;
u=SA\Sb;
%u=X\A;

figure(3)
plot(u);

if Ncells ==1
    cut=(AnodicWidth+1)+(MembraneWidth+2)+(CathodicWidth+1)*Ncells;

else
% cut=(AnodicWidth+1)+(MembraneWidth+2)+(CathodicWidth+1)*Ncells ...
- (Ncells-1);
    cut=SystemWidth;

end

% xlswrite('generatedMatrix.xlsx',A)
% xlswrite('generatedMatrixA1.xlsx',A1)

% xlswrite('generatedMatrix1.xlsx',Sb)
Z=vec2mat(u,cut);

% xlswrite('generatedMatrix2.xlsx',u)
% xlswrite('generatedMatrix3.xlsx',Z)

figure(4)
surf(Z)

%break
end
```